

Retrospective clonal analysis of the developing mouse heart

Tesis Doctoral

**Ghislaine Lioux
Enero 2019**

**Universidad Autónoma de Madrid
Facultad de Ciencias
Departamento de Biología Molecular**

Universidad Autónoma de Madrid
Facultad de Ciencias
Departamento de Biología Molecular



Tesis Doctoral

Retrospective clonal analysis of the developing mouse heart

Memoria presentada por:

Ghislaine Lioux

Director:

Dr. Miguel Torres Sánchez

Centro Nacional de Investigaciones Cardiovasculares (CNIC)

Madrid 2019

Table of contents

Summary.....	1
Resumen.....	3
Introduction.....	5
1.1 A Brief historical aside.....	5
1.2 Heart anatomy and function.....	6
1.3 Embryonic heart development.....	8
1.3.1 Formation of the four-chambered heart.....	8
1.3.2 Contribution of cardiac lineages during development.....	11
1.4.1 The cardiac lymphatics, an important component of the heart for a long time in oblivion.....	18
1.4.1 The role of Retinoic signalling in the four chambered-heart.....	24
Objectives.....	27
Results.....	29
1. Random retrospective clonal analysis successfully targets heart progenitors.....	29
2. The epicardium and arterial mesothelium do not belong to the same lineage.....	32
3. AMCs derive from the splanchnic mesoderm related to the Second heart field.....	36
4. AMCs are clonally related to vascular cells of the OFT.....	39
5. AMCs give rise to smooth muscle and endothelial cells of the great arteries.....	41
6. OFT proximal clones give rise to LECs.....	45
7. Lymphatic endothelial cells of the ventral and dorsal parts of the heart arise from distinct sources of progenitors.....	50
8. The second heart field contributes to the ventral but not to the dorsal lymphatic vasculature.....	57
9. The lymphatic vasculature of Tbx1 null-mice is altered in the dorsal part of the heart but fails to form in the ventral part of the heart.....	61
11. The Pulmonary artery contains a lymphvasculogenic niche of progenitors.....	64
.....	66
12. The mesothelium and sub-mesothelium of the arteries exhibit lower Raldh2 levels than their ventricular counterparts.....	66
13. RA signalling plays a role in cardiac lymphatic development and maturation.....	68
Supplementary material.....	74
.....	78
.....	80
Material and methods.....	82
1. Animal procedures.....	82

1.1 Mice strains	82
1.2 Tamoxifen preparation and maternal administration	83
1.3 Maternal administration of Retinoic acid:	83
1.4 Embryo harvest	84
1.5 Neonatal heart harvest.....	84
1.6 Clonal analysis	84
1.7 Mouse blood serum preparation	85
2.Tissue processing.....	85
2.1 <i>In situ</i> hybridisation on Paraffin sections	85
2.2 Immuno-histochemistry and immuno-fluorescence.....	86
3. Epicardial and arterial mesothelial dissection.....	90
4.Ex vivo explants and culture	90
5. Tissue imaging	91
6.RNA extraction and RNA sequencing:	92
7.RNAseq analysis.....	92
Discussion.....	95
Existence of a niche of LEC progenitors in the pulmonary artery	95
A Role for AMCs in lymphangiogenesis?	97
What about the Aorta?	100
The heterogeneous origins of the cardiac lymphatic vasculature	101
The lymphangiogenic properties of SHF progenitors introduce the concept of organ-specific lymphatic development	104
Conclusions	106
Bibliography	108

List of Abbreviations:

<p>AHF: Anterior heart field AMC: Arterial mesothelial cell Ang: angiopoietin Ao: Aorta AP: Arterial pole AVC: Atrioventricular canal BEC: Blood endothelial cell BMP: Bone Morphogenetic Protein Calp: Calponin CHD: Congenital heart defect CNCC: Cardiac neural crest cell CV: cardinal vein CVC : Coronary vascular cell DAB : diaminobenzidine tetrahydrochloride EC: Endothelial cell ECM: Extracellular matrix EMT: Epithelial to mesenchymal transition EPDCs: Epicardial derived cells ESC: Embryonic stem cell EpiCs: Epicardial cells Fb: Fibroblast Fgf: Fibroblast growth factor FHF: First heart field 4-OHT: 4-hydroxy-Tamoxifen ISH: In situ hybridization IVS: Interventricular septum LECs: Lymphatic endothelial cells LMCs: Lymphatic smooth muscle cells LN: Lymph node LS: lymph sac KO: Knock-Out LV: Left Ventricle MEF2C: Myocyte enhancer factor 2C MHC: Ms: Mesothelium nPEC: Non-proepicardial epicardial cell Nrp: neuropilin OFT: Outflow tract PA: Pulmonary artery</p>	<p>PE: Proepicardium Prox1: Prospero homeobox1 PS: Pimitive streak RA: Retinoic acid RERT: polr2a-CreERT2 RNAseq: RNA sequencing RV: Right ventricle SHF: Second Heart Field SHF-EpiCs: Second Heart Field derived Epicardial Cells SM: Smooth muscle Tbx18: T-box18 Tgf-β: Transforming Growth Factor-β Tom: Td Tomato SMC: Smooth muscle cells VEGF: vascular endothelial growth factor VP: Venous pole Valv: valvular mesenchymal cells WT: Wild type Wt1: Wilms tumor 1</p>
---	--

Summary

The cardiac OFT is composed of endothelial cells (ECs), smooth muscle cells (SMCs), fibroblasts (Fbs) and Cardiomyocytes (CMs) known to derive from neural crest and second heart field (SHF) progenitors. The OFT is also covered by a mesothelial sheet of arterial mesothelial cells (AMCs) continuous with the epicardium. While the epicardium arises from the proepicardium, the early progenitor of AMCs is unknown.

Using mesothelial and SHF related Cre lines we identified the origin of AMCs to be in the dorsal pharyngeal mesoderm. During a systematic analysis of cardiac lineages by random clonal labelling in developing mouse hearts, we found that AMCs shared a clonal relationship with cells of the great arteries. AMC clones were of different nature along the great arteries. On one hand, distal AMCs in both vessels were clonally related to Fbs, SMCs and ECs. On the other hand, the proximal AMCs of the Pulmonary artery (PA), were clonally related to Fbs, SMCs, CMs and lymphatic endothelial cells (LECs) of the ventral part of the heart. These clones however, were never found together with lymphatic clones of the dorsal part of the heart suggesting multiple origins for cardiac lymphatic vessels. Fate mapping of VEGFR3+ progenitors at different stages showed that whereas dorsal lymphatics derive from pre-existing lymphatic vessels, formation of ventral lymphatics involves the late recruitment of non-lymphatic cells. Using a range of SHF-specific Cre lines, we found that SHF-derived cells form ventral but not dorsal cardiac lymphatics. These observations suggest that SHF progenitors are recruited in the mesothelial-sub-mesothelial region of the PA. To test this hypothesis, we transplanted portions of PA mesothelial/sub-mesothelial layers from fluorescent donors into wild type E14.5 hearts. Donor tissue invaded the host myocardium, forming lymphatic vessels. The exploration of molecular cues involved in the formation of that niche showed that *Raldh2* is downregulated at transcriptional and protein levels in proximal AMCs. Moreover, the loss of RA signalling in mesothelial cells resulted in immature lymphatic vessels while an excess of RA triggered lymphatic hyper-remodelling.

These data show that part of the ventral lymphatics form by recruitment of SHF progenitors at a vasculogenic niche specified in a low *Raldh2* environment.

Resumen

El tracto de salida cardíaco (OFT) está compuesto por células endoteliales (EC), células de músculo liso (SMC), fibroblastos (Fbs) y cardiomiocitos (CM) que derivan de los progenitores de la cresta neural y del segundo campo cardíaco (SHF). El OFT está recubierto por una capa de células mesoteliales arteriales (AMCs) continua al epicardio. El epicardio proviene del proepicardio. Sin embargo, el progenitor temprano de las AMCs está desconocido.

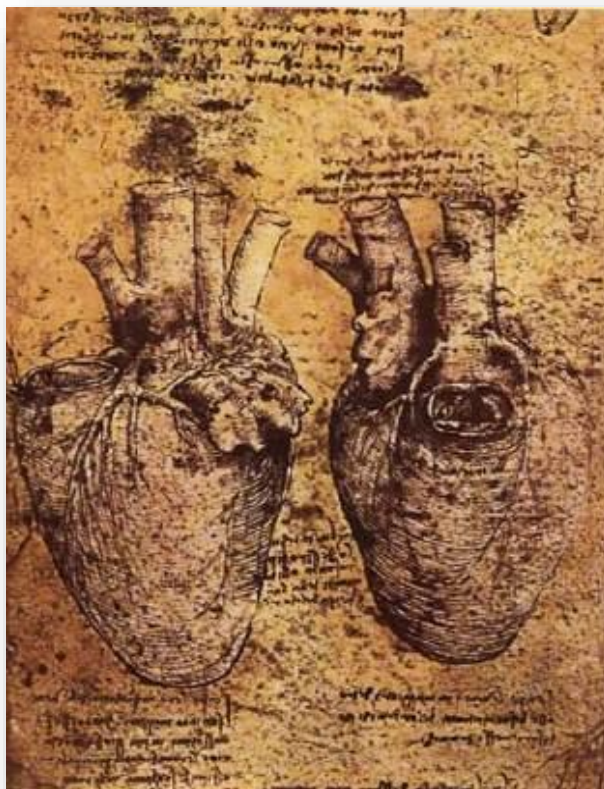
Mediante el uso de líneas Cre de mesotelio y de SHF, identificamos el origen de las AMCs en el mesodermo faríngeo dorsal. Durante un análisis sistemático de los linajes cardíacos mediante el etiquetado clonal aleatorio en corazones de ratones en desarrollo, encontramos que las AMCs comparten una relación clonal con las células de las grandes arterias. Los clones de AMCs eran diferentes según su posición en las grandes arterias. Por un lado, las AMCs distales en ambos vasos eran asociadas clonalmente con Fbs, SMC y EC. Por otro lado, las AMC proximales de la arteria pulmonar (AP) eran asociadas clonalmente con Fbs, SMC, CM y células endoteliales linfáticas (LEC) de la parte ventral del corazón. Sin embargo, estos clones no solapan con los clones linfáticos de la parte dorsal del corazón, lo que sugiere múltiples orígenes para los vasos linfáticos cardíacos. El trazado de los progenitores VEGFR3 + a diferentes estadios, demostró que los linfáticos dorsales derivan de vasos linfáticos preexistentes mientras que la formación de linfáticos ventrales implica el reclutamiento tardío de células no linfáticas. Usando un abanico de líneas Cre específicas del SHF, Recapitulamos el desarrollo de los linfáticos ventrales exclusivamente. Esto sugiere que los progenitores del SHF se reclutan en la región mesotelial/sub-mesotelial de la AP. Transplantamos trozos de mesotelio / sub-mesotelio de la AP de donantes fluorescentes a corazones de tipo salvaje a E14.5. El Tejido donante invadió el miocardio del recipiente, formando vasos linfáticos. La exploración de señales moleculares involucradas en la formación de ese nicho mostró que *Raldh2* está regulado a la baja a nivel transcripcional y proteico en las AMCs proximales. Además, la pérdida de señalización del Ácido Retinoico (AR) en las células mesoteliales resultó en vasos linfáticos inmaduros, mientras que un exceso de AR desencadenó una hiper-remodelación linfática.

Estos datos muestran que parte de los linfáticos ventrales se forman mediante el reclutamiento de progenitores de SHF en un nicho vasculogénico especificado en condiciones de bajo niveles de *Raldh2*.

Introduction

1.1 A Brief historical aside

The role and function of the heart have been a subject of debate for more than 0.2000 years as people knew about its existence since ancient times. In the Egyptian, Greek and Roman antiquity, the heart was considered as the seat for emotions, courage, intelligence and memory, hence the expression “learn by heart”. In the IInd century, the Greek physician Galen challenged the theory of Aristotle and other of his ancestors to place the brain as the holder of cognitive functions. Heart anatomy became clearer in the XVIth century as Leonardo da Vinci represented the human heart with unprecedented accuracy (**picture.1**) and the Spanish theologist Miguel Servet discovered pulmonary circulation in 1546. A century later, the English physician William Harvey’s breakthrough taught us about the existence of the blood circulation (*De Motu Cordis* 1628). Surprisingly, the dichotomy heart/brain remained for centuries as it had not been firmly established



Picture 1. Heart and its blood vessels, Leonardo da Vinci 1508

which of these organs was responsible for human emotions. It took the onset of the XIXth century to start understanding that mental functions are organized in different brain regions as postulated by the German neuroanatomist Franz Joseph Gall. The heart is now recognised as a vital blood pumping organ and the debate has definitely closed as the South African surgeon Christiaan Barnard performed the first successful heart transplantation in 1967. Nowadays human hearts are “interchangeable” and death is no more pronounced at the arrest of the heartbeat but when brain activity is no longer detectable. In spite of it all, the heart remains as a symbol of love and some people, like myself, are still compelled to “think with their heart”.

1.2 Heart anatomy and function

The vertebrate heart is the powerful pump which supplies the entire body with blood, oxygen and nutrients. Its role is so vital that it is the first organ to form during development. It starts contracting shortly after its formation as the need for nutrients and waste removal as the embryo grows can no longer be sustained by diffusion. Defects affecting heart formation are responsible for a substantial loss of fetuses and embryos before birth, accounting for 30% of human pregnancies (Bruneau, 2008). In addition, Congenital heart defects (CHDs) are the most common type of birth defects. According to the Centre for Disease Control and prevention, 3% of the population is born with a CHD (Fahed et al., 2013; Parker et al., 2010). CHDs range from simple conditions to more severe life-threatening symptoms requiring specific treatments. The occurrence of CHDs reflects how strict cardiac formation must be orchestrated to produce a heart that remains fully functional throughout lifespan.

The mammalian heart is a highly organized structure which can be divided into a left and a right compartment. Each compartment is itself composed of two adjacent chambers: one atrium and one ventricle (Fig.1). Systemic deoxygenated blood enters the right atrium through the superior and inferior caval veins, reaches the right ventricle and is pumped out to the lungs via the pulmonary artery. On its way out from the lung, the blood which is newly oxygenated, runs through the pulmonary veins to re-enter the heart

via the left atrium. The blood passes to the adjacent left ventricle and is expelled through the ascending aorta to irrigate the body and the heart itself via the coronary arteries. The entrance and exit of blood in each of the four heart chambers is regulated by the opening and closing of specific valves (Fig.1).

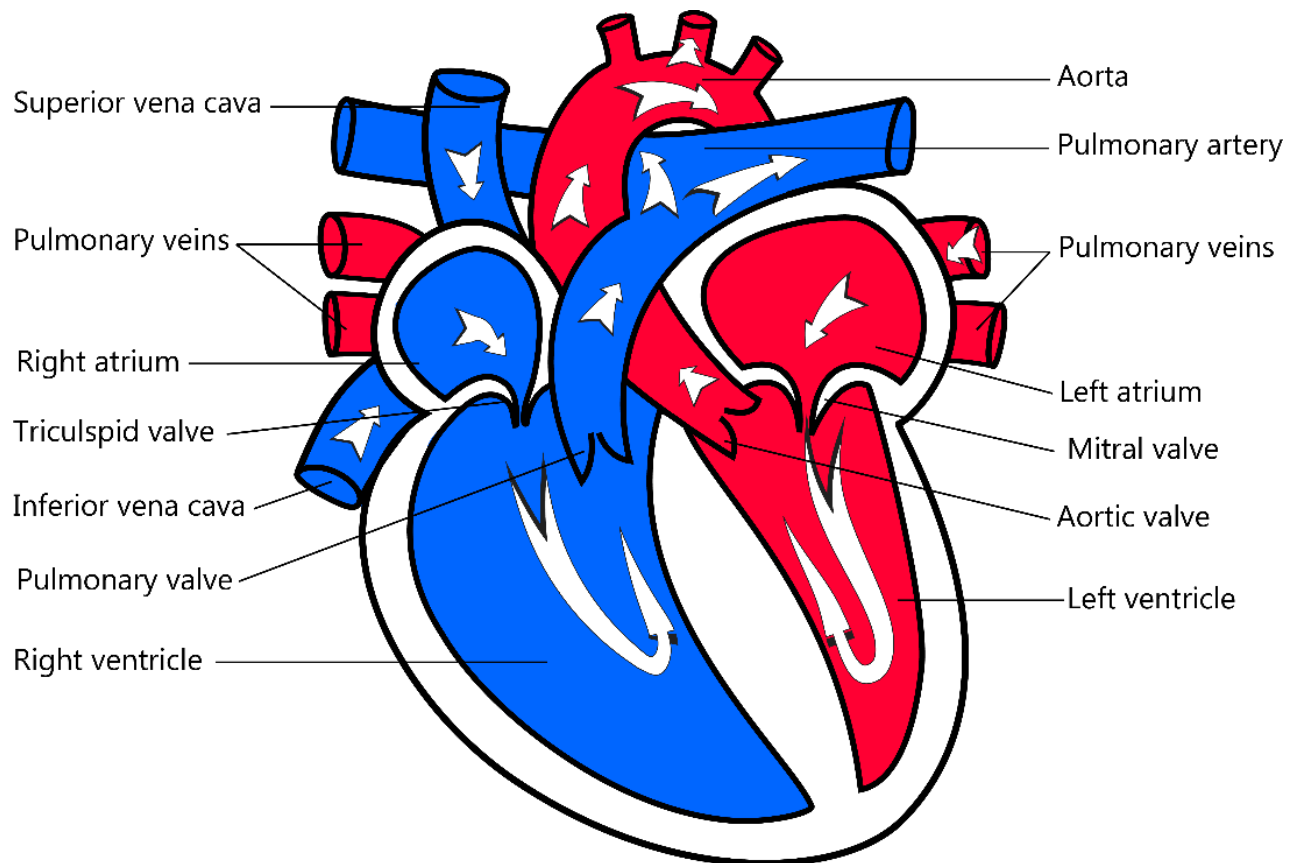


Figure 1. The mature mammalian heart and its blood flow.

The heart is formed of four chambers: the right atrium, the right ventricle, the left ventricle and the left atrium. Systemic deoxygenated blood enters the heart through the caval veins into the right atrium and passes to the right ventricle to exit through the pulmonary trunk. The blood is then oxygenated in the lungs and enters the left ventricle through the pulmonary veins connected to the left atrium. Once in the left ventricle, the blood is pumped out through the aorta and distributed to the body.

The heart chambers are grossly composed of 3 layers from the outside to the inside:

- the epicardium
- the myocardium

-the endocardium.

All layers contain a variety of specialized cell types. The myocardium contains cardiomyocytes, smooth muscle cells/pericytes, fibroblasts, endothelial cells and innate immune cells. Heartbeat depends on the work in concert of contractile cells: the cardiomyocytes. Cardiomyocyte function is coordinated by electrical impulses regulated by cells of the conduction system. Cardiomyocytes virtually occupy the majority of the heart volume but only account for about 50% of all cardiac cells (Banerjee et al., 2007). Fibroblasts are structural cells which secrete extracellular matrix (ECM) proteins to maintain tissue architecture. Endothelial cells are of two types in the heart: cells that cover the lumen of arteries, veins and capillaries and endocardial cells that cover the lumen of the heart. Smooth muscle cells and pericytes are associated to hearts vessels and capillaries, respectively, to regulate changes in vessel pressure. On its external surface, the heart is covered by a monolayer of epicardial cells. The epicardium is mostly composed of mesothelial cells which are pavement like-cells that line serous cavities offering a slippery protecting surface. The epicardium is associated to cell types also present in other organs such as macrophages, nerve fibres, glial cells and lymphatic endothelial cells (LECs).

Cardiac structure is the result of tightly regulated developmental processes. Understanding Cardiogenesis is thus of importance for the aetiology of CHD and for potential stem cell therapies to treat heart failure. From the standpoint of mammalian cardiogenesis, the mouse is the best described model. In addition, heart physiology, anatomy and development are highly conserved between mice and humans (Moon, 2008). We will thus describe cardiogenesis referring to mouse models unless otherwise stated.

1.3 Embryonic heart development

1.3.1 Formation of the four-chambered heart

The heart is the first organ to form shortly after gastrulation (Fig. 2). The first heart progenitors appear at embryonic day E6.5 (E6.5) when epiblast cells ingress through the

primitive streak (PS) to form the lateral plate mesoderm as shown in mouse (Lawson et al., 1991; Tam and Behringer, 1997) as well as chick embryos (Kirby, 2007). As cardiac cells emerge from the PS they start expressing *Mesp1* (Mesoderm Posterior 1), a key regulator of cardiac specification (Saga et al., 1999, 2000; Lescroart et al., 2014). Myocardial specification depends on molecular cues from the hypoblast such as transforming growth factor family β (TGF- β) factors in the chick and from the endoderm in the mouse (Nijmeijer et al., 2009). At E7.5, heart precursors consist of two mesodermal pools of cells on each side of the ventral mid-line. By embryonic day E7.75 these two cardiogenic regions fuse at the mid-line, under the head folds, forming an already beating cardiac crescent (Moorman et al., 2003; Wagner and Siddiqui, 2007). The cardiac crescent expresses markers of cardiovascular commitment such as *Gata4*, *Nkx2.5*, *Hand2*, *Mef2c*, *Tbx20*, *myocardin* (Bondue A. et al., 2008; Bondue A. and Blanpain, 2010). The cardiac crescent is a two-layered structure composed of endocardium in the inside and myocardium in the outside. The heart tube is originally attached to the body wall via the dorsal mesocardium (Abu-Issa and Kirby, 2008; Vincent and Buckingham, 2010). As the heart tube elongates it closes dorsally starting from the caudal to the cranial region by a 'zipping like' process as the dorsal mesocardium breaks down leaving the heart 'hanging' by his poles (Arguello et al. 1975; Moreno-Rodriguez et al. 2006). In parallel, the heart tube undergoes rightward looping so that both poles of the tube are aligned on the anterior-posterior (AP) axis (Buckingham et al., 2005). The pole moving anteriorly becomes the arterial pole while the pole moving posteriorly becomes the venous pole of the heart. The atria and inflow region form at the venous pole of the heart while the Outflow tract (OFT) is formed at the arterial pole of the heart. At E10,5 the future atria are still connected, so are both ventricles. The connection of each atrium to its respective ventricle is made by the atrioventricular canal (AVC). By E14,5 the organization plan of the heart is established:

- the four cardiac chambers are separated by interatrial and interventricular septa.
 - the pulmonary and caval veins take root in the inflow region of the heart.
 - the Pulmonary artery and aorta take root in the the OFT region.
- the connections between chambers, veins and arteries are delimited by valves for the regulation of blood flow.

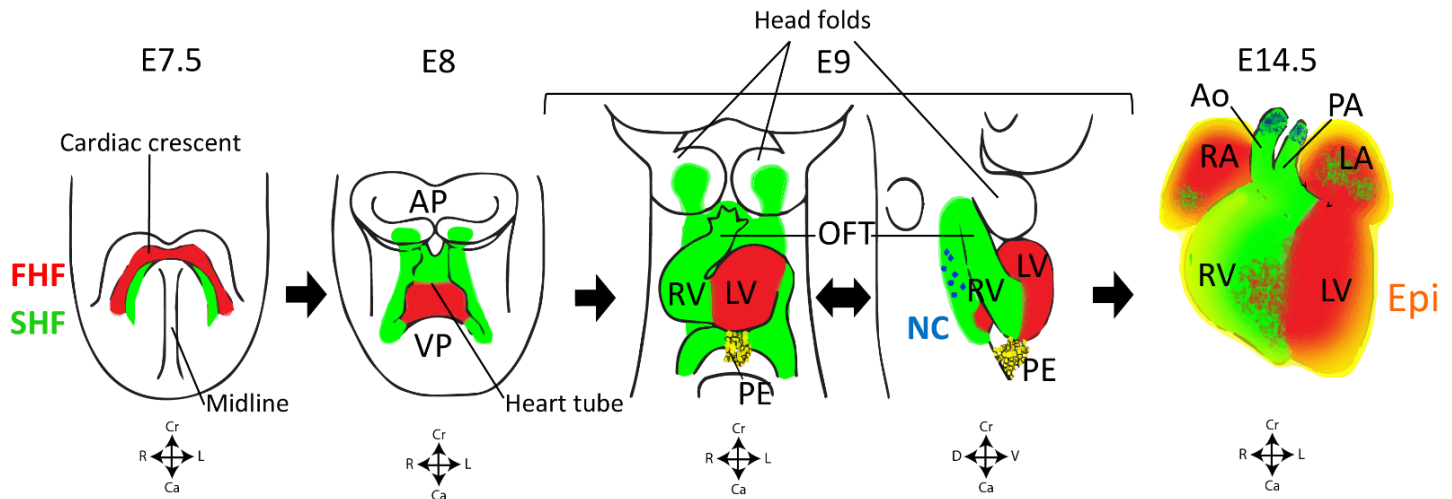


Figure 2. Overview of early mouse heart development.

Cardiac mesodermal cells are located in the cardiac crescent under the head folds at E7.5. At that stage two cardiac fields are distinguishable: the first heart field (FHF in red) and second heart field (SHF in green). At E8.5 the heart tube rapidly elongates undergoing rightward looping. At E10.5 different cardiac regions are apparent: the left and right atria (LA and RA), the left and right ventricles (LV and RV) and the outflow tract (OFT). Extracardiac heart progenitors are present in the proepicardium (PE) and Neural crest (NC) at E9. The cardiac anatomical plan is established at E14.5 as the four heart chambers are separated. The heart pumps out blood through the aorta (Ao) and pulmonary artery (PA). Cr: Cranial; Ca: Caudal; Epi: Epicardium; R: right; L: left. Cartoon adapted from Stéphane D. Vincent and Margaret E. Buckingham, 2010).

According to the segmental hypothesis, the primary heart tube was thought to contain progenitors of all cardiac chambers, organized as independent segments along the arterial-venous axis (Davis 1927; Srivastava & Olson 2000). This segmental model of myocardial cell regionalization proposes that each segment gives rise to a specific cardiac chamber (reviewed in Buckingham M. et al., 2005; Van Den Berg and Moorman, 2009)). The ballooning model now shows that the early heart tube is mostly fated to become the left ventricle and provides a scaffold for the addition of further cell lineages. According to this model, both ventricular chambers balloon out from the outer curvature of the looping heart tube (Moorman et al., 2003).

In the following chapter we will describe the lineages that have been identified to contribute to the myocytic and non-myocytic cells of the heart. They are mainly of three

sorts: the cardiogenic mesoderm cells (CMC), the proepicardium (PE), and cardiac neural crest cells (CNCCs).

1.3.2 Contribution of cardiac lineages during development

The Second Heart Field

The concept that all prospective cardiac chambers are not present in the heart tube was introduced by the work of Viragh and Challice in 1973 as they described cells undergoing an epithelial to myocardial transition at the border between the heart tube and the adjacent pharyngeal mesoderm (Viragh and Challice, 1973). Later on, De la Cruz and colleagues demonstrated that when disconnecting the cephalic end of chick embryonic hearts from the body wall, they failed to further elongate (Argüello et al., 1975). In another series of experiments, they showed that iron particles placed in the cephalic end of the heart tube reached the ventricular septum (separation between both ventricles) at later stages (de la Cruz et al., 1977). It took two more decades until three independent teams identified an external source of cardiac progenitors in the mesoderm. (Kelly et al., 2001; Mjaatvedt et al., 2001; Waldo et al., 2001; reviewed in Kelly, 2012). These progenitors lie medially and posteriorly to the heart tube in the pharyngeal mesoderm (Fig. 2). Because such cells are added secondarily, they are termed Second Heart Field (SHF) while cells of the cardiac crescent are referred to as the First Heart Field (FHF) (Kelly, 2012; Spater et al., 2013). Lineage tracing experiments using the *Islet1-Cre* line (Cai C.L. *et al.*, 2003) as well as retrospective clonal analysis with the *nlaacZ* reporter gene (Meilhac et al., 2004) showed that SHF cells express the LIM homeodomain transcription factor *Islet1* (*isl1*) and are added at both the arterial and venous pole of the primary heart tube. *Isl1* expression is crucial for SHF contribution as *isl1* mutants form a linear heart tube that fails to loop and elongate (Cai C.L. *et al.*, 2003). Sigolène Meilhac and colleagues used rare random cell labelling to perform unbiased cell fate analysis at E8.5 (Meilhac et al., 2003). Clones were found restricted to the left ventricle / inflow region or contributing to the outflow or outflow / inflow regions. The first class of clones corresponds to FHF contribution and the second class to SHF contribution as defined by *Isl1* expression. Altogether these experiments show that the FHF mainly gives rise to the left ventricle and atria and shows early

expression of myosin light chain 2 Mlc2. The SHF contributes to the right ventricle, Outflow tract (OFT), inflow region (venous pole) and part of the atria and expresses *isl1* (Fig. 2). Further studies identified the SHF as a vast pool of progenitors, itself organised into subdomains.

The experiments of embryo labelling in culture (Kelly et al., 2001; de la Cruz et al., 1977; Waldo et al., 2005), documented previously, show that SHF progenitors are patterned along the antero-posterior axis since the site of labelling in the SHF accurately predicts the part of the heart that is labelled in the end. The SHF can indeed be divided in subdomains. The Anterior heart field (AHF) contributes to the right ventricle and OFT (Kelly R.G. et al., 2001; Waldo et al., 2001; Zaffran S. et al., 2004) and expresses a variety of specific transcription factors such as *Fgf8*, *Fgf10*, *Tbx1*, *six2* (Zhou et al., 2017) and a *Mef2c* specific enhancer. In contrast, the pSHF predominantly contributes to the venous pole and more particularly to atrial and atrioventricular septa as well as to part of the OFT (Galli et al., 2008; Bertrand et al., 2011; Rana et al., 2014). The pSHF expresses Hox genes such as *Hoxb1* (Bertrand et al., 2011; Roux et al., 2015) and other genes also present in the FHF like *Tbx5* and *Osr1* (Xie et al., 2012; Devine et al., 2014). The most posterior portion of the SHF mesenchyme is distinct because it does not express the transcription factors *Nkx2.5*. Instead, these cells express *Tbx18* and will be giving rise to the myocardium of the caval veins (Christoffels et al., 2006).

T-box-containing transcription 1 (*Tbx1*) is a major regulator of SHF deployment. This gene is the major candidate in 22q11 deletion syndrome or DiGeorge syndrome characterised by craniofacial and cardiac defects (Zhang Z. et al., 2006) (Théveniau-Ruissy et al., 2008). Even though *Tbx1* is a marker of AHF, *Tbx1* mutation results in abnormal development of AHF derivatives as well as pSHF derivatives. *Tbx1* null embryos result in short and narrow embryonic OFT and present a persistent truncus arteriosus (absence of septation between the Aorta and Pulmonary artery) (Jerome and Papaioannou, 2001; Théveniau-Ruissy et al., 2008; Rana et al., 2014) due to the deregulation in the AHF. Defects accountable to a deregulation of pSHF progenitors also occur in *Tbx1* null embryos which present atrioventricular septal defects and defects of the dorsal mesenchymal protrusion (DMP) (Rana et al., 2014). Moreover, *Hoxb1*-expressing progenitor cells fail to contribute to the shortened OFT in *Tbx1*^{-/-} embryos.

Fate mapping of Tbx1 expressing cells revealed contribution to the proximal OFT and myocardium at the base of the pulmonary trunk (Brown et al., 2004; Huynh et al., 2007) consistent with the heterogeneity of myocardial progenitors in the arterial pole.

SHF cellular contribution

The pharyngeal mesoderm is a source of a variety of cell types as it is capable of giving rise to cardiac cells as well as head muscle cells in the embryo (Lescroart et al., 2010). In the heart, the SHF not only provides cardiomyocytes (Kelly R.G. et al., 2001; Waldo et al., 2001; Zaffran S. et al., 2004) but also non-myocytic cells. Ablation experiments in chicks and lineage tracing experiments in mice showed that the pharyngeal mesoderm is the source of smooth muscle cells at the base of the great arteries (Saga et al., 2000; Sun et al., 2007; Waldo et al., 2005). Smooth muscle contribution follows myocardial addition from the SHF between stages HH14 and 18 in the chick (Waldo et al., 2005b; Ward et al., 2005). Endothelial cells are also added at the arterial pole deriving from SHF mesoderm of posterior pharyngeal arches (3,4,6) (Wang et al., 2017).

SHF contribution and specification are spatiotemporal processes in which SHF cells are organised along the antero-posterior axis and are deployed at the hearts poles giving rise to different components. Isl1 expressing embryonic stem cells (ES) placed in culture behave as multipotent progenitors since they result in clonally related clusters of cardiomyocytes, endothelial and smooth muscle cells (Moretti et al., 2006). Similarly human foetal Isl1+ cells (Laugwitz et al., 2005) give rise to the same cell types (Bu et al., 2009). SHF cells are also responsible for large parts of the conduction system (Miquerol et al., 2013) and coronary arteries (Théveniau-Ruissy et al., 2008; Chen et al., 2014; Ivins et al., 2015). However, it remains unclear whether all SHF progenitors are multipotent and whether multipotency is a property of SHF cells *in vivo*.

We will now discuss other heart lineages essential for coronary vasculature formation.

The Proepicardium, epicardium and Epicardial derived cells (EPDCs)

The proepicardial organ (PEO) is a transitory mesodermal structure that forms posterior to the venous pole in the dorsal pericardial wall (Männer, 1992) (Fig. 2). Around E9.5, cells from the PEO migrate onto the looping heart and encapsulate the myocardium to form the epicardium. The epicardium becomes the outermost layer of the heart and is composed of mesothelial cells. Around E11, a subpopulation of epicardial cells undergoes an epithelial to mesenchymal transition (EMT) regulated by Snail and slug transcription factors (von Gise and Pu, 2012) resulting in epicardial derived cells (EPDCs). EPDCs invade the subepicardial and myocardial space to generate a variety of cell types (Wessels and Perez-Pomares, 2004, Carmona et al., 2010). EPDCs express the transcription factors *Wt1*, *Tbx18*, *Tcf21*, *scx* and *Sema3D*, as well as the retinoic acid (RA) synthesising enzyme *Raldh2*.

Retroviral cell labelling in chicks as well as Cre-based lineage tracing experiments in mice showed that EPDCs contribute to the coronary blood vasculature and to cardiac fibroblasts (Mikawa and Fischman, 1992; Mikawa and Gourdie, 1996; Pérez-Pomares et al., 2002; Guadix et al., 2006; Katz et al., 2012). Besides, EPDCs populate the atrioventricular cushions giving rise to the future tricuspid and mitral valves. The *annulus fibrosus* also originates from EPDCs (Dettman et al., 1998, Männer, 1999, Wessels and Perez-Pomares, 2004). Contribution of EPDCs to cardiomyocytes has been described but is still controversial since *wt1cre* and *tbx18cre*, the lines used to trace the fate of epicardial cells, produce recombination of the cardiomyocyte lineage independently of that in the epicardium (Zhou et al., 2008a, Cai et al., 2008, Rudat and Kispert, 2012; Villa del Campo et al., 2016). Katz and colleagues however, reported a modest contribution of the epicardium to the myocardial lineage using Semaphorin 3D (*Sema3D*) and Scleraxis (*Scx*) as epicardial cre drivers.

The epicardium extends until the base of the OFT where the pulmonary artery and aorta take root. Both vessels are covered by a sheet of mesothelial cells contiguous with the epicardium. Nevertheless, arterial mesothelial cells are not of PE origin (Männer, 2013; Pérez-Pomares et al., 2003). They have been described instead as derivatives of the cephalic pericardium. Their exact origin, function and fate however is still unclear.

In addition to cellular contribution, the epicardium provides trophic factors to the underlying myocardium, including retinoic acid (RA), fibroblast growth factors (FGFs) and signals arising from the extracellular matrix (ECM) (Niederreither et al., 1999; Chen et al., 2002; Merki et al., 2005) . Such signals promote the maturation of the myocardium and maintain its mitotic activity. Moreover, studies in adult mice, have shown its activation in response to organ damage and during regeneration upon injury. Indeed, adult epicardial cells resume embryonic programs to create new vasculature (Smart et al., 2007) and cardiomyocytes (Smart et al., 2011) after myocardial infarction.

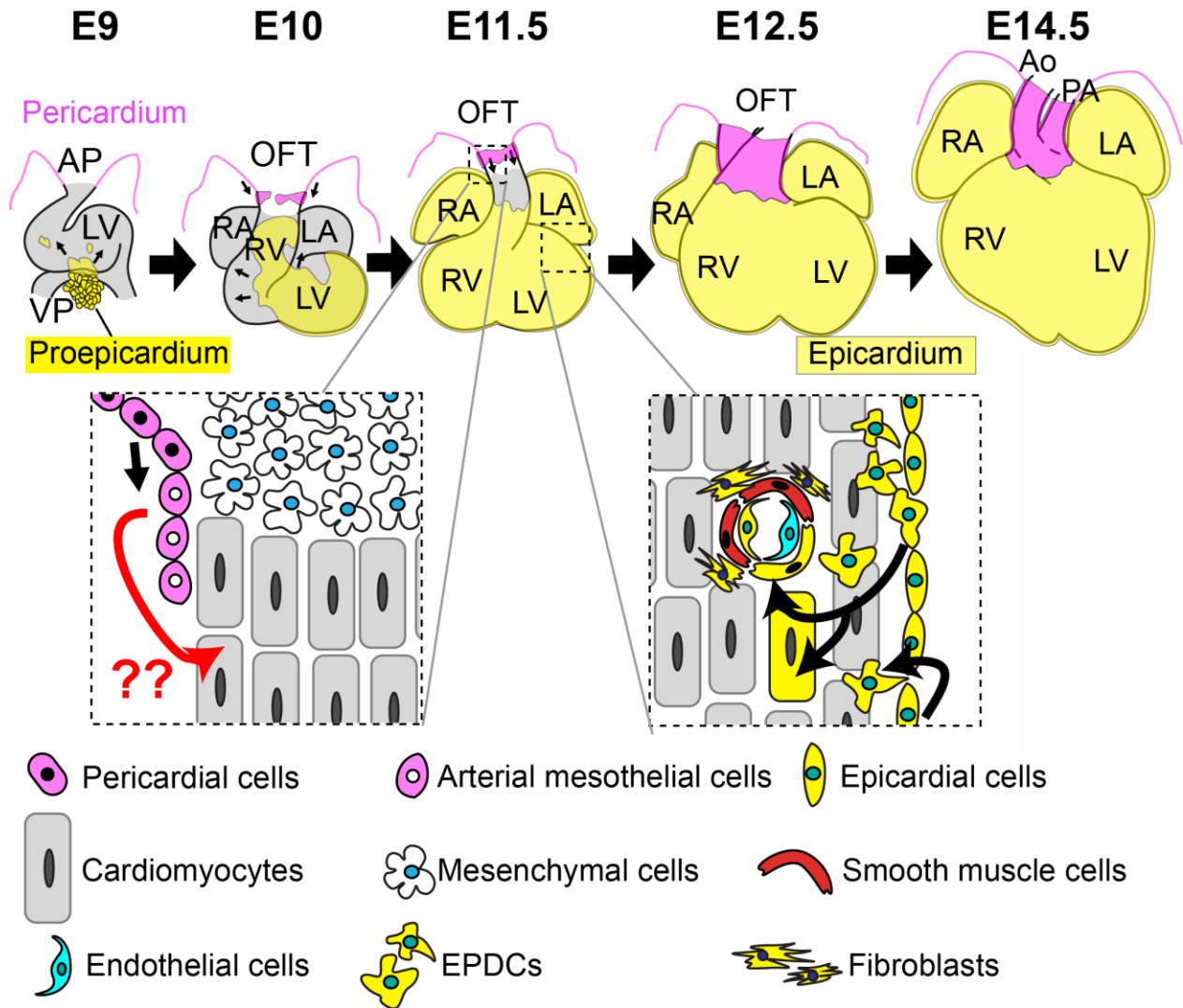


Figure 3. Formation of the mesothelium of the heart and great arteries

Around E9 cells from the proepicardium (yellow) start spreading over the myocardium (grey). At E10, cells of the cephalic pericardium (purple) give rise to arterial mesothelial cells (AMCs) crawling down the OFT's surface. By E11.5, the epicardium is covering the majority of the heart to the exception of the mesenchymal portion of the OFT. Epicardial cells go through EMT producing EPDCs that invade the myocardium (right caged box). These cells give rise to the fibroblasts, smooth muscle and endothelial cells of the coronary vessels as well as few cardiomyocytes (the epicardium and its derivatives is represented in yellow). In parallel, the arterial mesothelium follows its course invading the mesenchymal surface of the OFT (left caged box). It is not known whether arterial mesothelial cells contribute to the heart or arteries. By E12.5 the heart and OFT are entirely encapsulated by both mesothelia with no overlap. At E14.5 the epicardium and AMCs share a border at the frontier between the myocardium and the great arteries. AP: Arterial pole, VP: Venous pole, OFT: Outflow tract, RA: Right atrium, LA: Left atrium, RV: Right ventricle, LV: Left ventricle, Ao: Aorta, PA: Pulmonary artery.

The cardiac Neural crest cells (NCs)

The neural crest is a population of multipotent progenitors arising from the dorsal neural tube at mid-gestation between the mid-diencephalon and the posterior border of somite 3 (Keyte and Hutson, 2012). The properties of cardiac neural crest cells (CNCCs) were discovered by Margaret Kirby and colleagues in 1983. Using quail-chick chimeras and ablation experiments in avian embryos, they found that CNCCs delaminate and migrate towards the heart, invading the mesodermal core of the pharyngeal arches 3, 4, and 6 (Kirby et al., 1983) (Fig. 3). In mice, cre-lox based strategies were later employed to trace the fate of neural crest cells using Wnt1-cre, Pax3-cre, P0-cre, and PlexinA2-cre (Brown et al., 2001; Jiang et al., 2000; Lee et al., 1997).

CNCCs contribute to the smooth muscle of the pharyngeal arch arteries at the arterial pole of the heart around E10.5 in mice (Fig. 3) (Bergwerff et al., 1998). Neural crest cells from the arches migrate to the arterial pole of the heart and induce outflow tract remodelling around E12.5. During OFT remodelling, extracellular matrix (ECM) components are secreted into the space between the endothelial and myocardial layers forming the so called “cardiac jelly”. The cardiac jelly is then colonized by mesenchymal cells derived by EMT from the OFT endothelium and the neural crest to form the endocardial cushions, bulks of the future semilunar valve leaflets. (Eisenberg and Markwald, 1995; Markwald et al., 1981; Sugishita et al., 2004). The swelling of these cushions is thought to promote the fusion of endothelial cells at the centre of the OFT thereby giving rise to the aortopulmonary septum (reviewed by Navarro-Aragall et al., 2018). The aortopulmonary septum divides the truncus arteriosus (common arterial outflow) into the base of the pulmonary artery and aorta (Waldo et al., 1998, 1999). SHF-derived SMCs and myocardium from the OFT wall populate the emerging septum to complete septation through myocardialisation, a process by which the septum becomes muscular (Kelly et al., 2001; van den Hoff et al., 1999). The aortopulmonary septum later attaches to the IVS sealing the base of the aorta to the left ventricle and the base of the pulmonary artery to the right ventricle. CNCCs further contribute to heart development providing a variety of cell types. Indeed, the distal smooth muscle layer of the great arteries (Fig. 2) as well as the smooth muscle layer of the coronary arteries at the base of

the heart and in the IVS are of neural crest origin (Arima et al., 2012). Moreover, CNCCs give rise to the entire parasympathetic innervation of the heart (Kirby and Stewart, 1983).

Multiple signalling pathways are implicated in CNCCs migration and specification, the major players being BMP, Wnt, FGF-8 and semaphorin signalling. In the absence of neural crest, outflow tract septation is compromised leading to persistent truncus arteriosus (PTA) or common arterial trunk (CAT) (Hutson and Kirby, 2007). This condition causes the mixing of oxygenated and deoxygenated blood which is lethal, unless surgically corrected shortly after birth. CNCCs ablation also affects SHF's addition leading to a shortened OFT and heart looping defects. This phenotype is mostly due to altered FGF-8 levels, which keeps SHF progenitors in a proliferative state that impedes their further migration and differentiation (Waldo et al. 2005; Ilagan et al. 2006; Scholl and Kirby 2009).

We have summarised the origin of the myocytic as well as non-myocytic cells of the heart and their early origin. However, cardiac cells added to the heart during late development can also have a crucial role. It is the case of the embryonic lymphatic system which have received little attention as compared to the blood vessels. We will thus discuss the formation, function and origin of the lymphatic system in the next chapter.

1.4.1 The cardiac lymphatics, an important component of the heart for a long time in oblivion

The lymphatic vasculature: development and function

Lymphatic vessels are crucial for organ homeostasis through the transportation of immune cells, lipids and toxins and drainage of interstitial fluids (Harvey and Oliver, 2004). The origin of the lymphatic vasculature is yet the center of a century-old debate.

Performing ink injection experiments in pig embryos, Florence Sabin described a centrifugal model in which endothelial cells bud from the cardinal veins to form the entire lymphatic vasculature (Sabin, 1902). According to this model, the entire peripheral lymphatic vasculature develops by endothelial sprouting and remodeling of primarily formed lymph sacs (angiogenesis). A few years later, Huntington and McClure reported a

centripetal theory in which lymph primordia derive de novo from the mesenchyme independently of veins (vasculogenesis) (Huntington and McClure, 1910). The reconversion of blood circulating cells to a lymphatic fate has been proposed more recently (Maruyama et al., 2005; Sebzda et al., 2006). In agreement with Sabin's model, veins are now commonly accepted as the main source for lymphatic vessels in zebrafish (Küchler et al., 2006; Okuda et al., 2012; Yaniv et al., 2006) and mouse models (Srinivasan et al., 2007; Yang et al., 2012).

Murine LECs specify during mid-gestation in the wall of the anterior cardinal veins. At day E9.75, a subpopulation of venous endothelial cells acquires a lymphatic progenitor identity as the result of COUP-TFII, Sox18 and Prox1 transcription factor expression (François et al., 2008; Lee et al., 2009; Sabin, 1902; Srinivasan et al., 2007; Wigle et al., 2002). (Fig. 3). These cells delaminate from the veins to form lymphatic primordia or lymph sacs. The lymphatic vasculature originates from the further sprouting of the cardinal veins, lymph sacs and inter-somitic vessels (ISVs) (François et al., 2012; Yang et al., 2012) (Fig. 3).

Prospero-related transcription factor Prox1 has been identified as the key determinant of lymphatic cell fate (Hong et al., 2002; Johnson et al., 2008). In Prox1-null embryos, sprouting from the veins is still observed but vascular sprouts present blood rather than lymphatic endothelial characteristics (Wigle and Oliver, 1999; Wigle et al., 2002). As a result, Prox1-deficient mice are devoid of lymphatic vasculature (Wigle and Oliver, 1999) reflecting a failure in lymphatic specification (Wigle et al., 2002). Reciprocally, *Prox1* overexpression is sufficient to direct endothelial cells (ECs) towards a lymphatic fate both *in vitro* (Hong et al., 2002) and *in vivo* (Kim et al., 2010).

The cardinal veins are certainly the main source of lymphatic vasculature however, various studies support an alternative mesenchymal source for lymphatic endothelial cells (LECs) (Buttler et al., 2006; Ny et al., 2005; Papoutsis et al., 2001; Schneider et al., 1999; Wilting et al., 2000a, 2006) (Fig.3). Moreover LECs of different organs like the heart (Klotz et al., 2015), the skin (Martinez-corrall et al., 2015; Pichol-Thieuvend et al., 2018) and the mesentery (Stanczuk et al., 2015) were shown to have, at least in part, alternative developmental origins. We are only starting to understand the molecular, developmental

and functional differences endowing lymphatic vessels in different organs. Little is known about organ lymphatic patterning and its origin as lymphatic vessels have for a long time been seen as passive conduits returning tissue fluids to the blood circulation. We now know that organ lymphatics play major physiological and pathophysiological tissue-specific roles. In particular, cardiac lymphatic disturbance leads to heart defects such as endocardial edema, cardiac valve deformation, coronary arterial injury, conduction alterations, fibrosis, and poor heart performance in animal and human heart studies.(Ludwig et al., 1997; Wang et al., 2009) (Miller et al., 1964; Kline et al., 1964; Xu et al., 2007). Reciprocally, lymphangiogenesis can improve heart function after injury (Taira et al., 1990; Klotz et al., 2015). Getting insights into cardiac lymphatics and their origin has thus gained importance in the etiology of cardiac diseases and the field of organ repair.

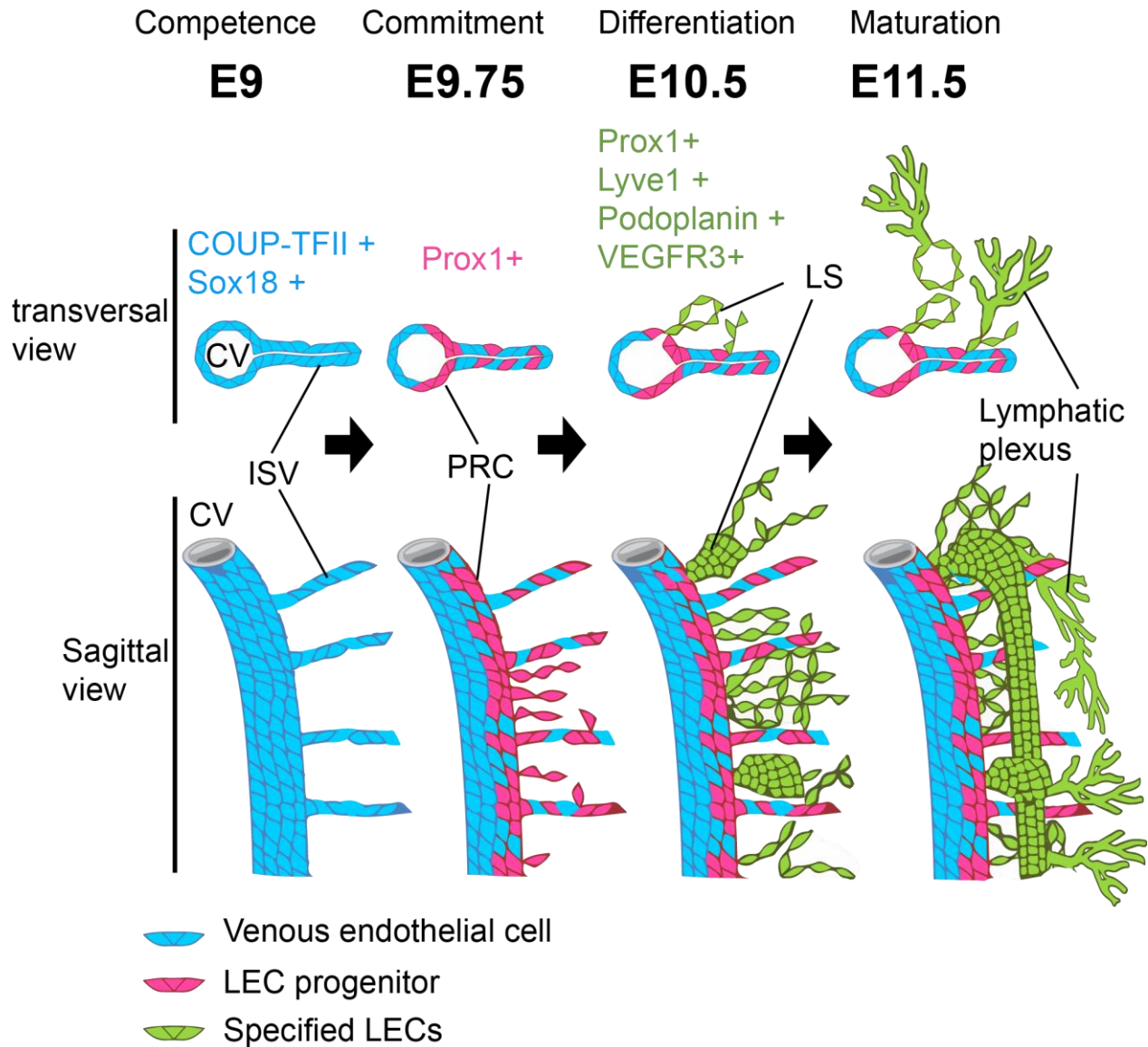


Figure 4. Specification and development of the lymphatic system.

Around E9 the expression of Coup-TFII, a venous identity marker, triggers the expression of Sox18 in a subset of cardinal vein endothelial cells (pink). Sox18 directly activates Prox1 expression forming “prox1-rich clusters” (PRCs) distributed along the cardinal veins. Lymph sacs, originate from the PRCs between E10-E11.5. Prox1 expression also triggers the formation of lymphatic structures in the inter-somitic vessels (ISVs). The lymphatic vasculature (in green) forms by sprouting from the PRCs, the lymph sacs and the ISVs. Sprouting, proliferation and migration of LECs away from the cardinal veins depends on vascular endothelial growth factor receptor 3 (Vegfr-3) expression.

(Cartoon adapted from Ying Yang et al. 2012).

The cardiac lymphatic system

Cardiac lymphatics were initially described by Olaus Rüdbeck in 1653 and further studied two centuries later by the anatomist Constant Sappey followed by Lewis R. Shore at the beginning of the 20th century. Studies in monkeys, rodents, and birds showed that cardiac lymphatic vasculature development succeeds that of the coronary blood vessels (Flaht et al., 2012; Wilting et al., 2000b). In mammals, the flow of lymph through the cardiac lymphatic vessels depends on heart contraction (Alexander et al., 1998; Levick, 1990; Mehlhorn et al., 1995). In the adult, lymph flows throughout three plexuses located in the sub-endocardium, myocardium, and sub-epicardium (Ruszynak et al., 1969). These plexuses feed into larger lymphatic vessels that follow the path of the main coronary arteries. The lymph returns to the venous system at the junction with the thoracic duct and subclavian vein. Development of the murine cardiac lymphatic plexus is limited to the subepicardial area before birth. Postnatally, this plexus reaches the myocardium and sub-endocardium following a base-to-apex gradient. Cardiac LECs as well as systemic LECs are characterised by the expression of Prox-1, Lyve-1, VEGFR3, Podoplanin, VEGFR2, CD144, CD31 and Tie2 (Flaht-Zabost et al., 2014; Karunamuni et al., 2010). VEGFR3 has been shown to be crucial for cardiac lymphatic specification even though it is also expressed in BECs until E14.5 (Hägerling et al., 2013; Kaipainen et al., 1995). Mice expressing a soluble VEGFR3 protein were used to trap the VEGFR3 ligands, VEGFC / VEGFD, inhibiting the VEGFR3 pathway. Transgenic mice developed lymphatic hypoplasia in many organs including the heart and presented a regression of already existing lymphatic vessels (Mäkinen et al., 2001). As a consequence, mice develop severe prenatal and postnatal oedema, including pericardial fluid accumulation. Another set of experiments knocking out VEGFC resulted in the blockage of lymph sac formation, reflecting the role of VEGFR3 signalling in LEC sprouting from the cardinal veins (Kaipainen et al., 1995; Karkkainen et al., 2004).

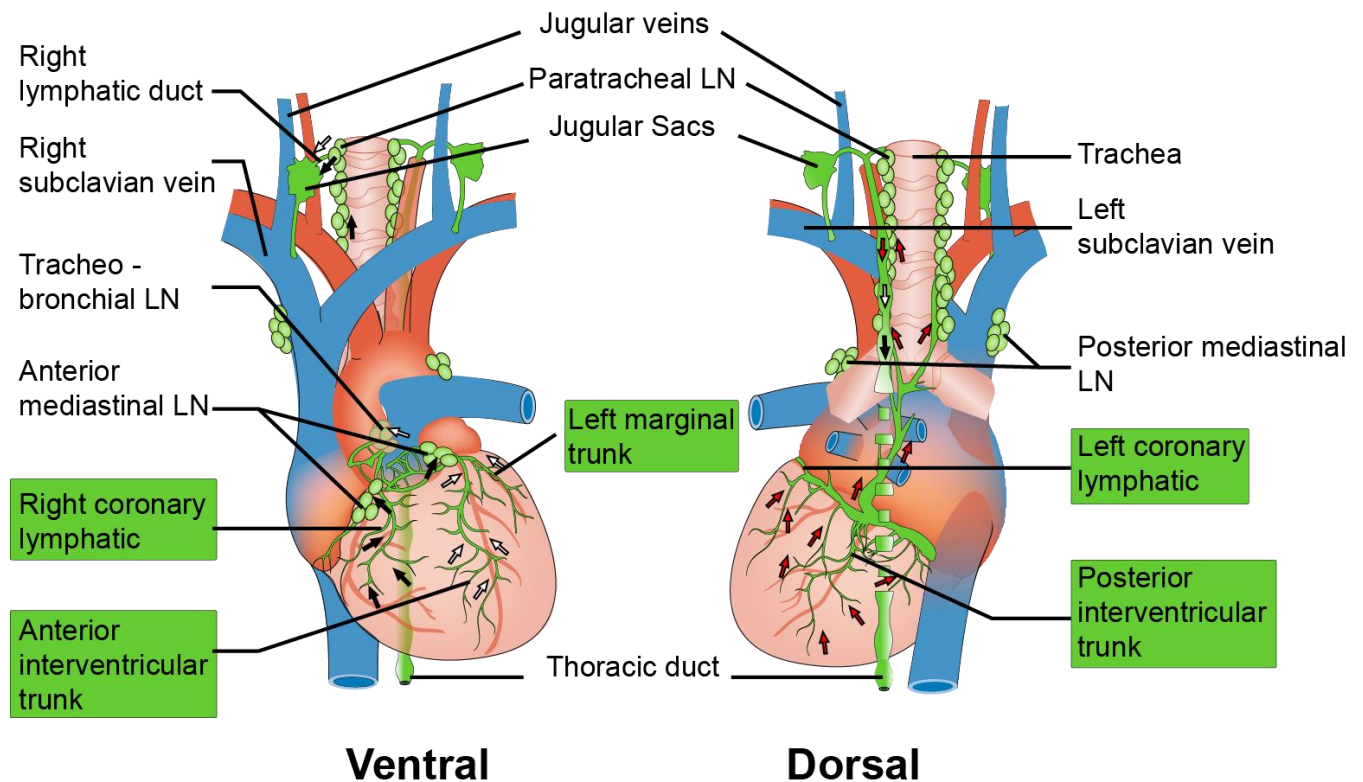


Figure 5. Prenatal cardiac lymphatic system organisation in mammals.

In the mammalian heart, three plexuses have been identified: the right coronary lymphatic follows the path of the right coronary artery, runs upwards to the right side of the pulmonary trunk, enters the mediastinal lymph node (LN), continues superiorly through the paratracheal LNs and drain into the right lymph sac (black arrows). The anterior interventricular and left marginal trunks originate in the left ventricle, follow the path of the left coronary artery, enter the tracheobronchial LN and drains into the right jugular lymph sac (white arrows). Lymph from the posterior interventricular trunk runs along the coronary sinus in the atrioventricular sulcus of the dorsal aspect of the heart and reaches the paratracheal lymph nodes (red arrows). All efferent extra-cardiac collectors finish their path in the thoracic duct. All lymphatic key players are represented in green. LN: Lymph node. (Cartoon adapted from E. Brakenhielm and K. Alitalo ,2018).

Direct connections of the developing cardiac lymphatics with the jugular lymphatic sac (JLS) were noted by Kampmeier in 1928, arguing for a venous origin of cardiac LECs. Recent work by Klotz and colleagues showed that most of the lymphatic vasculature in the heart is of venous origin using a Tie2-Cre transgene (Klotz et al., 2015). However, the group observed incomplete recombination of cardiac LECs by Tie2-Cre recombination,

suggesting that not all cardiac lymphatics are of venous origin. They reported instead the possible origin of cardiac LECs from the Yolk Sac (YS) haemogenic endothelium using fate mapping of $\text{Pdgfr}\beta$ + progenitors. However, Ulvmar and colleagues later demonstrated that $\text{Pdgfr}\beta$ -Cre transgene cannot be used to trace non-venous progenitors as it recombines part of the cardinal vein and jugular lymph sacs (Ulvmar et al., 2016). These results indicate substantial heterogeneity of cardiac lymphatic cells and highlights the limitations in determining the origins and mechanisms of lymphatic vasculature development. In rodent and avian hearts, lymphatic vessel formation has been suggested to originate from Prox-1-positive cells/strands migrating along the great arteries (Flaht et al., 2012; Karunamuni et al., 2010; Wilting et al., 2007), long after the onset of coronary vessel formation. More generally, these data illustrate the limitations of using constitutive Cre lines in lineage tracing experiments, and the need of alternative methods describe the origin of cardiac lymphatic vessels. As a result, understanding the mechanisms and origins of the cardiac lymphatic system demands further analysis.

1.4.1 The role of Retinoic signalling in the four chambered-heart

The effects of Retinoic acid (RA), the active metabolite of vitamin A, in cardiac development have been mostly studied in early embryos since RA signalling is crucial for SHF deployment and posterior domain delimitation (Ryckebusch et al., 2008). In the epicardium, RA signalling regulates myocardial proliferation (Chen TH et al., 2002; Stuckmann et al., 2003). RA signalling in the epicardium depends on the retinaldehyde dehydrogenase (*Raldh2*) enzyme responsible for RA synthesis. *Raldh2* is highly expressed in the epicardium but not in the myocardium (Moss et al., 1998) since the mesothelial gene *Wt1* activates its expression (Guadix et al., 2011). *Raldh2*^{-/-} mutant hearts present reduced myocardial density (Lin et al., 2010) and a downregulation of Fgf signalling, important for myocardial growth. In addition, mutation of the retinoid X receptor RXR, affects epicardial EMT thus compromising coronary artery development (Lin et al., 2010). Wang and colleagues found that pharmacological inhibition of RA synthesis led to myocardial thinning and aberrant coronary vessel formation/ remodelling. Interestingly,

excessive RA levels in mice deficient for the retinaldehyde reductase DHRS3 also resulted in altered coronary vessel morphology and reduction in coronary density and heart coverage (Wang et al., 2018a).

The role of RA on cardiac lymphatic development has not been investigated yet. However, a role for RA in lymphangiogenesis has been suggested by studies showing that exposing developing embryos to excessive doses of RA increased the number of Prox1-positive LEC precursor cells in mouse and *Xenopus* embryos (Marino et al., 2011). Moreover, RA has been shown to promote lymphatic vascular regeneration in a mouse model of lymphedema (Choi et al., 2012). Interestingly, endothelial cells of the cardinal vein exhibit asymmetric RA levels. The region of LEC progenitor specification exhibits low levels of RA as compared to the ventral side of the cardinal vein (Bowles et al., 2014). Consistently the dorsal portion of the cardinal veins (Lymphatic specification territory) expresses the RA-degrading enzyme Cyp26 while the ventral portion expresses Raldh2. In addition, excessive RA levels in *Cyp26b1*^{-/-} mutants result in enlarged lymph sacs. Conversely, the inhibition of RA signalling in *Cyp26b1* gain of function showed alteration in lymph sac formation. These data, are calling for the investigation of RA role in cardiac lymphangiogenesis since they suggest that low RA levels are necessary for lymphatic progenitor specification, while higher levels would allow lymphatic sprouting and expansion.

Objectives

The doctoral thesis aimed at describing the lineage tree of the heart during development. A broad analysis of heart lineages taking into account all cardiac lineages had never been performed before. Moreover, it was not clear how cardiac cell types relate to each other and if cardiac lineages are multipotent at the heart tube stage. At the light of recent studies about the SHF as a potential multipotent source of cardiac progenitors as well as compelling evidence for a heterogeneous origin of cardiac lymphatic endothelial cells the main objectives of this study were as follow:

- Generating a bank of clones for the identification of heart lineages.
- Explore the differences between epicardial clones and arterial mesothelial clones in terms of contribution and origin.
- Check if all the vascular cells of the great arteries derive from multipotent progenitors in the pharyngeal mesoderm.
- Investigate the dynamics of lymphatic formation through the study of cardiac lymphatic clones.
- Confirm or refute hypotheses, based on random single cell labelling, with the use of tissue specific -Cre lines.

Results

1. Random retrospective clonal analysis successfully targets heart progenitors

We first wanted to understand the variety and potential of cardiac progenitors, at the heart tube stage. To target all cardiac progenitors in an unbiased manner, we employed random single cell labelling. We used transgenic mice carrying a tamoxifen inducible Cre recombinase (Polr2a-CreERT2 named RERT) as well as two reporters (Rosa26R-LacZ and Rosa26R-EYFP) (Fig. 6A). All transgenes were driven by ubiquitous promoters so that every cell of the embryo is susceptible to recombine and express one of the reporters. Tamoxifen was administered to mice at E8.5 to trigger permanent reporter expression in few embryonic cells and their progeny. Embryos were harvested at E14.5 when the organization plan of the heart is established and heart lineages are advanced in differentiation. Since Cre-mediated recombination is tamoxifen dose-dependent we first titrated the tamoxifen dose necessary to label single cell progenitors at clonal density. The ideal dose should be high enough to trigger the recombination of various cells but low enough for their progeny not to overlap during embryonic tissue growth.

We initially administered 0.15mg of tamoxifen to pregnant mice. We were able to successfully target heart progenitors since YFP+ (brown) or LacZ+ (blue) cells could be recovered in the heart of various embryos at E14.5 (Fig. 6B-D). However, no YFP/ LacZ double positive cells were ever found. This shows independent recombination of the YFP and LacZ reporters. Moreover, recombined cells were mostly found as single-reporter coherent cell clusters in the heart, indicating that we generated a large proportion of clonal cell groups (Fig. 6E-E’’).

Recombination is achieved at clonal density when a cluster of labelled cells can be considered as clonal with high confidence. We thus considered clusters of labelled cells (as isolated coherent group of cells) and assessed whether they were clonal (Fig. 6E,E’’) according to their colour. Clusters of cells containing YFP+ as well as LacZ+ cells (defined as bicolour clusters) originate from the recombination of independent progenitors followed by the spatial overlap of their progeny during tissue growth. We thus estimated the

frequency of bicolor clusters in order to choose the appropriate tamoxifen dose to perform clonal analysis.

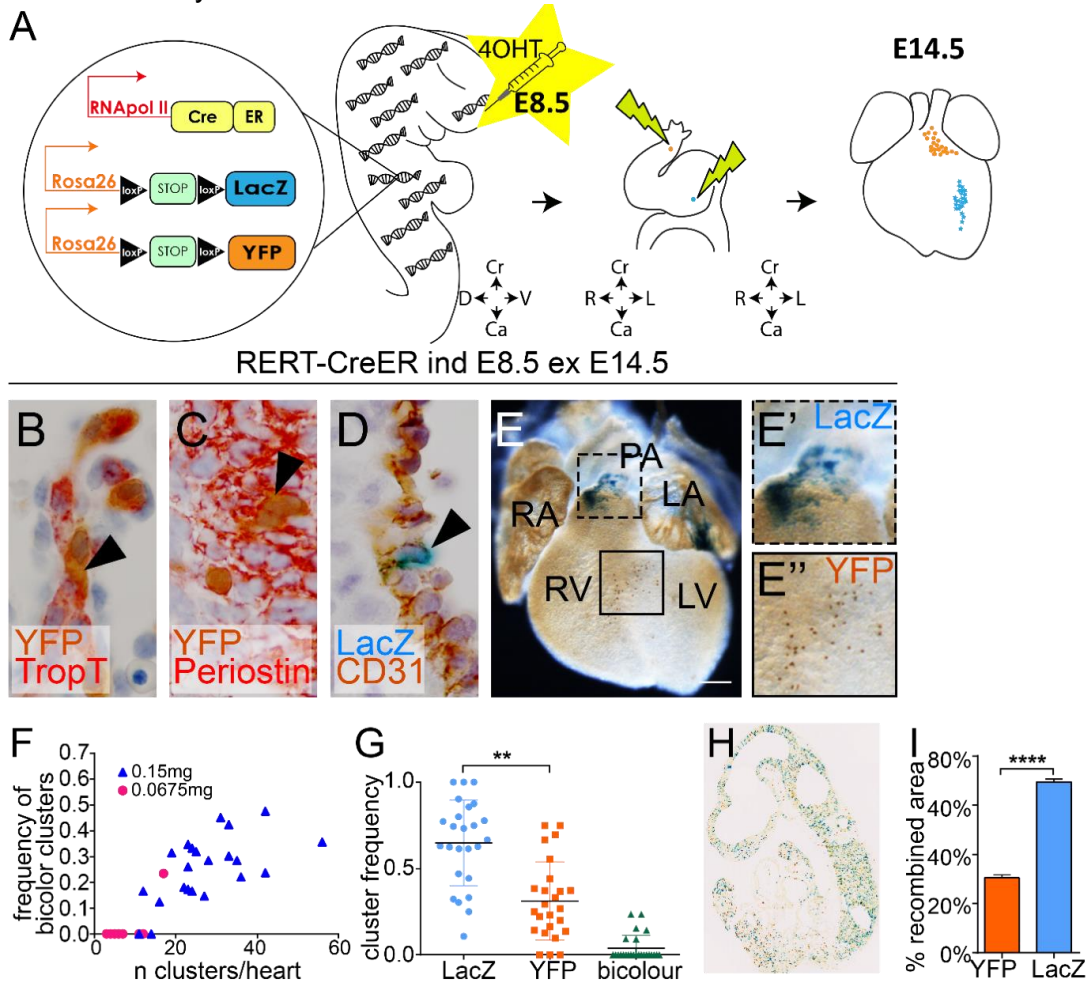


Figure 6. Retrospective clonal analysis: experimental setting.

(A) Transgenic mouse embryos with a tamoxifen inducible Cre recombinase (RERT) and two reporters (Rosa26R-LacZ; Rosa26R-EYFP). All constructs are driven by ubiquitous regulatory regions so that any embryonic cell can be randomly labelled. A low dose of tamoxifen was administered to pregnant females at E8.5 to trigger few labelling events. Labelled cells are analysed at E14.5. Cardiomyocytes (B), fibroblasts (C) and endothelial cells (D) were found (arrowheads). Nuclei were counterstained with hematoxylin (grey/purple). (E) LacZ+ and YFP+ clusters can be viewed as blue and brown clusters in whole mount. (E', E'') high magnification of boxed area in E. (F) Comparison of the occurrence of bicolor clusters in function of the number of clusters per heart using two different tamoxifen doses (blue: 0.15mg, pink: 0.0675mg). (G) Frequency of LacZ+ vs YFP+ and bicolor clusters in all litters. Paired t test **p = 0.015. (H) transversal section of an E9.5 RERT embryo induced at E8.5 with a high dose of tamoxifen. (I) Quantification of the embryonic surface recombined into LacZ vs YFP. ****p < 0.0001. Cr: Cranial; Ca: Caudal; R: right; L: left; 4OHT : 4 hydroxy-Tamoxifen (A), TropT: Troponin T (B), Pulmonary artery (PA); RA: Right atrium; LA: Left atrium; RV: Right ventricle; LV: Left ventricle (E). Scale bar: 200µm. (E).

The administration of 0.15mg of tamoxifen produced a significant number of bicolour clusters, we thus lowered the tamoxifen dose to 0.0675mg. As expected, the administration of 0.0675mg of tamoxifen resulted in hearts with fewer bicolour clusters (Fig. 6F). As a result, we generated a collection of 737 E14.5 hearts using 0.0675mg of tamoxifen to perform clonal analysis. The frequency of LacZ⁺ cell clusters was higher than that of YFP⁺ cell clusters (Fig. 6G). We thus sought to determine the frequency of recombination of each reporter for future calculations used to infer or reject clonal relationships. Embryos were induced with a high dose of tamoxifen (1mg) at E8.5 and harvested a day after so that the map of positive cells would directly reflect the efficiency of recombination. LacZ⁺ cells represented 69.42% of the recombined area compared to 30.57% for YFP⁺ cells, confirming a differential recombination efficiency (Fig. 6H).

We experimentally determined the frequency of bicolour clusters in the collection as 0.038 (Fig. 6G). Bicolour clusters represent only part of all polyclonal clusters, because independent progenitors can also be recombined in the same colour by chance. The frequency of mono-colour polyclonal clusters is estimated as a function of the frequency of bicolour clusters and the frequencies of single-colour clusters, which is biased towards the production of LacZ⁺ clusters (see materials and methods). The estimated frequency is $0,038 \times 1.95 = 0,074$, meaning that mono-colour cell clusters have an estimated 92.3% chance to be clonal.

The collection of hearts was screened for clusters of labelled cells. Each cluster was systematically assigned an ID and characterized in whole mount and on sections according to its colour, cell type(s) and anatomical position. As expected, our method targeted all cardiac lineages since all cardiac cell types were labelled. A general primary analysis of all cardiac lineages led us to focus on clones which contained different cell types and whose origin and specification were still unclear. Cell clusters were classified according to the cell type(s) they contained such as: Cardiomyocytes (CM), endocardial cells, Endothelial cells (ECs), Fibroblasts (Fbs), valve mesenchymal cells (valv) Smooth muscle cells (SMCs), epicardial cells and arterial mesothelial cells (AMCs). Strikingly, approximately 80% of clones consisted of a single cell type showing that as early as E9, most heart progenitors are already specified and maintain lineage decisions until E14.5.

As expected, heterogeneous clones were found in the Outflow tract (OFT), in the epicardium and in the valves. On one hand, the OFT region is known to derive from multipotent sources of progenitors: The Second heart field (SHF) and the Cardiac neural crest cells (CNCCs). On the other hand, the epicardium is known to undergo Epithelial to mesenchymal transition (EMT) after colonizing the myocardial surface and provide the heart with smooth muscle cells, fibroblasts, endothelial cells and according to some studies, cardiomyocytes.

The epicardium extends up to the base of the OFT where the pulmonary artery and aorta take root. Both vessels are covered by a sheet of mesothelial cells contiguous and continuous with the epicardium. We first sought to confirm what had previously been described in chick embryos (Pérez-Pomares et al., 2003; Männer, 2013)(Männer, 2013; Pérez-Pomares et al., 2003) by ruling out the possible lineage relationship between the epicardium and Arterial mesothelial cells (AMCs). We later investigated the lineage relationship between AMCs with cells of the great arteries and the heart, which had not been described before.

2. The epicardium and arterial mesothelium do not belong to the same lineage

In order to understand the lineage relationship between epicardium and AMCs, we screened the collection of hearts for AMC and epicardial clones. If epicardial cells and AMCs are related, we should be able to observe single clones containing both mesothelial types at frequencies above those resulting from random polyclonality. We first studied the distribution of labelled cells in the epicardium and the mesothelium of the great arteries (Fig. 7). From the collection of 737 hearts, 82 (~11%) contained exclusively epicardial clusters, 10 (~1.4%) contained exclusively AMC clusters and 13 (~1.8%) contained both (Fig. 7A-C). The distribution pattern of epicardial clones is consistent with their proepicardial origin. Epicardial clones appear as large groups of cells colocalizing the surface of the heart as well as the sub-epicardial space (Fig.7B-B'; S1A-F). In addition, various epicardial clusters were found within a same heart. For hearts containing more than one epicardial cluster, the frequency of colour coincidence between clusters co-occurring in the same heart was much higher than expected for random independent

events and 7 hearts with 4-6 colour-coincident clusters were found (Fig. S1A-F). These data suggest a clonal origin of single-colour multiple clusters found in the epicardium. The results are compatible with the recombination of single cells in the E9 proepicardium and their proliferation before colonization of the heart surface at different locations. Furthermore, these results show that single proepicardial cells proliferate, migrate and mix extensively with neighbours during myocardial surface colonization. The absence of clusters extending across the border between arteries and myocardium also suggested a lineage restriction between AMCs and epicardium. To further study this aspect, we determined the colour coincidence between AMC and epicardial clusters in the 12 hearts in which both were observed. In this sample, the colour of all epicardial clusters within a same heart was the same, despite the fact that 5 out of 12 hearts contained more than two clusters. In only 5/12 hearts there was a colour match between AMC and epicardial clusters, while in 7/12 hearts the colours did not match. Even when the colours between AMCs and epicardial cells did not match 3 and 4 colour-matched epicardial clusters could be found (two hearts). These results are compatible with random independent recombination of AMC and epicardial precursors, as the expected matched/non-matched proportion deduced from the recombination frequencies is 5.09/6.91, assuming a single recombination event in each precursor type.

To corroborate the results obtained by clonal analysis we used the tamoxifen inducible mesothelial specific WT1-creERT2 line (Fig. 7D,E) and induced recombination at different stages. Since WT1 is expressed in both populations, we reasoned that the timing of labelling of the two populations should depend on whether they originate from single or distinct populations. Detection of the Oestrogen receptor protein (ER) by immunofluorescence at E9 in WT1creERT2 embryos, confirmed that Cre recombinase is expressed in the proepicardium (Fig. 7F,F'') and in few epicardial cells (Fig. 7F,F') at the moment of induction. Therefore, at this stage, only the proepicardium and no other mesothelial lineages express Wt1Cre. We thus administered tamoxifen at E8.5 to trigger Cre-mediated recombination in proepicardial and epicardial cells. As expected, a significant number of epicardial cells were labelled in the ventricles and atria (Fig. 7D). In the Outflow tract (OFT), however, no positive cells could be observed (Fig. 7D). These data not only show that AMCs are not coming from the proepicardium but also that

epicardial cells are not capable of reaching the great arteries. It therefore suggests the existence of a lineage restriction boundary at the interface between the myocardium and the great arteries.

These results prompted us to investigate when AMCs appear in the OFT. After performing WT1 immunofluorescence in embryos ranging from E8 to E13, we were able to observe the first AMCs around E10.5/E11 (Fig. S2 A,B arrowheads). We thus wondered if we could target AMCs by inducing WT1creERT2 embryos at E9.5 (Fig. 7E). In that setting, some LacZ⁺ AMCs were observed in the great arteries of E14.5 embryos (Fig. 7E). To challenge the work of J.M. Perez Pomares and colleagues, we assessed the possible cephalic pericardial origin of AMCs. To do so, we analysed ER protein location at E10 (presumed stage of maximal induction after E9.5 TM injection). In addition to epicardial cells (Fig. 7G,G''), some pericardial cells expressed the Cre recombinase (Fig. 7G,G'). These results show the pericardial origin of the OFT mesothelium, which agrees with previous observations in chick embryos (Pérez-Pomares et al., 2003).

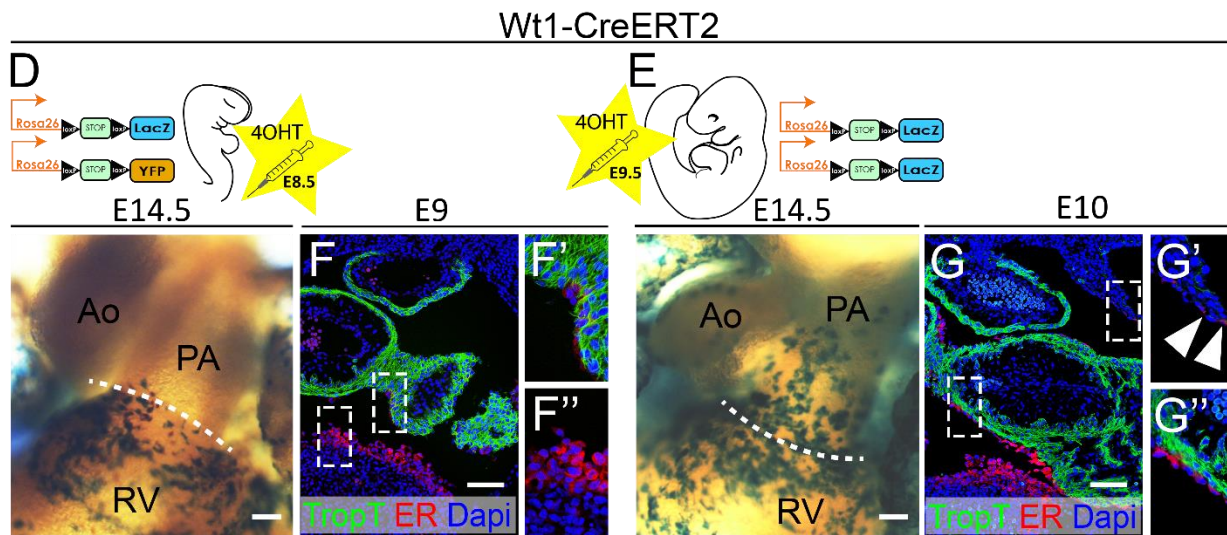
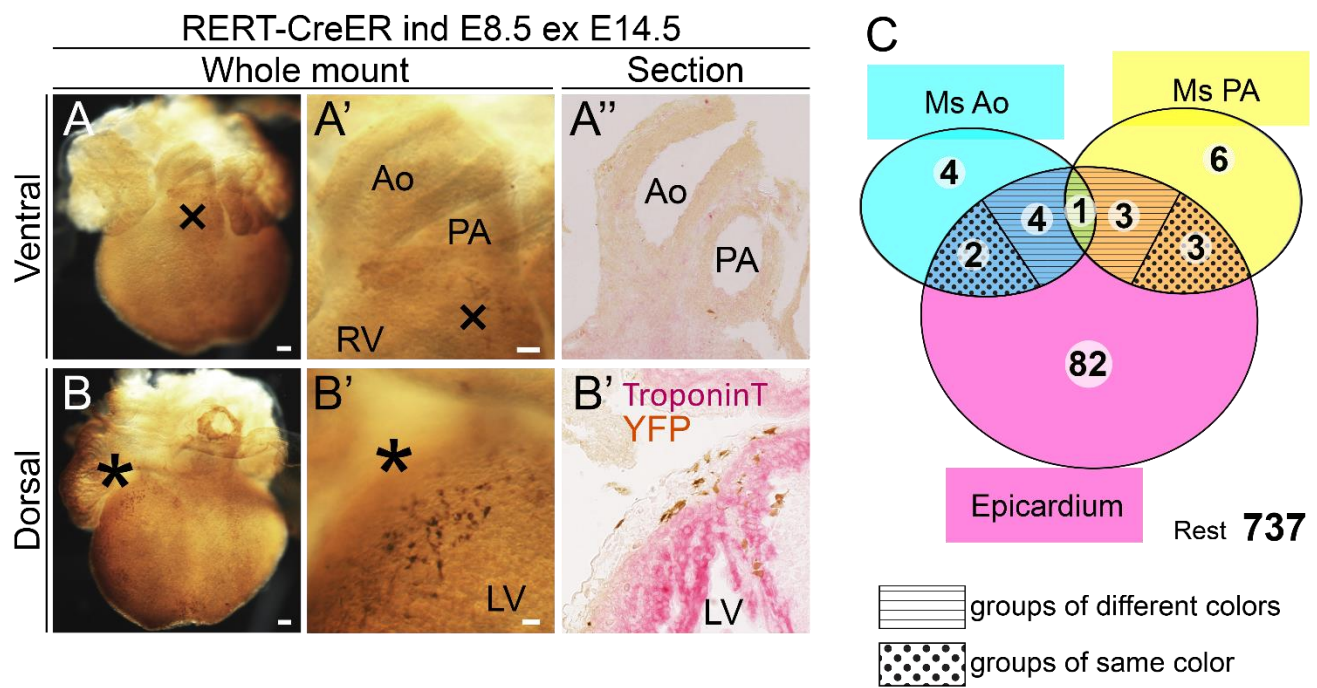


Figure 7. Arterial mesothelial clones are of non-proepicardial origin

(A) Whole mount ventral view of a specimen of the collection. (A') high magnification of the OFT area specified with a cross in A. (A'') Section of A' confirming the absence of YFP+ cells in AMCs. (B) Whole mount dorsal view of the same heart. (B') high magnification of a YFP+ epicardial clone seen in B (area of the star). (B'') frontal section of the same area revealing YFP+ epicardial cells and EPDCs. (C) Diagram of the hearts classified according to three categories: Hearts that contain AMCs in the Aorta (blue circle), Pulmonary artery (yellow circle) or epicardial clones (pink circle). The rest of the collection is indicated outside of the circles. Hearts with more than one category are at the intersection of the circles. The polka-dot and striped areas indicate if AMCs and epicardial cells are of a same or of a different colour respectively. (D-G'') samples from *Wt1creERT2* embryos. E14.5 hearts in (D) and (E) correspond to embryos induced at E8.5 and E9.5 respectively. In D no AMCs can be observed in contrast to E. The dashed lines represent the border of the myocardium with the great arteries. (F-F'') and (G-G'') show the localization of the Cre recombinase (ER) in red. The myocardium can be appreciated in green. (F') and (G'') are high magnifications of ER+ epicardial cells seen in the boxed area of (F) and (G) respectively. (F'') and (G') are high magnifications of ER+ proepicardial cells and pericardial cells (arrowheads) seen in the boxed area of (F) and (G) respectively. All scale bars: 100µm. Ao: Aorta; PA: Pulmonary artery; RA: Right atrium; LA: Left atrium; RV: Right ventricle; LV: Left ventricle. Ms: Mesothelium (C). TropT: Troponin T; ER: Oestrogen receptor (F,G).

3. AMCs derive from the splanchnic mesoderm related to the Second heart field

The cephalic pericardium, because of its location, is most likely derived from the splanchnic mesoderm related to the Second heart field (SHF). In addition, OFT cells such as myocardial, smooth muscle and endothelial cells are known to derive from SHF progenitors (Kelly et al., 2001; Sun et al., 2007; Wang et al., 2017). We therefore investigated the possibility of a SHF-related origin for AMCs. To do so, we used various Cre lines labelling SHF derivatives and related splanchnic lineages and checked if they labelled AMCs. Using the constitutive *Mef2c-AHF-Cre* transgene line, combined with the ROSA26R-TdTomato (Tom) reporter, we observed that the entire mesothelium of the great arteries was labelled (WT1/Tom double positive cells) (Fig. 8A,A',B). Reciprocally, labelled cells were not found extensively in the epicardium, however some labelling was detected in the epicardium of the ventricles in 3/6 hearts (Fig. 8A,A',B). Since *Mef2c*-cre recombines a variety of cardiac progenitors, we hypothesized that some hearts exhibited Tom + epicardial cells due to residual recombination in the proepicardium (Fig. 8B). Indeed, the proepicardium of 2/6 of the embryos analysed at E9.5 had Tom + cells in the proepicardium (Fig. 8B). These events of recombination in the proepicardium can thus

account for the number of hearts with Tom + epicardial cells at E14.5. In contrast, 100% of E14.5 hearts presented Tom + AMCs, suggesting their origin in lineages related to the anterior SHF (Fig. 8A,A',B). Tom + To further verify the specificity of AMCs to SHF-related lineages, we used the Rosa26R-TdTomato reporter recombined with *isl1*-Cre, which labels the SHF and related splanchnic cells. The observation of such hearts by confocal microscopy revealed the presence of Tom + AMCs along the great arteries (Fig. 8C,C'). In order to confirm these results, we sought to trace the fate of single SHF progenitors labelled at E8.5. To do so, we used the tamoxifen inducible *isl1*-mER-Cre-mER line with the Rosa26-YFP reporter. After low-density induction at E8.5, we studied the distribution of YFP + cells at E16.5. YFP + AMCs were found together with SMCs and ECs in the great arteries. About 80% of *isl1*-mER-Cre-mER hearts at E14.5 exhibited positive cells in the mesothelium of the great arteries (Fig. 8E). The ventricular epicardium as well as the proepicardium of the embryos analysed, at E14.5 and E9.5 respectively, were devoid of Lineage + cells (Fig. 8E). Smooth muscle cells and cardiomyocytes of the pulmonary trunk are derivatives of the pSHF (Bertrand et al., 2011; Rana et al., 2014; Waldo et al., 2005). Since AMCs are found together with those cells, they might as well derive from posterior SHF progenitors. To test this hypothesis, we traced the fate of late *isl1*+ progenitors (Fig. S3A,B). We found that embryos induced at E9 more consistently recapitulated AMC and AMC-related cells labelling than induction at E8.5. The use of the *Hoxb1*-Cre line that targets pSHF progenitors also resulted in the labelling of AMCs (Fig. S3C).

Altogether, these data show that AMCs originate from SHF-related lineages. Nonetheless It is still unclear whether *in vivo* SHF progenitors are multipotent or, alternatively, whether heterogeneous progenitors give rise to distinct cell populations in the heart and OFT. Heterogeneous AMC clusters found using *isl1*-mER-Cre-mER lineage tracing suggest that AMCs could be related to the cells of the great arteries (Fig. 8E). In a second phase, we thus studied OFT randomly generated clones, to explore the possible lineage relationships between AMCs and other SHF-derived cells in the arterial pole.

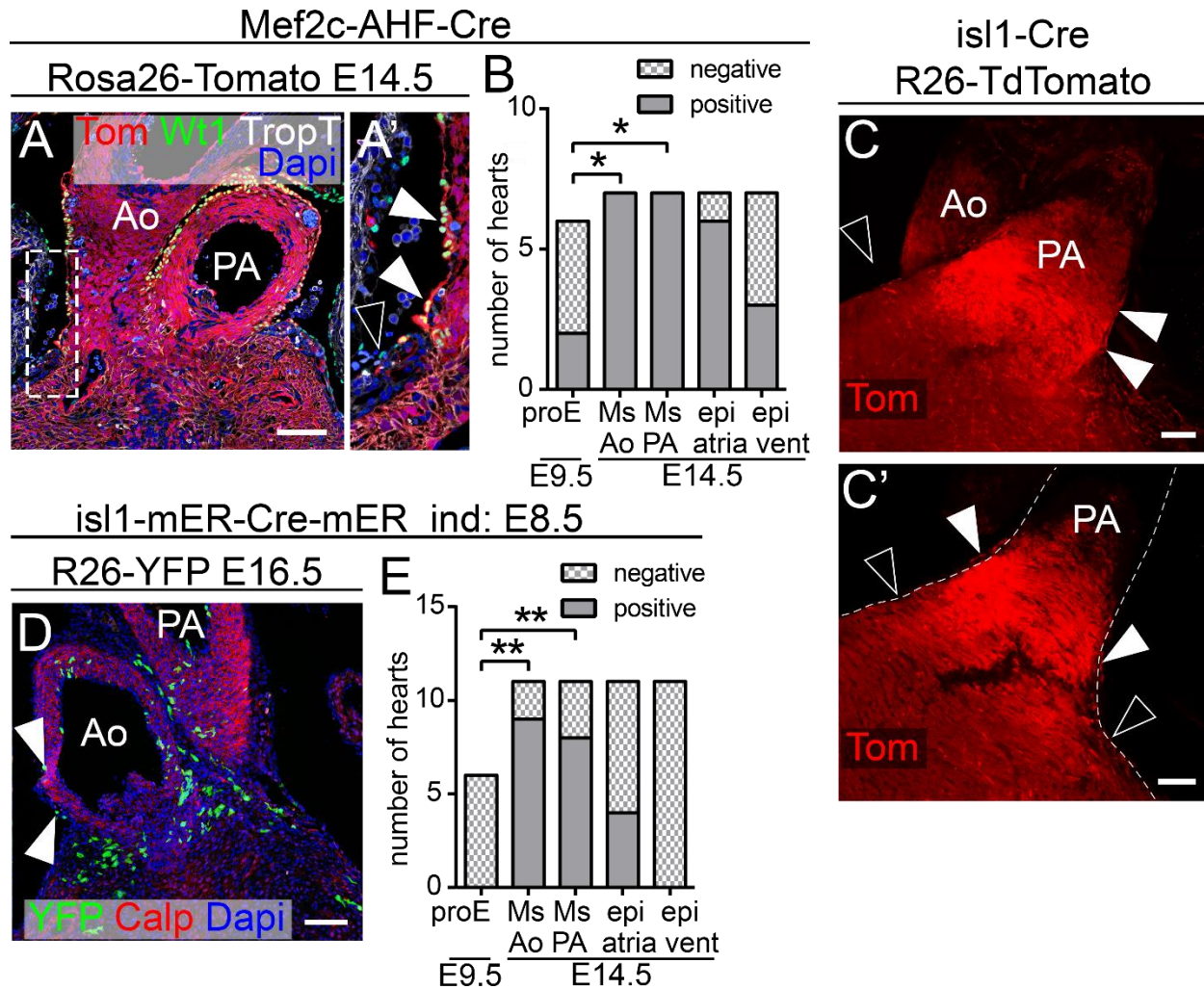


Figure 8. Arterial mesothelial cells derive from Second heart field-related progenitors

(A-B) Mef2c-AHF-Cre lineage tracing. (A) Heart section showing OFT Tom + cells at E14.5. AMCs and epicardial cells can be distinguished in green (Wt1). (A') high magnification of the boxed area in A showing the presence of Tom + AMCs (white arrowheads) and Tom - epicardial cells (Black arrowhead). (B) Graph representing the number of individuals containing lineage + cells in the tissues indicated on the x-axis. (C) Lineage tracing of isl1-Cre embryos at E16.5. Maximum Z projection of the OFT. (C') Optical section of heart in C, the dashed line follows the path of the sub-epicardium and sub-mesothelium. The presence of Tom+ AMCs (white arrowheads) and Tom- epicardial cells (Black arrowheads) can be appreciated. (D-E) isl1-mER-Cre-Mer lineage tracing of embryos induced at E8.5. (E) Heart section showing YFP+ AMCs (arrowheads), SMCs and ECs. (F) Graph representing the number of individuals containing lineage + cells in the tissues indicated on the x-axis. All scale bars: 100µm. Ao: Aorta; PA: Pulmonary artery; ProE: Proepicardium; vent: ventricle Ms: Mesothelium (B,E). Calp: Calponin (D)

4. AMCs are clonally related to vascular cells of the OFT

Analysis of E14.5 hearts with randomly induced clones showed labelled cells in the arterial poles. Different cell types could be found such as endothelial cells (ECs), fibroblasts (Fb), Smooth muscle cells (SMCs), AMCs, valvular mesenchymal cells (valv) and cardiomyocytes. We focused on clusters containing AMCs and investigated whether they contained other cell types as well. Interestingly all AMCs clones also contained cells in the inner layers of the Pulmonary artery (PA) and Aorta (Ao). To determine whether these clusters arose from independent events of recombination or rather from the recombination of multipotent progenitors, we used statistical analysis. We classified labelled cell clusters by their composition of cell types and by their proximity to the heart (Fig. 9, S4). Using Fisher's contingency test, we found that AMCs are clonally related to cells of the great arteries labelled cell clusters by their composition of cell types and by their proximity to the heart (Fig. 9, S4). The first category extends over the distal part of the great arteries (Fig. 9A Blue cells), while the second category is located in the proximal portion of the pulmonary artery (Fig. 9A Yellow and pink cells). The identification of cell types in both categories by immunohistochemistry revealed that distal clones contained ECs, SMCs, Fb and AMCs (Fig. 9C-C''²). In contrast, proximal clones contained AMCs (Fig. 9B, D''¹, D''², E''²), SMCs (Fig. 9B, D''¹, D''²), CM and valvular mesenchymal cells (Fig. 9B, D'-E''²). Proximal clones also contained endothelial-like labelled cells around blood cells in the wall of the pulmonary artery in the region adjacent to the ventricle (Fig. 9A, D''¹, D''²). Such cells organise as tubes in close proximity to the AMCs. Because of their morphology and localisation, they will be referred to as coronary vascular cells (CVC). In addition to the presence of AMCs, the majority of proximal clones in the pulmonary artery (10 out of 13 groups) showed disperse epicardial cells extending over the myocardium at the base of the PA (Fig. 9E''³). Nonetheless, these cells are not comparable to proepicardial-derived epicardial cells because they are scarce and do not expand over the ventricle. These results agree with the observed leakiness of the border between AMC and epicardial cells. This border is "hermetic" to Proepicardial-derived

epicardial cells (cf Fig. 7D) but allows arterial clones to migrate towards the ventricle. Since these cells overlie the myocardium, they should be named epicardial cells by definition. Since they derive from the SHF, we will name them SHF-derived Epicardial Cells (SHF-EpiCs).

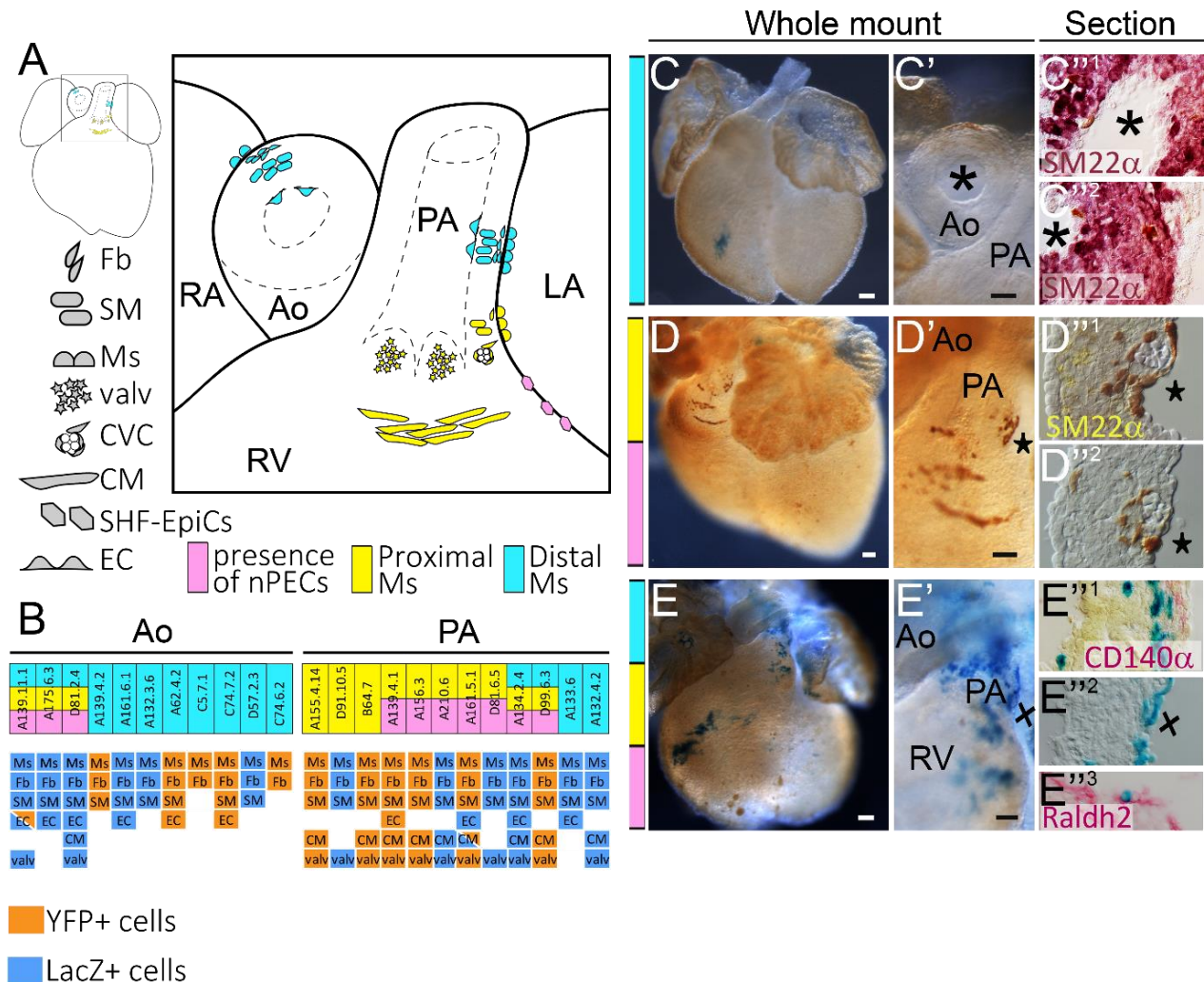


Figure 9. AMCs are clonally related to cells of the great arteries

(A) Scheme of categories of AMC clones and cell types. (B) Description of AMCs clusters per cell type. (C-C'') Example of YFP + distal clone. (C''1, C''2) Sections of the area in C'. YFP + ECs and YFP + SM22α + SMCs can be appreciated. (D-D'') Example of a YFP + proximal clone. (D''1, D''2) Sections of the area in D'. YFP + CVCs are found around erythrocytes (E-E'') Example of a LacZ + proximal clone (E''1- E''3) Sections of area in E'. (E''1) LacZ+ fibroblasts and and endothelial cells. (E''2) LacZ+ AMCs. (E''3) LacZ+ SHF-EpiCs. Fb: Fibroblast; SM: Smooth muscle; Ms: Mesothelium; valv: valvular cells; CVC: coronary vascular cell; CM: Cardiomyocyte; SHF-EpiCs: SHF-derived epicardial cell; EC: Endothelial cell (A,B) All scale bars: 100μm. Ao: Aorta; PA: Pulmonary artery; RV: Right ventricle; (C-E').

All together, these results show that AMCs are clonally related to cells of the great arteries, reflecting multipotent properties their progenitors. Furthermore, different lineages with different potentialities contribute to the mesothelial layer in this region, with proepicardial-derived cells contributing to the ventricle, SHF-derived cells contributing to the OFT and base of the arteries and SHF-related splanchnic mesoderm contributing to the distal arterial mesothelium.

On one hand, it was known that SHF progenitors give rise to smooth muscle cells, endothelial cells and cardiomyocytes of the arterial pole. However, no link between these cells and the AMCs was ever documented. On the other hand, the epicardium is known to undergo EMT and provide the heart with the same cell types. We thus wondered if AMCs in the distal region of the arteries could have the same properties as their epicardial counterparts. Furthermore, we have described a new SHF-derived mesothelial population and we wanted to know if they undergo epithelial to mesenchymal transition (EMT) to contribute to cells of the inner layers.

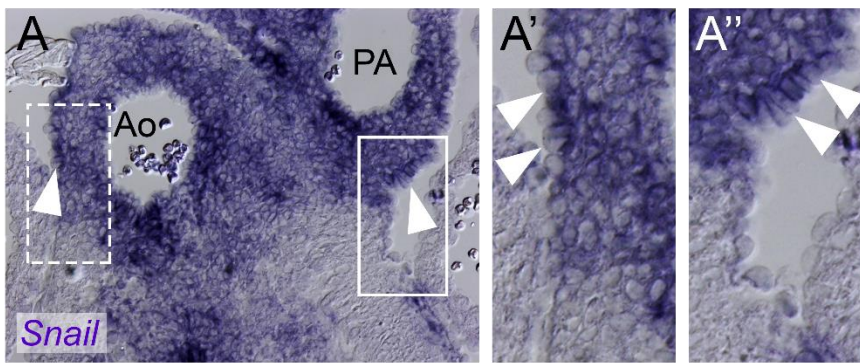
5. AMCs give rise to smooth muscle and endothelial cells of the great arteries

If AMCs are contributing to the great vessels through a mechanism of EMT, they should be expressing EMT markers. Known key regulators of EMT are the Snail family genes (Alberga et al., 1991; Carver et al., 2001) also essential to the formation of epicardial derived cells (EPDCs) (Martínez-Estrada et al., 2010). We first sought to check the presence of *snail* transcription factors in the great arteries at E12.5 by in situ hybridization (ISH). As a result, *snail* transcripts were detected in the arterial mesothelium (Fig. 10A-A'' arrowheads) and through the great arteries but seemed absent from the adjacent myocardium (Fig. 10A-A''). The expression of Snail gene in AMCs suggests that the EMT pathway is active in these cells and therefore they have the potential to invade and contribute to inner layers.

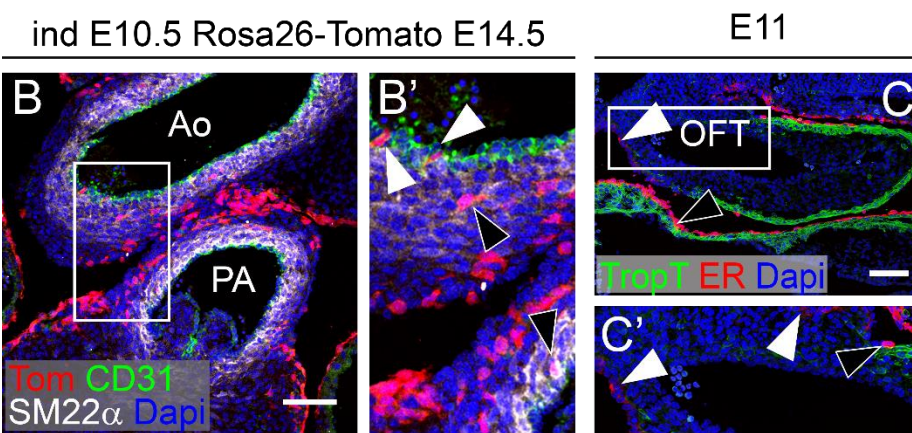
To further test this hypothesis and assess the possible contribution of AMCs to cells of the great arteries, we performed lineage tracing with the Wt1-CreERT2 line and the tomato reporter. We previously showed that AMCs appear in the OFT as early as day E10.5 (52A), we thus administered tamoxifen to mice at that stage and studied the distribution of tomato+ cells at E14.5. AMCs were successfully labelled at that stage (Fig.10 B). Immunofluorescent staining for CD31 (in green) and SM22 α (in white) revealed the presence of tomato+ endothelial cells and SMCs respectively (Fig. B,B'). Detection of the Oestrogen receptor protein (ER) by immunofluorescence at E11, confirmed that Cre recombinase is neither expressed in ECs nor in SMCs at the moment of induction (Fig. 10C,C'). ER was found expressed in the arterial mesothelium and epicardium instead (Fig. 10C,C'). These data, together with previous clonal analysis in which we showed no cross-contribution between the arterial and ventricular mesothelial clones, imply that AMCs are giving rise to SMCs and endothelial cells in the great arteries.

We wanted to know if the plastic properties of AMCs are extensive to later developmental stages or are taking place at a restricted stage. To address that issue, we additionally induced the Wt1-CreERT2 line at E11.5 or E12.5 and studied the distribution of Tom + cells in the great arteries at E14.5 (Fig. S5C,D). As a result, Tom + SMCs as the as Tom + ECs could be found in the Ao and PA (Fig. S5C-D'). These results reflect plastic of continuously providing cells to the Ao and PA during at least 3 days of development.

WT E12.5



Wt1-CreERT2



Wt1-Cre
Rosa26-TdTomato E14.5

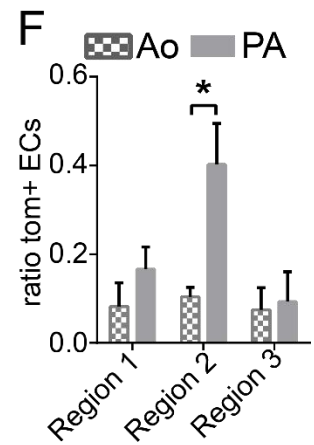
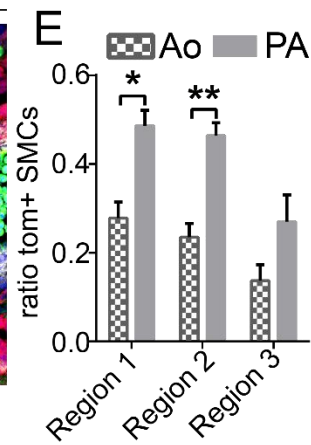
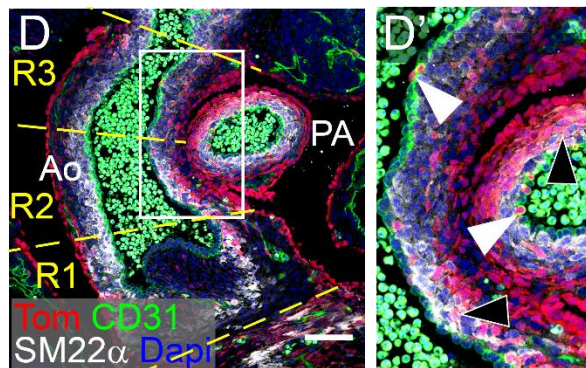


Figure 10. AMCs give rise to the smooth muscle and endothelial cells of the great arteries

(A) *In situ* hybridization of *Snail* on E12.5 sections showing the presence of positive AMCs (arrowheads). (A') and (A'') are high magnifications of the dashed and solid boxed areas in A. They show the presence of positive AMCs in the Ao and PA (arrowheads). (B-C') Wt1-CreERT2 hearts (B) Wt1 progenitors induced at E8.5 shows Tom+ cells in the AMCs, Smooth muscle (SM22 α +) and endothelial cells (CD31+) of the Ao and PA. (B') high magnification of the boxed area in B. white arrowheads point at ECs while black arrowheads point at SMCs. (C) localisation of the ER protein at the time of induction. White arrowhead points at positive AMCs, black arrowhead points at positive epicardial cells. (C') high magnification of boxed area in C. White arrowheads point at positive AMCs, the black arrowhead points at positive epicardial cells. (D-F) Lineage tracing of Wt1-Cre. (D) The great arteries can be divided in 3 regions as shown in the Ao with the yellow dashed lines. (D') High magnification of the boxed area in D. Example of a YFP+ proximal clone. White arrowheads point at Tom+ ECs (CD31+), the black arrowhead points at Tom+ SMCs (SM22 α +). (E) Quantification of Tom+ SMCs shows higher contribution to the PA (F) quantification of Tom+ ECs shows similar contribution between Ao and PA to the exception of region 2. All scale bars: 100 μ m. Ao: Aorta; PA: Pulmonary artery (A,B,D,E,F). OFT: Outflow Tract (C). R: Region (D)

These data suggest that part of the arterial inner layers are generated by EMT from a primary mesothelial progenitor state. We next sought to determine if AMC-derived cells accounted for an important part of the great arterial inner layers.

To assess the global extent of AMC contribution, we traced their fate using the constitutive Wt1-Cre line (Fig. 10D,D'). After harvesting and sectioning hearts at E14.5, we quantified the proportion of Tom+/SM22 α +/out of the entire smooth muscle population (Fig. 10E). We also quantified the proportion of Wt1 lineage endothelial cells, calculating the number of Tom+/CD31+ cells out of all CD31+ cells (Fig. 10F). All quantifications were done according to cell location along the Ao and PA proximo-distal axes. The subdivisions were as follow: “region 1” for the area adjacent to the myocardium, “region 3” for the area adjacent to the cephalic pericardium and “region 2” in the transition zone between both. About 50% of the pulmonary artery SMCs were contributed by the Wt1 lineage in regions 1 and 2, while the proportion dropped to 25% in region 3. Contribution of the Wt1Cre lineage to SMCs in the Aorta was consistently about half of that observed in the PA for all sub-regions (Fig. 10E). Regarding ECs, the contributions oscillated between 10-15% for the different regions of the PA and Ao, with the exception of the intermediate PA's region 2, in which the contribution was notably higher; 40% (Fig. 10F).

The fact that fewer smooth muscle cells were found in the distal part of the arteries (about 30% for the PA and 15% for the Ao (Fig. 10D,E) reflects the preferential contribution of Cardiac neural crest cells (CNCCs) over SHF cells to the distal OFT. In sum, these results provide compelling evidence showing that a substantial part of SHF-related progenitors contribute to the OFT and arterial roots through an intermediate state as AMCs, which then undergo EMT and contribute to various inner lineages.

Wt1-CreERT2 lineage tracing recapitulated the formation of distal clones (described in the previous chapter) since they are composed of SMCs and ECs. Proximal clones, however, were not represented since no cardiomyocytes were observed at the base of the PA. It is therefore likely that AMCs do not give rise to cardiomyocytes at the base of the PA. The fact that proximal clones could not be recapitulated, suggested their non-mesothelial origin which prompted us to study in detail the nature of these proximal clones.

6. OFT proximal clones give rise to LECs

As mentioned above, proximal clones arise from the deployment of SHF progenitors at the arterial pole. We assumed that proximal clones have not fully differentiated and expanded at E14.5, so we decided to study them at later stages. We reproduced the clonal analysis experiment inducing RERT mice at the same stage as previously (E8.5) but harvesting embryos half a day later at E15. In order to analyse the clones by confocal microscopy, we used the Rosa26-Td-Tomato and Rosa26-GFP reporters.

Out of a total of 240 hearts, three presented OFT proximal mesothelial clones (Fig. 11A,F"). These clones (GFP + cells in this example) are composed of AMCs expressing the Wt1 protein (Fig. 11B), cardiomyocytes expressing Troponin T (Fig. 11C), valve mesenchymal cells, CVCs and sub-epicardial endothelial cells forming a vascular network (Fig. 11A). The vascular structures found, express lymphatic endothelial cell (LEC) markers. Indeed, GFP + cells express the lymphatics determining gene Prox1 (Fig. 11C,E)

and Lyve1 (Fig. 11B,D,F-F'). As described above, this type of clones includes epicardial cells of SHF origin, which we called SHF-EpiCs. Interestingly, SHF-EpiCs-, unlike their immediate neighbours, are negative for Wt1 (Fig. 11F-F' black arrowhead), suggesting they have a different nature than the mesothelial arterial and proepicardial lineages. Instead, SHF-EpiCs were positive for the lymphatic-specification gene Prox1 (Fig. 11E arrowhead). Altogether, these results unveil the presence of LECs in early proximal clones. While the epicardial layer of the OFT contains isolated Prox1 + cells, the sub-epicardium underlying this area contains LECs structured in an incipient vascular network. In the hearts presenting proximal AMC/ LEC clones, no labelled lymphatic cells were found in the rest of the heart. Moreover, we were not able to detect other lymphatic clones in the collection of hearts at E15. To investigate the evolution of coronary lymphatics in proximal AMC clones at the base of the PA, we aimed at investigating lymphatic clones even later in development.

After clonal labelling by TM injection at E8.5, E14.5 hearts with proximal OFT clones accounted for 2% of all generated hearts (13 out of 737 hearts) and 3% of hearts containing at least one clone (13 out of 420 hearts). Similarly, induced clones analysed in E15 hearts accounted for 3 out of 240 specimens. To study clones later during development we thus followed two strategies. On one hand, to increase the chance of targeting lymphatic clones and study their distribution, we chose to recombine progenitors at higher density (0.1mg of tamoxifen). In that instance, RERT embryos were harvested at E16.5. On the other hand, we chose to recombine progenitors at lower density (0.05mg of tamoxifen) and study clones at birth (p0). In that setting, we were able to analyse bigger cell clusters while maintaining the clonality of labelled groups.

Out of 71 E16.5 hearts, 9 lymphatic clusters were found (Fig.11G,G'; S6D), 6 of which extended predominantly in the ventral side of the heart, while the other three affected exclusively the dorsal part of the heart (two of them in the same heart) (Fig. S6C, D). However, the pattern of lymphatic clusters was different depending on their location in the heart; two main categories could be observed. Four of the nine LEC clusters, located in the ventral side of the heart, showed sparse and scattered cells (Fig.11G,G' S6A,B). On the other hand, two ventral LEC clusters and all three dorsal LEC clusters were dense

(Fig.11H,H', S6C,D). Interestingly, sparse ventral clones did not contribute to the dorsal part of the heart. The three sparse ventral clones co-localised with AMCs, SMCs, valvular cells, in the PA and CMs at the base of the PA. These ventral clones are thus the equivalent of the ventral proximal clones found at E15. However, AMCs were mostly found in the distal part of the PA (1/4 with proximal and distal AMCs, 3/4 with distal AMCs) suggesting that proximal AMCs do not stay at the surface of the PA. Dense ventral clones however, showed lymphatic outgrowths reaching the dorsal part of the heart in two instances (Fig. S6D). The dense clusters of the dorsal part of the heart however, did not show contribution to the ventral part of the heart (Fig.11H,H''; S6). Interestingly all dorsal clones had positive cells in extra-cardiac LECs in the cephalic region of the heart, suggesting their connection to the systemic vasculature. These data suggest that the origin and dynamics of formation of the cardiac lymphatic vasculature are different in the ventral and dorsal parts of the heart (Fig.11H,H'). Because the tamoxifen dose used in this experiment was high, numerous labelled cells of different cell types were found in the E16.5 hearts. High labelling density impedes to decipher precisely lineage relationships regarding ventral LECs and dorsal LECs (Fig. S6). We thus studied P0 hearts, induced at clonal density to challenge the observations made at E16.5.

The analysis of 130 P0 hearts labelled at low density spotted two very large lymphatic clones. One exclusively affecting the ventral part and one exclusively affecting the dorsal part of the heart. As previously observed in E16.5 clones, the dorsal lymphatic clone was dense and widely spread over the dorsal aspect of the heart (Fig.11L-L'). Unlike the dorsal clone, the ventral clone was composed of scattered cells. Tom + cells were mixed with clonally unrelated cells of the ventral lymphatic vascular tree (Fig.11I-K).

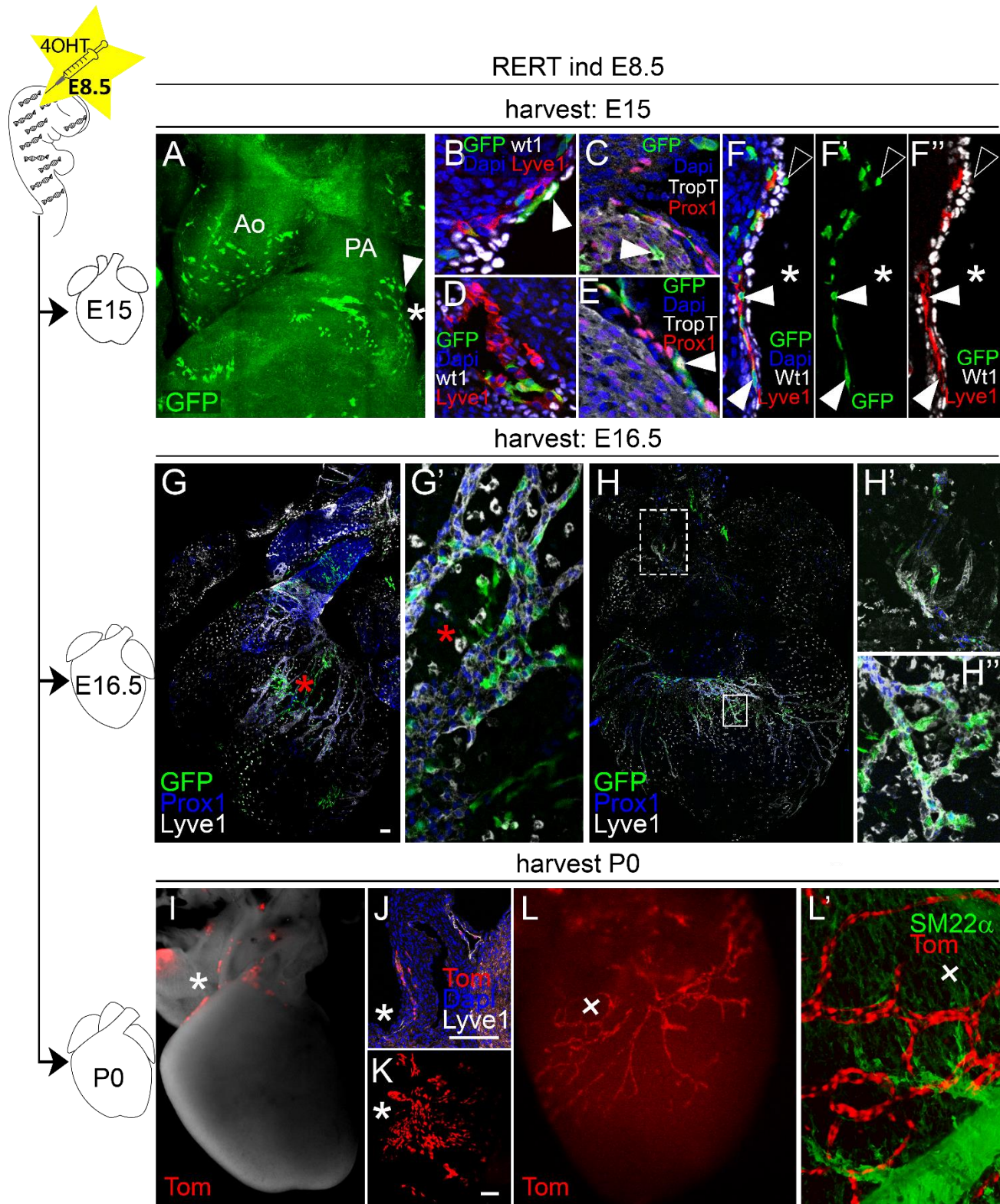


Figure 11. Proximal AMC clones form lymphatic vessels during late development

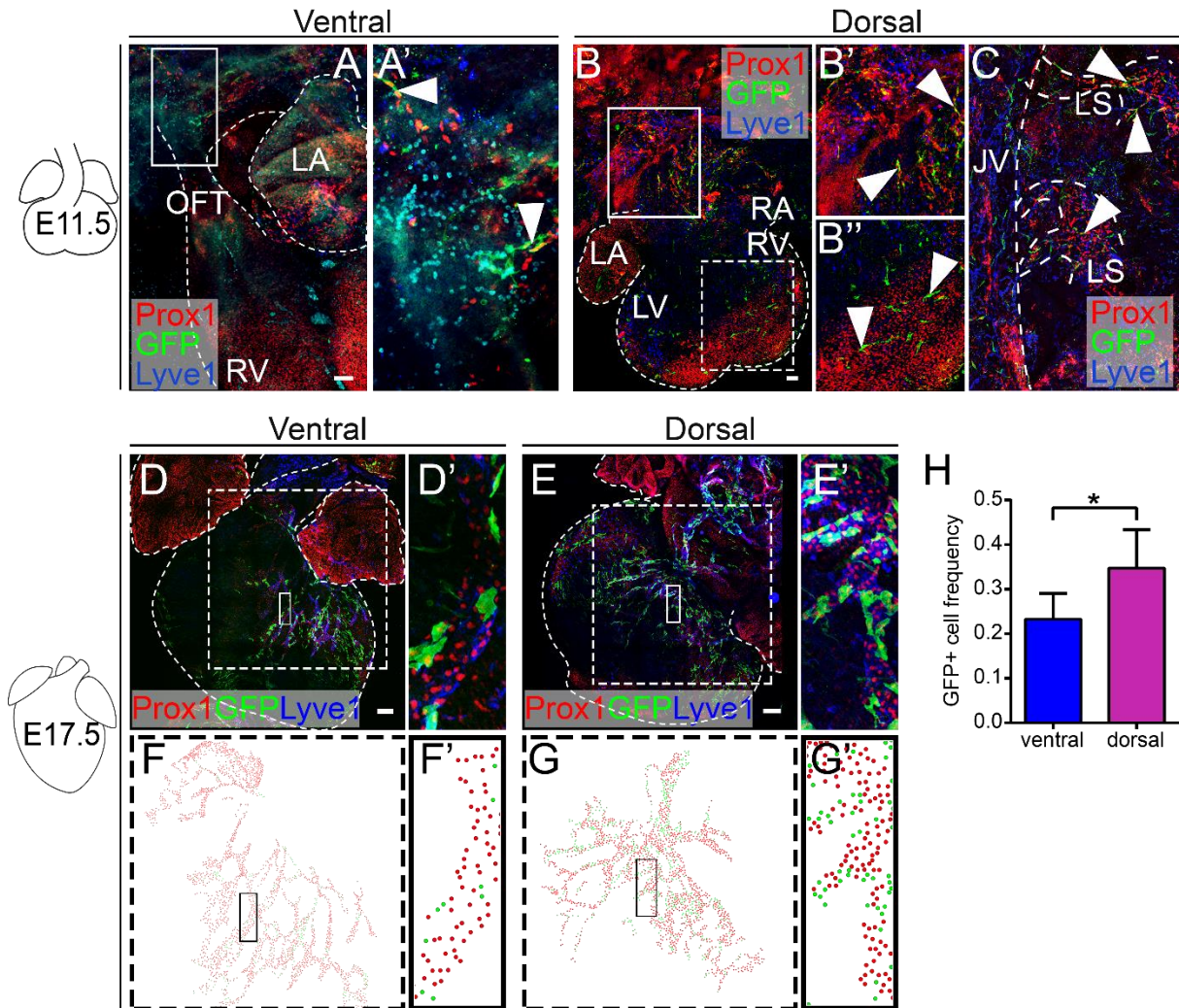
(A-F') Clone at E15. (A) Z-projection of a GFP+ clone. The arrowhead points at proximal AMCs. (B-F'') are sections of the PA (B) shows GFP+ LECs (Lyve1 +) and AMCs (Wt1 +). (C) shows GFP+ LECs (Prox1 +) and Cardiomyocytes (TropT + arrowhead). (D) shows GFP+ LECs (Lyve1 +). (E) shows GFP + SHF-EpiCs (Prox1 +). (F-F'') Area specified with an asterisk in A. They show the presence of GFP + Wt1- epicardial cells (black arrowhead) and GFP + sub-epicardial LECs (Lyve1 + white arrowheads). (G-G') Ventral GFP + LEC Clone at E16.5. (G) Maximal Z-projection of the entire ventral surface. (G') Z projection of 5 optical sections from the asterisk area in G. GFP + LECs are intermingled with GFP – LECs. (H-H') Dorsal GFP + LEC Clone at E16.5. (H) Maximal Z-projection of the entire dorsal surface. (H) high magnification of extracardiac GFP + LECs of the dashed box area in H. (H') high magnification of GFP + LECs of the solid box area in H. GFP+ cells are cohesive. (I-K) Ventral tom + P0 clone. (J) Tom + LECs (Lyve1 +). (K) Confocal Z- projection of the asterisk area in I. Cells are distributed on the ventricle (L,L') Dorsal Tom+ LEC P0 clone. LECs Tom + cells form an organised plexus. (L') confocal Z- projection of the cross area in L. Tom + cells are cohesive. All scale bars: 100µm. Ao: Aorta; PA: Pulmonary artery (A).

The heterogeneous pattern of lymphatic clones observed in this study, suggests the existence of different sources of LEC progenitors. The lymphatic vasculature had been shown to come from the specification of a subset of progenitors in the cardinal vein around E9.75 (Yang et al., 2012). Klotz and colleagues shown that not all cardiac LECs derive from the cardinal vein (Klotz et al., 2015). They suggested a complementary contribution from progenitors of the haemogenic endothelium in the yolk sac. Since we saw different patterns and limited cross-contribution between cardiac lymphatic clones of the ventral and dorsal parts of the heart, we hypothesised that both aspects of the heart may be colonized by different sources of progenitors. We hypothesised that the majority of dorsal lymphatic cells is coming from the cardinal vein dorsal clones are composed of extra-cardiac LECs as well as intra-cardiac LECs (Fig.11H,H'; Fig S5). Moreover, podoplanin staining in dorsal clones showed higher intensity level in Tom + extra-cardiac LECs than in Tom + cardiac LECs suggesting that they sprout from extra-cardiac vessels (Fig S5). In contrast, we assumed that a portion of ventral lymphatic clones must derive from an alternative source. Because LECs appeared associated to the SHF-EpiCs between E14.5 and E15 in proximal clones derived from the SHF, we hypothesized they might form by a process of vasculogenesis from SHF precursors in that time window. To challenge the idea of a heterogeneous origin for ventral versus dorsal cardiac lymphatic vessels, we decided to specifically trace the origin of lymphatic progenitors.

7. Lymphatic endothelial cells of the ventral and dorsal parts of the heart arise from distinct sources of progenitors

To investigate the degree of specification of cardiac lymphatic progenitors at different developmental stages, we used the VEGFR3-CreERT2 line, that targets all committed and differentiated LECs (Martinez-Corral et al., 2016). The fate of VEGFR3+ progenitors was traced with the Rosa26-mTmG reporter, so that every recombined cell is expressing the membrane GFP protein, (the un-recombined ones remain Tomato positive). Lymphatic progenitors specify and start expressing VEGFR3 around E10.5-E11.5 in the cardinal vein of mouse embryos (Yang et al., 2012). We thus induced hearts at E11.5, when cells start sprouting from cardinal vein-derived lymph sacs (LS). Since the peak of recombination takes place about 12 hours after TM administration (Hayashi and McMahon, 2002), harvesting hearts only 24 hours after induction is a valuable approach to map the location of recently recombined cells as well as to assess the rate of recombination. Therefore, embryos were first harvested at E12.5, to verify that recombination occurred in the cardinal vein (CV) and lymph sacs (LS). Since VEGFR3 is expressed in blood vessels at early stages (Martinez-Corral et al., 2016), we expected the recombination of some blood endothelial cells (BECs). As expected, GFP + cells were found in the cardinal vein, inter-somitic vessels (ISVs) and LS (Fig. 12C). Some GFP + cells in both the ventral and dorsal parts of the heart did not express Prox1, reflecting their possible blood endothelial nature (Fig. 12B,B’). Interestingly, some embryos exhibited GFP + cells in extra-cardiac lymphatics of the cephalic part of the heart both ventrally (Fig. 12A,A’) and dorsally (Fig. 12B,B’). After studying the pattern of recombination of VEGFR3+ progenitors a day after induction, we decided to study it at E17.5, when an established cardiac lymphatic vasculature is present. We reasoned that in the case all lymphatics of the heart derive by angiogenesis from pre-specified LECs, there should not be any difference in the proportion of VEGFR3-lineage+ LECs between the ventral and dorsal part of the heart. If, however, the ventral part of the heart depends on another source of progenitors that specifies later during development, there should be less VEGFR3-lineage +GFP + LECS in the ventral part than in the dorsal part of the heart.

Hearts were systematically stained for prox1 (red) and Lyve1 (blue) for the identification of LECs (Fig. 12 D-E'). Overall, less than half of Prox1+/Lyve1 + cardiac cells were GFP+ at E17.5 (Fig. 12), which agrees with the incomplete recombination of LECs observed at E12.5. We then measured the proportion of GFP + cells in the ventral and dorsal parts of the heart, calculating the ratio of Prox1 +/GFP + cells by all prox 1+/Lyve1 + cells (Fig. 12). GFP + cells of the dorsal part accounted for about 35% of all Prox1 +/Lyve1 + cells (Fig. 12E,E',G,G'). However, GFP + cells of the ventral part of the heart represented only 23% of ventral LECs (Fig. 12A,A',C,C',E). The proportion of GFP + cells of extra-cardiac lymphatic vessels should reflect the efficiency of recombination of early VEGFR3+ progenitors deriving from the CV. We thus quantified the proportion of GFP + cells in extra-cardiac LECs in lymphatic vessels of the vicinity of the jugular veins GFP +. The proportion of GFP + cells in extra-cardiac LECs, was found comparable to that of the dorsal part of the heart. Nevertheless, the proportion of GFP + cells in the ventral part was found significantly lower than that of extra-cardiac LECs. Consistently, the proportion of GFP + cells of the ventral part of the heart was found to be significantly lower than that of the dorsal part of the heart. These data suggest that while dorsal LECs mostly derive from the CV, part of the ventral lymphatic vasculature depends on another source. In turn, the presence of GFP + LECs in the ventral part of E17.5 embryos (Fig. 12D,D',F,F') as well as in extra-cardiac LECs of the cephalic part of the heart at E12.5 (Fig. 12A,A') indicates that part of ventral LECs also derive from pre-specified LECs, presumably from the CV.



We next labelled VEGFR3⁺ cells at different stages to gauge the onset of full LEC specification for ventral lymphatics. We followed the same strategy as before, but inducing at E12.5, followed by harvesting embryos at E13.5 to determine the sites of recombination and at E17.5 to determine the proportions of GFP⁺ + LECs in the established lymphatics. As previously, E13.5 embryos exhibited GFP⁺ cells in Prox1⁺ + LECs (Fig 13A-C') and Prox1⁻-BECs (Fig 13A,C'). Similarly, some embryos exhibited extra-cardiac GFP⁺ + LECs in the cephalic region of the ventral part of the heart (Fig. 13A,A'). Some GFP⁺ + LECs however, could be found on the pulmonary artery (Fig. 13A,A' Black arrow). In the dorsal part, however, LECs appeared arranged in a vascular lymphatic plexus connected to extra- cardiac lymphatic vessels (Fig. 13B). In another embryo (less advanced in development), we could appreciate extra-cardiac GFP⁺ + LECs growing towards the dorsal atrioventricular groove (Fig. 12C,C'). These data illustrate, the direct early contribution of pre-specified LECs, presumably from the cardinal vein, to the lymphatics of the dorsal part of the heart. Direct connection between the cardinal vein and to GFP⁺ + LECs in the ventral part, was not clear because of tissue orientation.

Foetuses labelled at E12.5 and studied at E17.5 showed a higher proportion of GFP⁺ + lymphatic cells GFP⁺ + (about 48-67%) (Fig. 13D-G'') than those induced at E11.5 (23-35%) (Fig 12H). If, as hypothesised previously, the alternative ventral LECs are not fully specified at E13, the gap between the proportions of GFP⁺ + cells of the ventral and dorsal parts should remain. Indeed, Prox1⁺/GFP⁺ + cells represented about 48% of all Prox1⁺ +/Lyve1⁺ + cells of the ventral part of the heart. In the dorsal part of the heart, however, Prox1⁺ +/GFP⁺ + LECs proportion remained significantly higher (67%) at this stage. Consistently, the proportion of GFP⁺ + cells in extra-cardiac LECs was similar to that of cardiac dorsal LECs but significantly higher than that of ventral LECs.

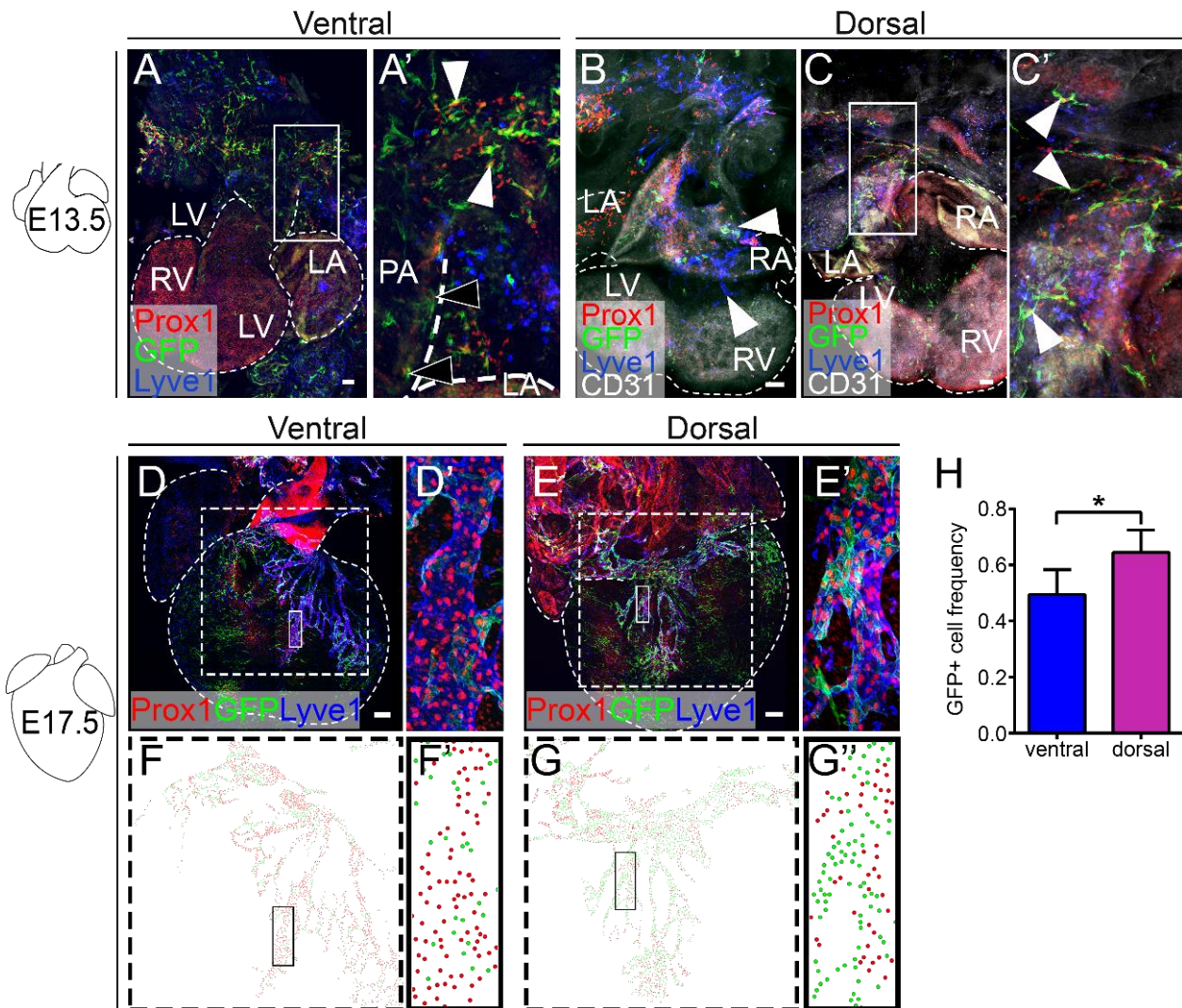


Figure 13. Cardinal vein VEGFR3 + lymphatic progenitors contribute only partially to LECs of the ventral part of the heart.

VEGFR3-CreERT2 lineage tracing of embryos induced at E12.5. (A-C') Z projections of embryos harvested at E13.5. (A) Ventral view. (A') High magnification of boxed area in A showing GFP + extra-cardiac LECs (arrowheads) and GFP + LECs on the PA. (B) Dorsal view showing a lymphatic plexus (Lyve1 +) connected to the extra-cardiac lymphatic vasculature (arrowheads). (C) Dorsal view of another embryonic heart (C') High magnification of solid boxed area in C showing extra-cardiac GFP + LECs migrating towards the atrioventricular groove (arrowheads). (D-H) Z projections of embryos harvested at E17.5. (D) Ventral view (D') High magnification of boxed area in D. (E) Dorsal view (E') High magnification of boxed area in E. (F) and (G) are maps of the boxed area in D and E respectively where the proportions of GFP + LECs (green) and GFP - LECs (red) can be appreciated. Similarly (F') and (G') are maps of the boxed area in D' and E' respectively. (H) Quantification of GFP+ LECs/ all LECs showing higher recombination in dorsal lymphatics. All scale bars: 100um. RV; Right ventricle; LA: Left atrium; RA: Right atrium; LV: Left ventricle (A,C).

VEGFR3-CreER; Rosa26-mTmG induction E14.5

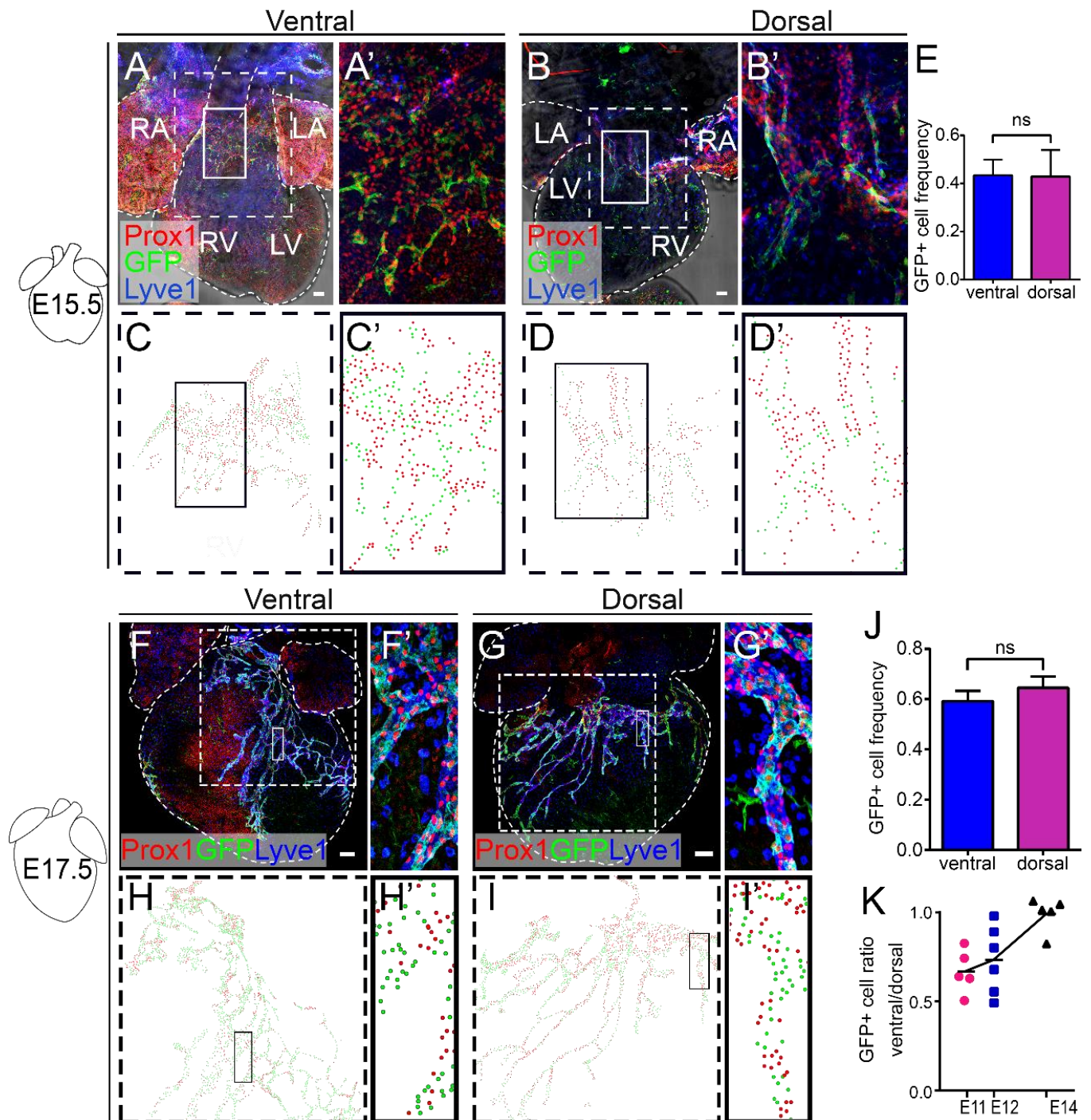


Figure 14. All VEGFR3 + lymphatic progenitors of the ventral part of the heart are specified by E15.5

(A-B') Z projections of embryos harvested at E15.5. (A) Ventral view (A') High magnification of boxed area in A. (B) Dorsal view (B') High magnification of boxed area in B. (C) and (D) are maps of the boxed area in D and E respectively where the proportions of GFP + LECs (green) and GFP – LECs (red) can be appreciated. Similarly (C') and (D') are maps of the boxed area in A' and B' respectively. (E) Quantification of GFP+ LECs/ all LECs showing equal contribution of VEGFR3 + to both parts of the heart. (F-G') Z projections of embryos harvested at E17.5. (F) Ventral view (F') High magnification of boxed area in A. (G) Dorsal view (G') High magnification of boxed area in B. (H) and (I) are maps of the boxed area in F and G respectively where the proportions of GFP + LECs (green) and GFP – LECs (red) can be appreciated. Similarly (H') and (I') are maps of the boxed area in F' and G' respectively. (J) Quantification of GFP+ LECs/ all LECs showing equal contribution of VEGFR3 + to both parts of the heart. (K) Evolution of the ratio of ventral GFP + LECs/ dorsal GFP + LECs at the different moments of induction. All scale bars: 100um. RV; Right ventricle; LA: Left atrium; RA: Right atrium; LV: Left ventricle (A,C).

We then sought to determine whether and when the contribution to ventral and dorsal LECs by VEGFR3+ progenitors matches. Embryos were induced with tamoxifen at E14.5 and harvested either at E15.5 or E17.5. Interestingly, E15.5 hearts displayed similar proportions of ventral and dorsal GFP + LECs (Fig. 14A-E). This means that by E14.5 both the progenitors of the ventral and dorsal parts of the heart are present. To confirm these observations, we studied the distribution of GFP + cells in E17.5 hearts. As expected, not only were the proportions of GFP + cells similar between both parts of the heart, but also they were maintained between E15.5 and E17.5 (Fig. 14J,K). Further quantification of extra-cardiac Lymphatic vessels, showed that the proportions of GFP + cells observed in the heart reflect the efficiency of recombination in extra-cardiac lymphatics.

Our results show different dynamics of cardiac LEC progenitor specification in dorsal and ventral regions of the heart. While full specification of dorsal heart lymphatics takes place between E12 and E13, the specification of ventral lymphatics lags behind this schedule and is only complete by E15. Together with the observed pattern of lymphatic vessel colonization of the dorsal and ventral parts of the heart, these results are compatible with the idea that early specified LECs, presumably from the cardinal vein, give rise to all dorsal LECs through angiogenesis but only to part of the ventral LECs.

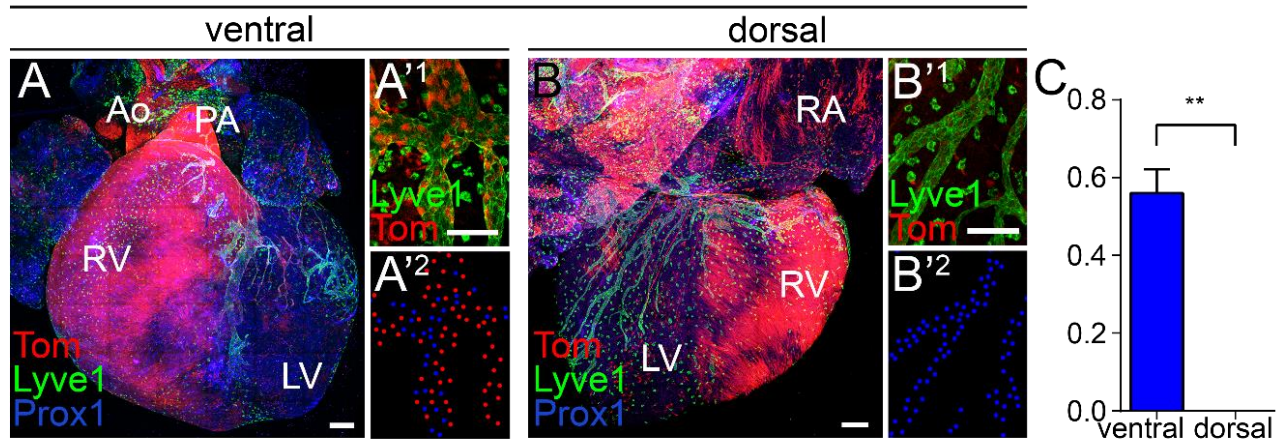
Instead, a substantial amount of ventral LECs depends on the contribution of another source of progenitors which are not fully specified until E15. The fact that dorsal LECs are not fully recombined is mostly a consequence of the incomplete efficiency of recombination. Even so, we found an increase in VEGFR3+ progenitors between E12 and E13, so we cannot rule out the specification of CV-independent VEGFR3+ progenitors between E12 and E13 and their later addition into the heart. Furthermore, these results do not exclude, the existence of other complementary cLEC progenitors, such as those reported by Linda Klotz and colleagues (Klotz et al., 2015), with a recombination efficiency similar to that of CV-derived precursors. These results support the existence of an alternative late-specified source for cardiac lymphatic endothelial cells contributing to the ventral part of the heart. Because AMCs derive from the SHF, and were found to be clonally related to a population of ventral LECs, we reasoned that this late specified population may correspond with the SHF-derived LECs.

8. The second heart field contributes to the ventral but not to the dorsal lymphatic vasculature

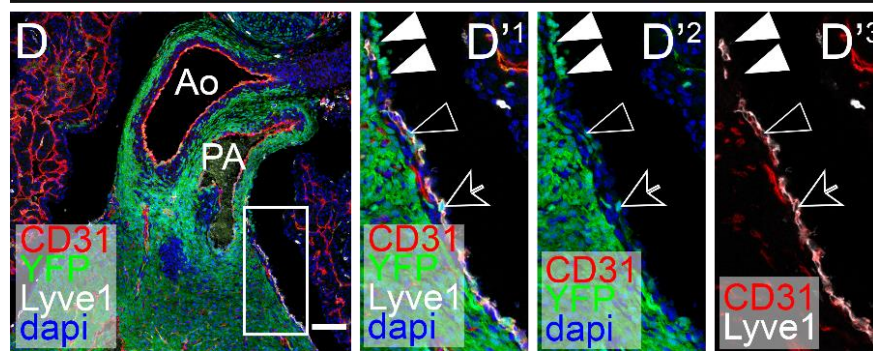
We sought to challenge the possible contribution of SHF progenitors to the lymphatic vasculature using a variety of Cre lines recombining the SHF. The first line we used was the *isl1*-Cre line combined with the Rosa26-Tdtomato reporter. Embryos were harvested at E17.5 in order to directly compare *isl1*-Cre hearts to VEGFR3-Cre hearts from the previous experiment. Hearts were immuno-stained in whole mount for Prox1 and Lyve1 markers. The ventral and dorsal surfaces of the hearts were acquired in 3D using confocal microscopy. As predicted by our previous results, Tom + cells were found in the lymphatic plexus of the ventral part of the heart (Fig. 15A-A'²). Strikingly, no tomato LECs were detected in the dorsal part of the same hearts (Fig. 14B-B'²). The quantification of Prox1 +/Lyve1 +/ Tom + cells showed that about 55% of all ventral LECs were labelled (Fig. 15C). However, no LEC was found to express the tomato reporter in the dorsal part of the heart (0 out of an average of 1341 cells per heart).

To corroborate these results, we used the Mef2c-AHF-Cre line, which labels the anterior heart field, combined with the Rosa26-YFP reporter. YFP+ LECs were studied on sections of E16.5 embryos. The presence of YFP +/Lyve1 +/CD31 + cells in the sub-epicardium of Mef2c hearts confirmed that SHF progenitors indeed contribute to ventral cardiac LECs (Fig. 15D-D'³ black arrowheads). The presence of proximal AMCs (Fig. 15D-D'³ white arrowheads). as well as SHF-EpiCs expressing Lyve1 and CD31 (Fig. 15D-D'³ black arrow) could be appreciated in these specimens.

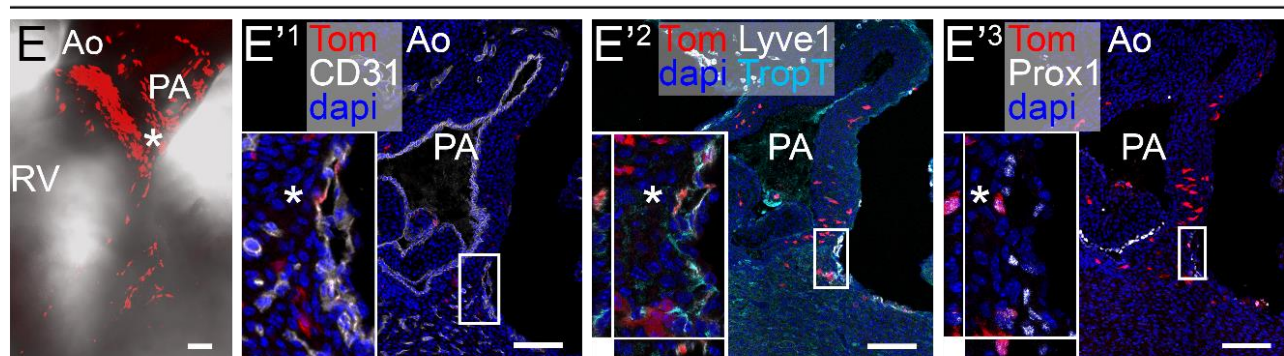
isl1-Cre; R26-Tdtomato E17.5



Mef2c-AHF-Cre R26-YFP E16.5



isl1-mER-Cre-Mer ; R26-Tdtomato ind: E9 harv: E16.5



Wt1-Cre
Rosa26-mTMG E16.5

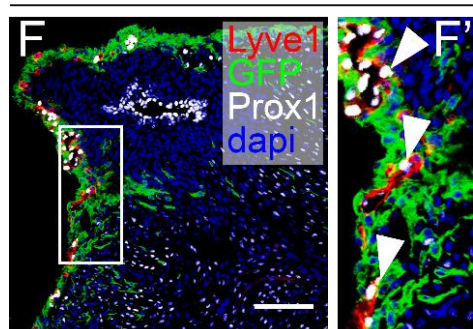


Figure 15. The SHF gives rise to cardiac LECs but not to dorsal LECs

(A-C) Isl1-Cre lineage tracing. Z projections of embryos harvested at E17.5. (A) Ventral view. (A'¹) High magnification of ventral Tom + dorsal LECs. (A'²) map of area in A'¹. Red points are Tom + LECs and blue points Tom - LECs (B) Dorsal view (B'¹) High magnification of dorsal Tom - dorsal LECs. (B'²) map of area in B'¹. (C) Proportions of Tom+ LECs/ all LECs in the ventral and dorsal parts of the heart showing that no LECs from the isl1 lineage form in the dorsal part. (D-D'³) Mef2c-AHF-Cre lineage tracing. Sections of embryos harvested at E16.5. (D'¹-D'³) High magnification of the boxed area in D showing YFP+ proximal AMCs (white arrowheads), sub-epicardial LECs (Lyve1 +/CD31+ black arrowhead) and SHF-EpiCs (Lyve1 +/CD31+ black arrow). (E-E'³) IIs1-mER-Cre-Mer lineage tracing of embryos induced at E9 and harvested at E16.5. (E) Whole mount Z projection of the Arterial pole area. The volume is visualised in the Brightfield. Sparse Tom+ cells are present in the ventricle. (E-E'³) heart sections of the area near the asterisk in E show that these cells are LECs (CD31 +, Lyve1 +, Prox1+). (F-F') Wt1-Cre lineage tracing of heart sections at E16.5. (F) Section of the base of the pulmonary artery. (F') High magnification of the boxed area in F showing that LECs are not GFP +. All scale bars: 100 μ m. Ao: Aorta; PA: Pulmonary artery; RV: Right ventricle; LV: Left ventricle; RA: Right atrium; (A,E'³).

To further validate these observations at lower recombination density, we used the inducible isl1-mER-Cre-mER mouse line with the Td-tomato reporter. In order to verify that posterior SHF progenitors are responsible for the development of ventral LECs, embryos were induced at E9 and harvested at E16.5. About 30% of the hearts analysed presented sparse tomato cells extending from the base of the pulmonary artery to the ventricle (Fig. 15E). Further immunofluorescence experiments on sections, showed that Tom + cells were positive for the pan-endothelial marker CD31 (Fig. 15E'¹) as well as the LEC marker Lyve1 (Fig. 15E'²) and Prox1 (Fig. 15E'³) confirming their LEC nature. Consistent with the SHF-origin deduced from the random clonal analysis study, Tom + cells include SMCs, valvular mesenchymal cells, Fbs, ECs, CMs and AMCs (Fig. 15E'³). Surprisingly, the majority of hearts displaying Tom + LECs did not contain proximal AMCs, while previous results showed their presence in E15 clones. These observations suggested a possible incorporation to the pulmonary artery or reconversion of AMCs into LECs between E15.5 and E16.5. In order to address the possible reconversion of proximal AMCs to a lymphatic fate we used the Wt1-Cre mouse line with the mTmG reporter. Hearts were harvested at E16.5 and co-stained for Prox1 and Lyve1. However, no GFP + LECs could be observed (Fig. 15F,F') indicating that WT1-expressing proximal AMCs do not give rise to LECs.

Altogether, these results identify the SHF as an additional source to CV-derived lymphatics for cLECs in the ventral part of the heart.

9. The lymphatic vasculature of Tbx1 null-mice is altered in the dorsal part of the heart but fails to form in the ventral part of the heart

Tbx1, is essential for SHF deployment and Tbx1 mutants present defects of the lymphatic vasculature (Chen et al., 2010). We thus sought to understand if Tbx1 mutation could cause defects specifically in SHF derived cardiac lymphatic vessels. To investigate whether Tbx1 loss of function would cause defects specific to the ventral cardiac lymphatic vasculature, we studied the hearts of Tbx1 mutant embryos. Tbx1^{-/-} hearts were harvested at E16.5, sectioned and stained by immunofluorescence for Lyve1, Prox1 and CD31 proteins (Fig. 16C-D''). WT littermates followed the same procedure and were used as controls (Fig. 16A-B''). As described in the literature, the hearts of Tbx1 mutants presented a common arterial trunk (CAT). The study of the three markers, identified extra-cardiac lymphatics located cranially to both the ventral and dorsal parts of the heart (Fig. 16A,A',B,B',C,C',D,D'). The presence and distribution of these extra-cardiac vessels was similar in mutant and WT hearts (Fig. 16A,A',B,B',C,C',D,D'). In the dorsal part of Tbx1^{-/-} hearts, we observed lymphatic vessels that seemed slightly less developed than in the dorsal part of WT hearts (Fig. 16B-B'',D-D'', E). The number of Prox1 +/CD31 + cells in the dorsal part of Tbx1^{-/-} hearts also seemed to be smaller, indicating a reduced cellularity of mutant lymphatic vessels (Fig. 16F), however, these observations were not found to be statistically significant. While the ventral part of WT hearts was covered of lymphatic vessels, in contrast, the ventral part of Tbx1 mutants displayed more severe defects than the dorsal part. Even though numerous Lyve1 + cells were observed (green) in the ventral part of Tbx1^{-/-} hearts, none co-localized with CD31 and Prox1 markers (Fig. 15A,A''¹, A''² arrowheads). The morphology of these Lyve1 + cells indicates that they are most likely Lyve1 + macrophages (Maruyama et al., 2005; Schledzewski et al., 2006). The ventral surface of Tbx1^{-/-} hearts was therefore completely devoid of LECs (Fig. 16E,F). The CAT of one of four mutant embryos presented immature lymphatic vessel

structures in the wall of the CAT which suggests that LECs form but fail to expand towards the ventricle. These results show that the cardiac lymphatic vasculature of Tbx1 mutants is more severely altered in the ventral part of the heart than in the dorsal part of the heart. Given the role of Tbx1 in deploying SHF progenitors at the arterial pole of the heart, these results support the involvement of the SHF in ventral cardiac lymphatic development.

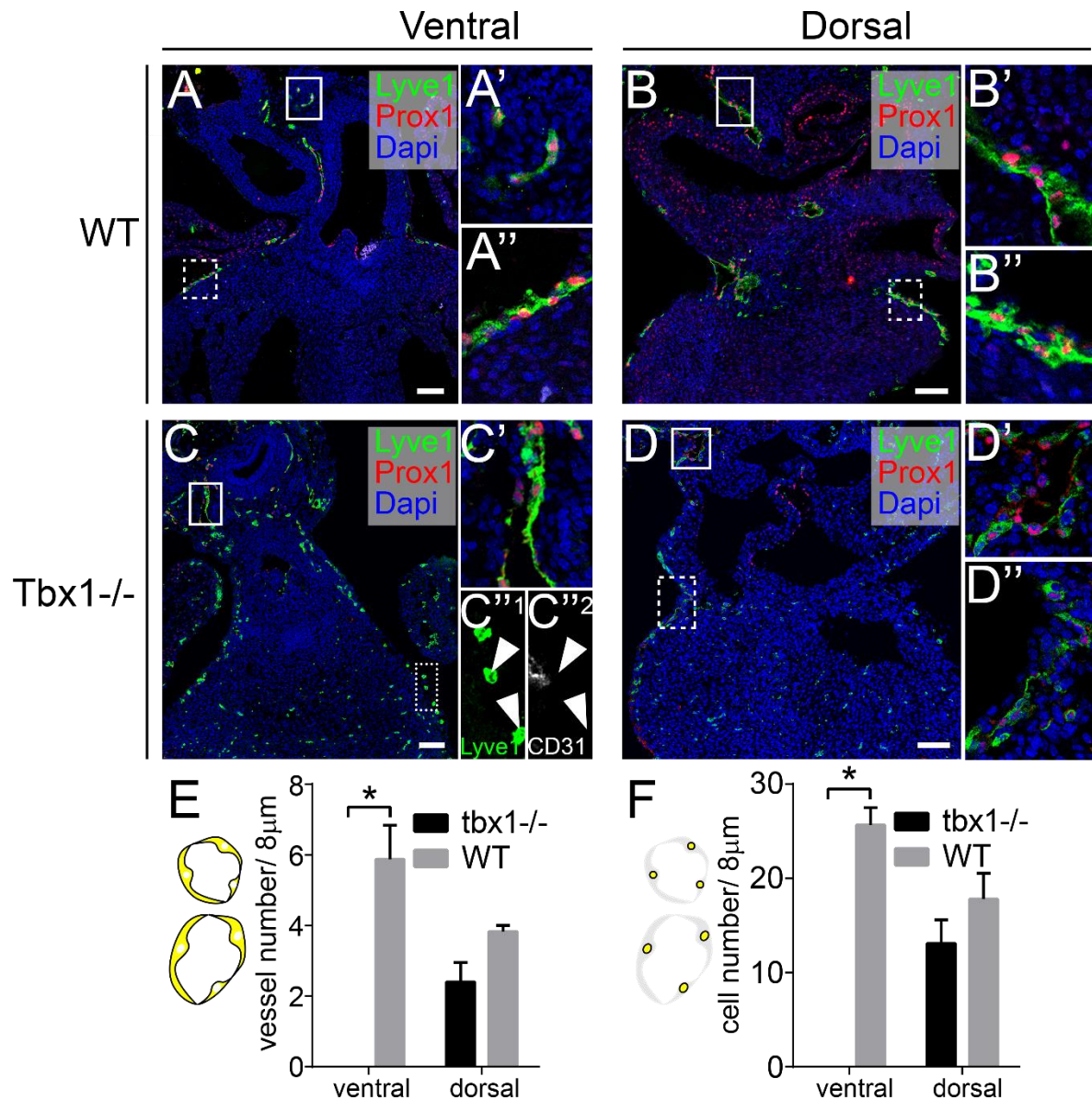


Figure 16. Tbx1^{-/-} hearts exhibit more severe ventral lymphatic defects than dorsal lymphatic defects

(A-B') Sections of WT hearts. (A) Ventral view. (A') high magnification of solid boxed area in A showing extra-cardiac LECs (Prox 1 +; Lyve1 +). (A'') high magnification of dashed boxed area in A showing cardiac LECs. (B) Dorsal view. (B') high magnification of solid boxed area in B showing extra-cardiac LECs. (B'') high magnification of dashed boxed area in A showing cardiac LECs. (C-D'') Sections of Tbx1^{-/-} hearts. (C) Ventral view. (C') high magnification of solid boxed area in B showing extra-cardiac LECs (Prox 1 +; Lyve1 +). (C''1) and (C''2) are high magnification of dashed box in C, showing that Lyve1 + cells (arrowheads) are not LECs (CD31-). (D) Dorsal view. (D') high magnification of solid boxed area in D showing extra-cardiac LECs. (D'') high magnification of dashed boxed area in D showing cardiac LECs. (E) LEC number/ section. No Lymphatic vessels were found in the ventral part of Tbx1^{-/-} embryos. (F) LEC number/ section. No LECs were found in the ventral part of Tbx1^{-/-} embryos. All scale bars: 100 μm.

11. The Pulmonary artery contains a lymphovasculogenetic niche of progenitors

These results together with data from the previous experiments suggest that SHF progenitors recruited to the mesothelial/sub-mesothelial region of the base of the PA. These progenitors might then become specified and LECs contribute to lymphangiogenesis in the ventral side of the heart. We next sought to address this hypothesis. To test this hypothesis and confirm the nature of lymphatic progenitors in this area, we performed tissue grafting and tissue culture techniques. We used E14.5 Wt1-Cre; Rosa26-mTmG hearts as fluorescent tissue donors and the hearts of their WT littermates as recipients (Fig. 17A). In these donor hearts, the mesothelial layer is GFP +, while the sub-mesothelial layer is Tom +. Portions of the mesothelial/sub-mesothelial layers of the proximal PA from donor hearts were peeled off. They were then transplanted onto the hearts of WT littermates in the area of the ventricle where the first ventricular lymphatic vessels are observed at E15.5 (ventricle portion under the base of the PA) (Fig. 17A,B). As a control, the epicardium and sub-epicardium of fluorescent donors was dissected from the same area and transplanted onto WT hearts (Fig. 17A,D). Transplanted hearts were then placed in culture for three days. In the donor tissue, un-recombined sub-mesothelial cells stay Tom + while recombined mesothelial cells are GFP + (Fig. 17A). It is thus possible to distinguish the fate of AMCs and epicardial cells (EpiCs), both GFP +, from the fate of sub-AMCs and sub-epicardial cells respectively, both Tom +. The heart sections of control transplants exhibited in most cases an “epicardial-like” layer made of GFP + cells continuous with the recipient’s epicardium (Fig. 17E,E’ white arrowheads, G). PA transplants, in contrast, showed much fewer cells staying on the outer surface of the heart (Fig. 17C,C’ dashed line G), indicating an increased invasive activity of AMCs with respect to EpiCs. Cells deriving from the Wt1 lineage (GFP +) predominate among those invading the myocardium in the case of epicardial orthotopic transplants (Fig. 17E,E’,G) while PA transplants showed a similar proportion of invading cells from the Wt1+ lineage (GFP +) and from the sub-mesothelium (Tom +). We performed an immunofluorescence staining for the lymphatic marker *prox1* in order to assess the presence of lymphatic cells derived from the transplant. In epicardial

transplants we did not find any Prox1 + cell derived from either GFP + or Tom + cell (Fig. 17C,E,E',F), however Prox1 + cells could be found in sub-epicardial cells of the host heart (Fig. 17E black arrowhead). In PA transplants GFP + cells of mesothelial origin did not contribute to Prox1 + cells, in contrast, the Tom + cells of sub-mesothelial origin organised into vascular tubes that expressed Prox1 (Fig. 17C,C' arrowheads, F). Occasionally, Tom + cells were seen in the epicardial layer. This observation agrees with the fact that in the clonal analysis some Prox1 +, WT1 - cells related by lineage with the sub-epicardial lymphatics appear in the epicardium close to the base of the PA. These results confirm that a population of WT1-negative sub-mesothelial cells at the base of the PA have the ability to form coronary lymphatic vessels. Equivalent cell populations in the adjacent epicardium, however, do not have this ability.

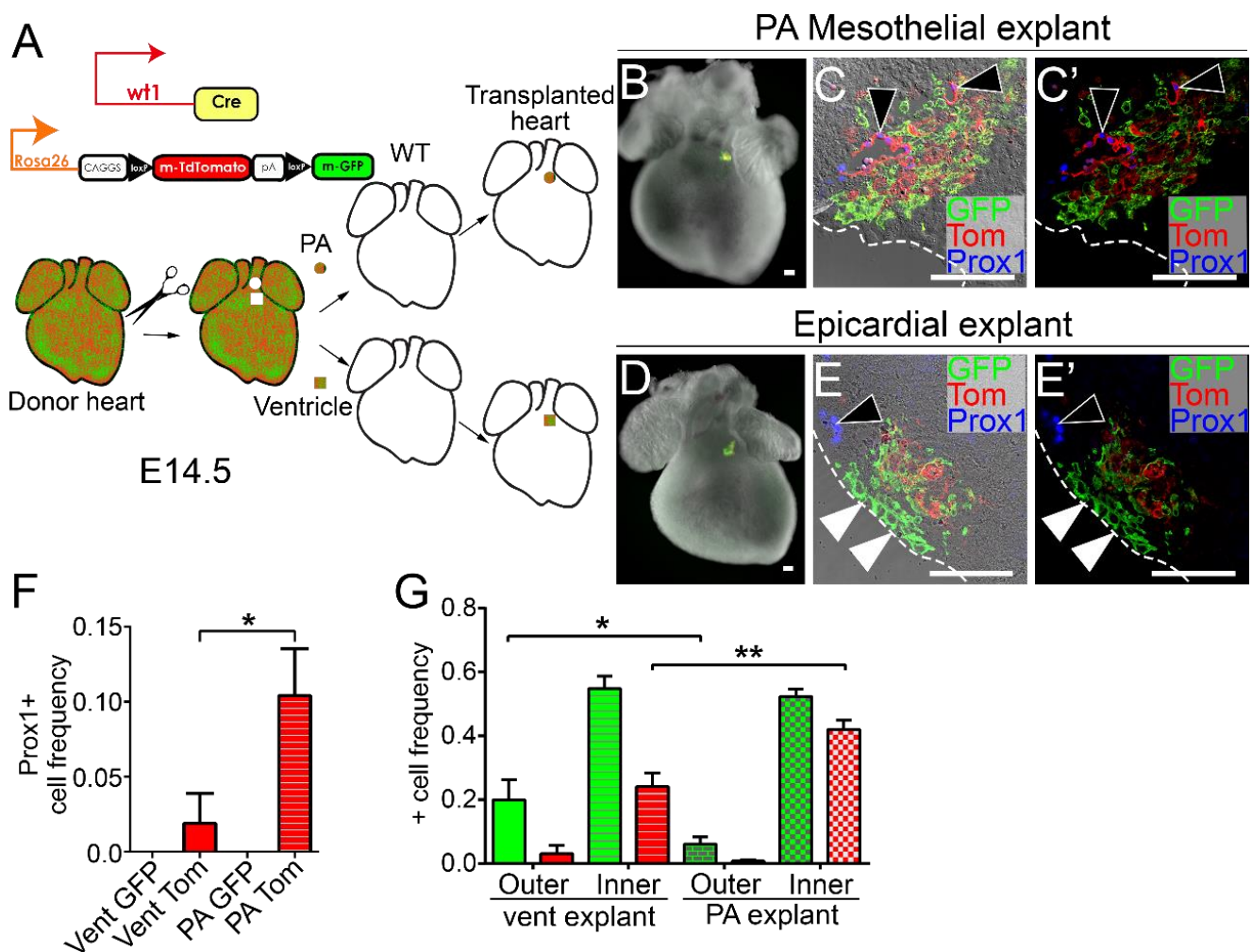


Figure 17. Pulmonary artery sub-mesothelium transplants give rise to lymphatic vessels.

(A) Wt1-Cre; mTmG mouse embryos were harvested at E14.5. Wt1-Cre; mTmG double heterozygous embryos were used as donors since they express GFP in the epicardium and AMCs. They also express Tomato in the sub-epicardium and the arterial sub-mesothelium. Their WT littermates were used as non-fluorescent recipients. The mesothelium of the PA (circle, homotypic) or the Epicardium of the ventricles (square, heterotypic) were transplanted into the ventricle of recipient hearts, at the base of the PA. (B) Whole mount picture of a heart with a heterotypic transplant. (C) and (C') are sections of the transplanted heart with and without the brightfield channel respectively. The dashed line represents the border of the epicardium. Tom +, Prox1 + LECs formed vascular tubes (black arrowhead). (D) Whole mount picture of a heart with a homotypic transplant. (E) and (E') are sections of the transplanted heart with and without the brightfield channel respectively. The dashed line represents the border of the epicardium. (E) Prox1 was expressed in the host tissue but not in the explant (black arrowhead). The epicardial cells of the explants form an epicardial layer continuous with the host's epicardium (White arrowheads). (F) Number of Prox1 + cells from the donor. The cells of the heterotypic donor formed LECs. (E) Distribution of fluorescent donor cells in the outer and inner layers of the heart. Heterotypic donor cells mostly invaded the heart. All scale bars: 100 μ m. PA: Pulmonary artery; Vent: Ventricle.

12. The mesothelium and sub-mesothelium of the arteries exhibit lower Raldh2 levels than their ventricular counterparts

Our results suggest that the proximal sub-mesothelium/mesothelium of the PA is a vasculogenic niche for the specification of SHF-derived ventral cLEC progenitors. In order to understand better the molecular cues that drive lymphatic specification in that region, we decided to identify differentially expressed genes between the arterial mesothelium/sub-mesothelium and the epicardium/sub-epicardium.

The mesothelium/ sub-mesothelium of the arteries and the epicardium/sub-epicardium of the ventricles of WT hearts was peeled off to study their respective transcriptome by RNA sequencing (Fig.18). Interestingly the mesothelium of the arteries presented a 3-fold decrease in Raldh2 expression compared to the epicardium of the ventricle (P-value: 0,0004). These results are similar to what was previously reported in chick embryos (Pérez-Pomares et al., 2003). Interestingly, analysis of RNA samples with the ingenuity pathway software showed an active network for endothelial cell movement and

vasculogenesis in AMCs and sub-AMCs (Fig. 18 A). In addition, analysis of upstream regulators showed inhibition of Wt1 gene and activation of the EMT-related gene Twist suggesting a loss in epithelial integrity (Fig. 18 B).

A

Top Regulator Effect Networks			
ID	Regulators	Disease & Functions	Consistency Score
1	BMP4,CRTC3,ESRRA,HBA1/HBA2,Hbb-b1,SKI,TRAP1	Biosynthesis of nucleoside triphosphate (+3 more)	9.827
2	CRTC3,ESRRA,KDM8,PCGEM1	Concentration of ATP (+1 more)	7.25
3	COMMD1,ESRRA,HBEGF,Hif1,KDM8,LONP1,PCGEM1	Concentration of ATP	6.455
4	BMP15,BMP6,HOXD3,MRTFB,PLIN5,RNF111	Cell movement of endothelial cells,Vasculogenesis	5.942
5	ESRRA,FOXO1,KDM5A,PIK3R1,REST	Biosynthesis of nucleoside triphosphate (+2 more)	5.63

B

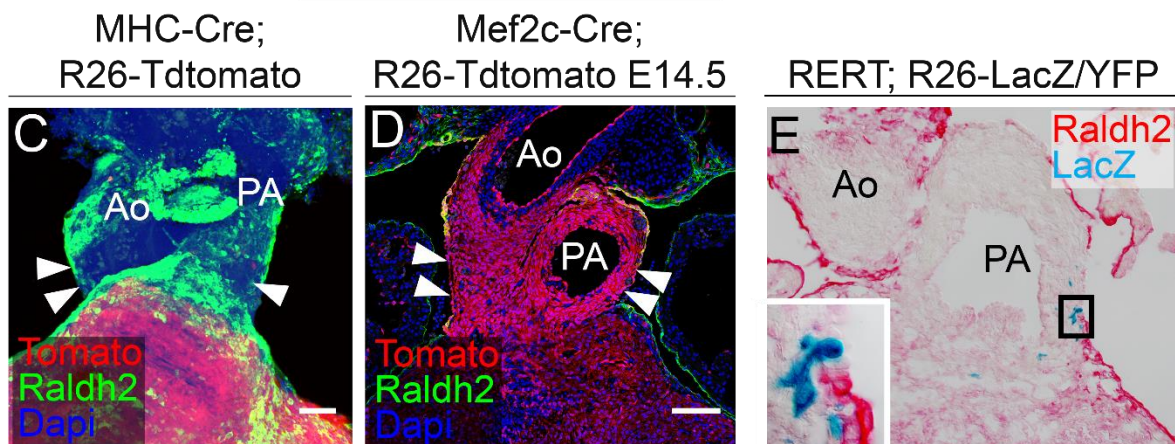
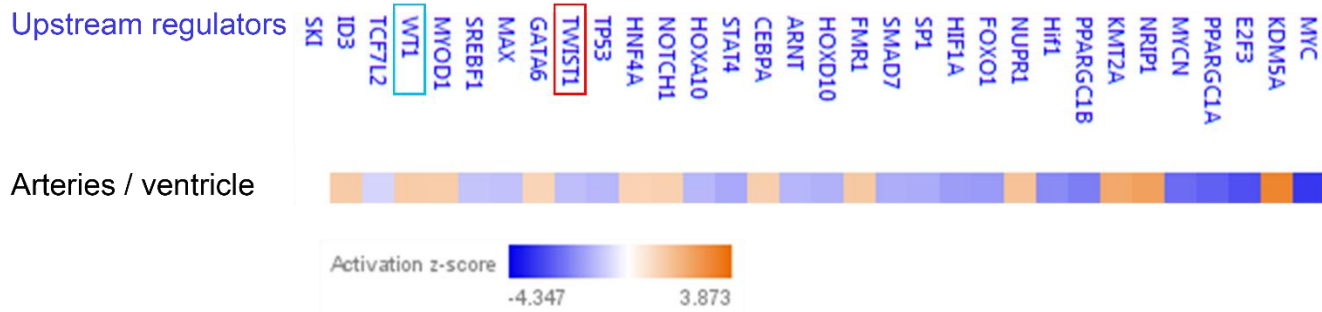


Figure 18. AMCs express low levels of Raldh2 compared to the epicardium

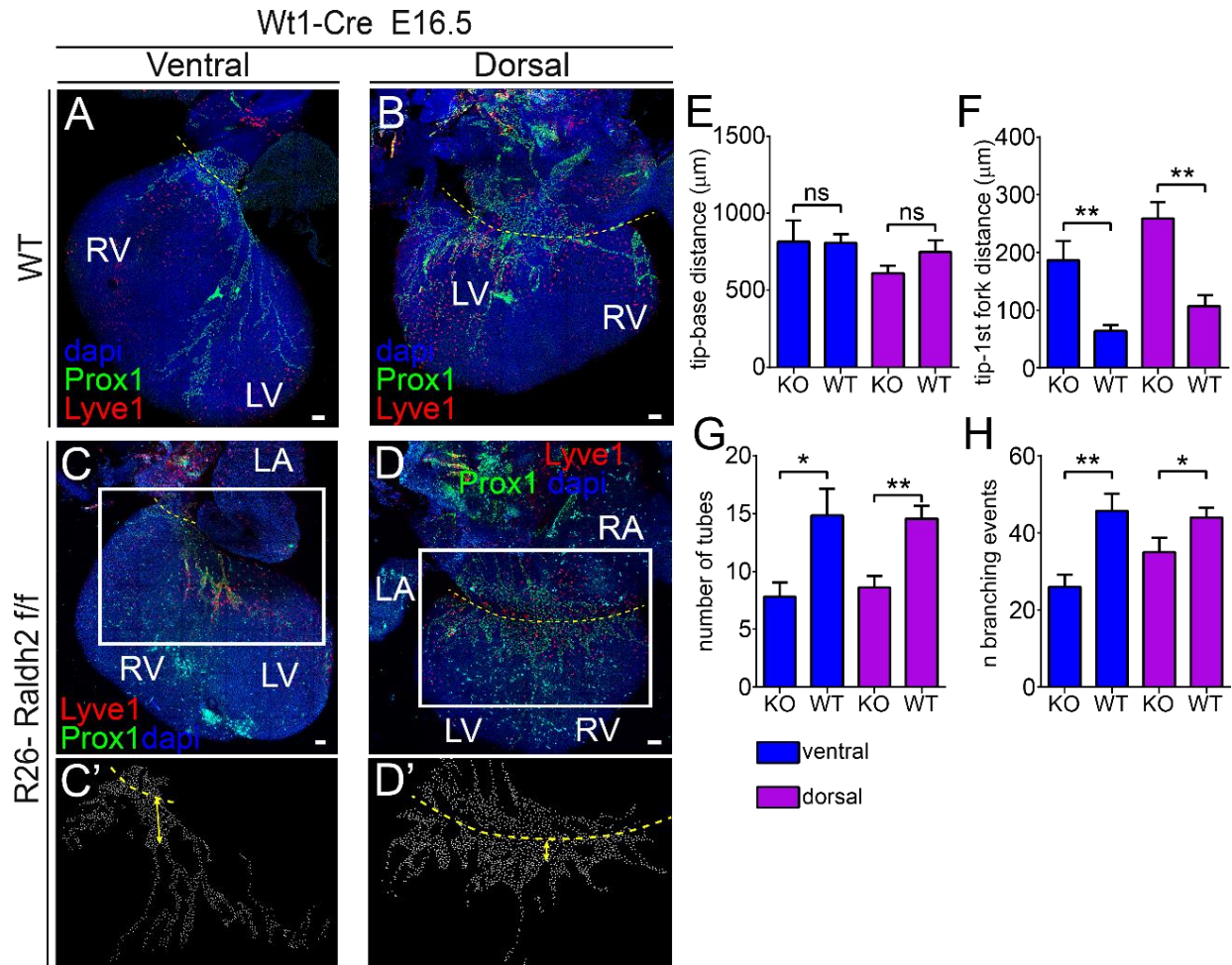
(A) Ingenuity pathway analysis of the regulator networks activated in AMCs as compared to epicardial cells of the ventricle. (B) Ingenuity pathway analysis of the upstream regulators activated and inhibited in AMCs as compared to epicardial cells of the ventricle. (C-E) All images were acquired in the OFT part of the heart at E14.5 (C) E14.5 heart showing the myocardium in red and Raldh2 expression in the heart epicardium and arterial mesothelium. The arrowheads point at low Raldh2 areas. (D) Mef2c-AHC-Cre used as a reference to identify

To confirm the results obtained by RNAseq, we studied *Raldh2* expression in the OFT at E14.5. MHC-Cre;Tdtomato hearts were used in order to identify the myocardium (in red) and were immuno-stained for RALDH2 protein (in green) (Fig.18C). Analysis of such hearts in whole mount showed that overall, epicardial cells and AMCs express high levels of RALDH2 (green), with the exception of the proximal AMCs (Fig.18C arrowheads), which exhibited lower to undetectable levels of RALDH2 (Fig.18C). To corroborate these observations, we employed the Mef2c-AHF-Cre; Rosa26-Tdtomato mouse line as a reference to distinguish AMCs (Tom +) from the epicardium. Hearts were sectioned and immuno-stained for RALDH2 protein at E14.5. As expected, a substantial portion of AMCs at the border with the myocardium exhibited low levels of RALDH2 (Fig.18D arrowheads). These data prompted us to wonder if proximal AMC clones include cells from the RALDH2-low zone. Hearts from the random clonal analysis were thus immuno-stained for RALDH2 (in pink) (Fig.18E). AMC cells belonging to clones containing AMCs and sub-epicardial cells invading the myocardial area were found located in the area with low RALDH2 levels (Fig. 18E). The singular behaviour of this mesothelial niche at the base of the PA therefore correlated with the only mesothelial areas of the whole cardiac region that do not express RALDH2, raising the possibility that low RA levels condition this niche.

13. RA signalling plays a role in cardiac lymphatic development and maturation

We next investigated whether Retinoic acid (RA) signalling was implicated in the specification of lymphatic progenitors. RA signalling has been shown to be essential for lymphangiogenesis at early stages (Bowles et al., 2014). In addition, RA is known to be important for the maturation and patterning of blood vascular cells (Lai et al., 2003; Wang et al., 2018b). We therefore hypothesised that low *Raldh2* levels might enable specification and expansion of LEC progenitors, while high *Raldh2* levels could promote angiogenesis and maturation of the lymphatic plexus in the ventricles.

To study the role of RA signalling in cardiac lymphatic vessel formation, we used embryos in which WT1-Cre drives the recombination of a *Raldh2* conditional Knock-Out (KO) allele in epicardial cells and AMCs. We sought to compare the state of maturation and remodelling of lymphatic vessels in mutant hearts compared to their WT littermates. Hearts were harvested at E16.5 and stained by immunofluorescence with Lyve1 and Prox1 antibodies. Additional immunofluorescence with Raldh2 antibody showed the total absence of RALDH2 protein in the mesothelium of mutant hearts compared to WT hearts (Fig S7). Mutant hearts exhibited altered lymphatic vasculature patterns in both ventral and dorsal parts of the heart (Fig. 19C-D') compared to Wild types (Fig. 19C-D). The state of maturation and patterning of a vascular plexus can be assessed looking at its degree of complexity. We thus analysed phenotypic markers of maturation such as the number of vascular branches, branching events and tubes (region in the centre of anastomosed branches). In general, the mutant lymphatic tree seemed more immature and with thicker vessels (Fig. 19A-B'). The base of the PA in the ventral part (Fig. 19A,C,C' dashed line) and the atrioventricular groove in the dorsal part of the heart (Fig. 19B,D,D' dashed line) were used as a reference to quantify the distances of the cardiac lymphatics. Even though KO lymphatic vessels generally reached the same total length as WT lymphatic vessels (Fig. 19E), the average distance from the base of the heart to the first lymphatic forks was bigger in the mutants (Fig. 19C',D', arrows F). This means that at the base of the PA and in the dorsal atrio-ventricular groove the lymphatic vasculature of WT hearts splits into various branches while mutant lymphatic vessels form extended sac-like structures before forming branches (Fig. 19D,D'). This suggests that the lymphatic vasculature of KO hearts is less remodelled than that of WT hearts. Consistently, KO hearts formed less lymphatic vascular tubes (Fig. 19G) and generated fewer branching events (Fig. 19H) than WT hearts. We have thus shown that epicardial RA signalling has an effect on the maturation of the cardiac lymphatic plexus. To confirm these observations, we aimed to perform the reciprocal experiment by exposing embryonic hearts to an excess of RA.



Since the part of the lymphatic vasculature derived from SHF progenitors is specified around E14, we decided to inoculate embryos at E13,5 with 6.75 mg of RA. Pregnant mice were either inoculated with RA (Fig. 20A-B') or sesame oil (controls) (Fig. 20C-D') to test two hypotheses. On one hand, we wanted to know if an excess of RA could affect the specification or differentiation of SHF-derived lymphatic progenitors at the base of the PA. On the other hand, we wanted to determine if an excess of RA could affect the ventricular lymphangiogenic process. Hearts were immuno-stained at E15 in whole mount for Lyve1 and Prox1 antibodies. The lymphatic vasculature of RA-treated hearts appeared more branched and composed of thinner vessels than that of untreated animals with an exacerbated effect on ventral lymphatic vessels (Fig. 20A-D, E). In addition, we observed a higher presence of one-cell wide capillaries in the ventral part of the heart (Fig. 20C-C'¹ arrowhead). Treated animals formed more discontinuous vessels and formed more branching events than untreated animals (Fig. 20C-C' arrowheads). In untreated embryos, LECs in the great arteries form sac-like vascular structures with large lumens and appear poorly remodelled compared to lymphatics in the heart (as described in chapter 4) (Fig. 20A-A'²). The LECs of embryos treated with RA formed an organised vascular plexus instead (Fig. 20C-C'²). Indeed, the lymphatic vessels on the PA of treated embryos was more branched (Fig. 20H) and presented more tubes as a result. In the dorsal part of the heart, the lymphatic vasculature seemed less affected (Fig. 20B-D'). However, it presented generally more branches and branching events. Overall, the average size of the branches was also smaller than untreated animals (Fig. 20B'-D').

Overall, it seems that RA triggers the premature remodelling of the cardiac lymphatic vasculature. RA also seems to promote the maturation of cardiac lymphatics since the lymphatic sac-like structures in the PA are not maintained in an immature state in untreated animals. The exacerbated phenotype in the ventral part of the heart is consistent with altered specification of Lymphatic SHF progenitors.

All together, we have shown that RA signalling is an actor of cardiac lymphangiogenesis. It seems that low *Raldh2* levels are necessary for the expansion of lymphatic progenitors (e.g. dilated lymphatic vessels in the case of *Raldh2*^{-/-} embryos)

while RA signalling is most likely responsible of the maturation and patterning of the primary lymphatic vasculature.

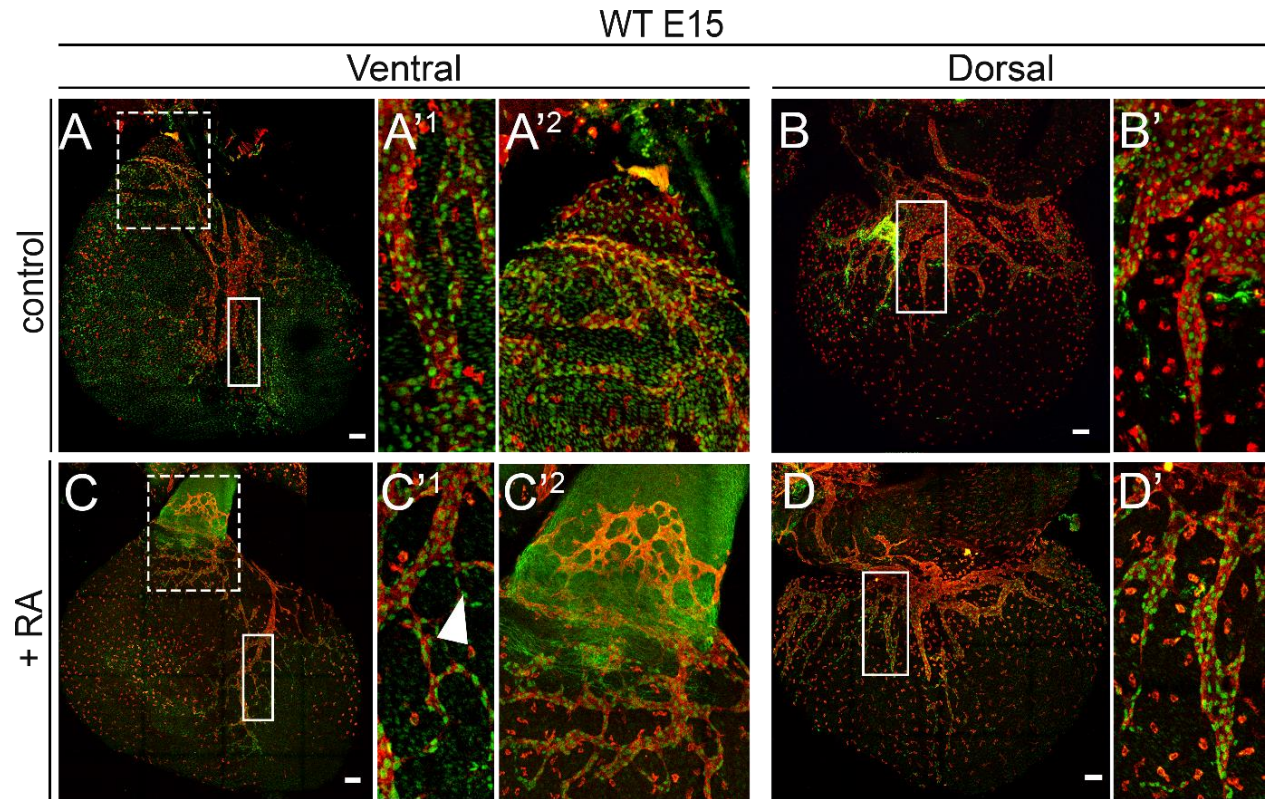


Figure 20. Excessive RA levels trigger the hyper-remodelling of the cardiac lymphatic vasculature

(A-B') Z-projections of untreated E15 hearts. A) Ventral view. (A') high magnification of solid boxed area in A showing the normal vasculature (Prox 1 +; Lyve1 +). (A'²) high magnification of dashed boxed area in A showing the sac like immature pattern of LECs of the Pulmonary artery(B) Dorsal view. (A') high magnification of boxed area in A showing the normal dorsal vasculature (Prox 1 +; Lyve1 +). (C-D') Z-projections E15 hearts treated with RA. C) Ventral view (C') high magnification of solid boxed area in C showing an hypoplastic and hyper-remodelled vasculature. More one-cell wide branches were found (white arrowhead). (C'²) high magnification of dashed boxed area in C showing hyper-remodelling and maturation of the PA lymphatic vasculature vasculature. (D) Dorsal view (D') high magnification of boxed area in D showing showing thinner vessels (Prox 1 +; Lyve1 +). All scale bars: 100 μ m.

As a summary, our results show that the SHF on one hand gives rise to the smooth muscle and the endothelium of the great arteries through EMT of distal AMCs. On the other hand, the second heart field gives rise to proximal AMCs together with sub-mesothelial lymphatic progenitors. These lymphatic progenitors in turn, start their

specification and differentiation at a localized vasculogenic niche of low-RALDH2 AMCs at the base of the PA. From this region, they migrate into the ventricular sub-epicardium and contribute to the ventral cardiac lymphangiogenesis. In parallel, the lymphatic vasculature deriving from the CV colonizes the heart surface by angiogenesis and cells from both origins intermingle exclusively in the ventral part of the heart. Finally, the maturation and patterning of the cardiac lymphatic vasculature is influenced by RA signalling cues from the epicardium.

Supplementary material

RERT-CreER ; Rosa26-LacZ/ YFP
ind E8.5 ex E14.5

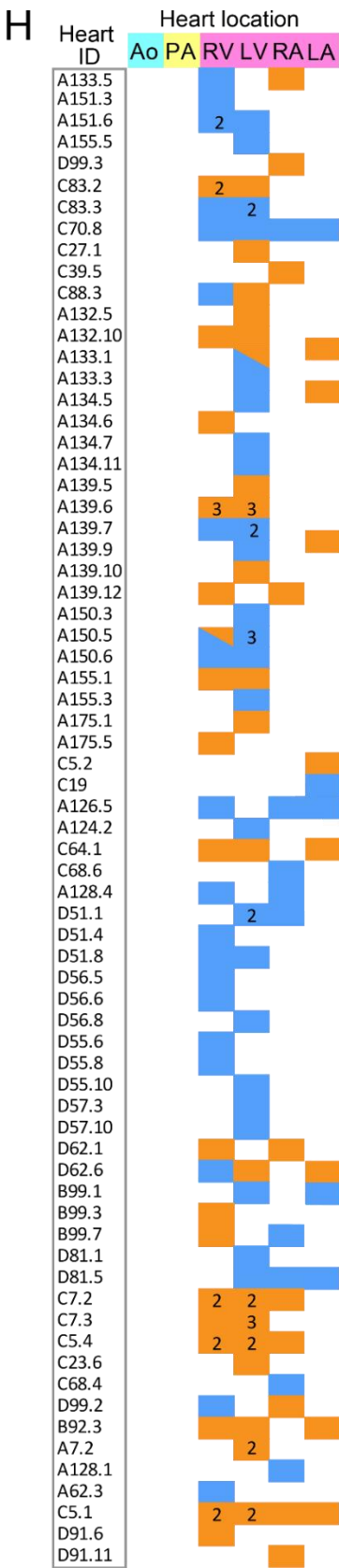
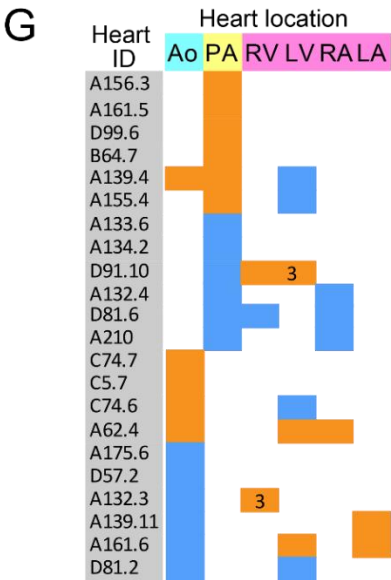
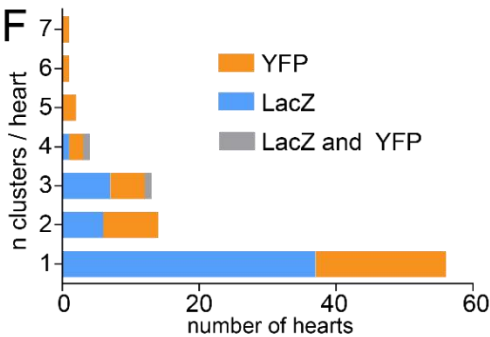
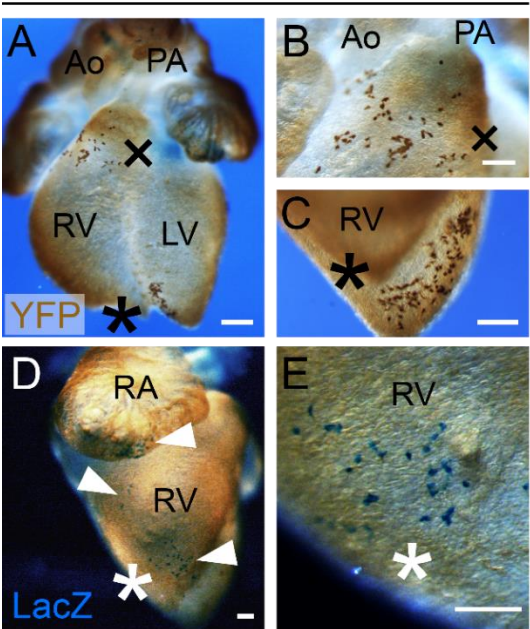


Figure S1. Epicardial and AMC clones

(A) Whole mount ventral view of a heart with YFP+ epicardial clusters. (B) high magnification of the OFT area specified with a cross in A. (C) high magnification of the area specified with an asterisk in A. (D) Whole mount of the lateral view of a heart with LacZ+ epicardial clusters. The arrows point at epicardial clusters (E) high magnification of the area specified with an asterisk in D. (F) Graph representing the number of hearts, in the collection, that present clusters from a range of 1 to 7. (F and H) Analysis of epicardial and arterial mesothelial cluster's colour and location. Hearts are classified by ID (left column). Brown and blue rectangles represent YFP+ and LacZ+ clusters respectively. A rectangle without number is equivalent to the presence of only one cluster. The numbers displayed on the rectangles indicates the respective number of clusters found in that colour. (H) represents all the hearts with epicardial clones but no AMCs in neither the Aorta (Ao) nor the Pulmonary artery (PA). (F) represents all the hearts containing AMC clones in the Ao or the PA and whether they contain epicardial clones too. Scale bar: 200µm (A), 100µm (B-E). Ao: Aorta; PA: Pulmonary artery; RA: Right atrium; LA: Left atrium; RV: Right ventricle; LV: Left ventricle (A-H).

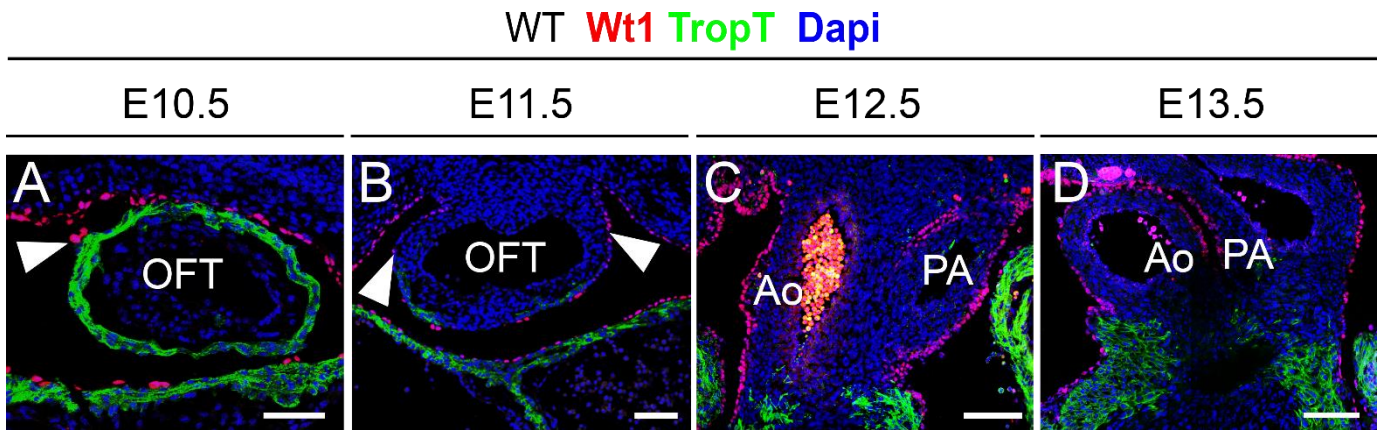
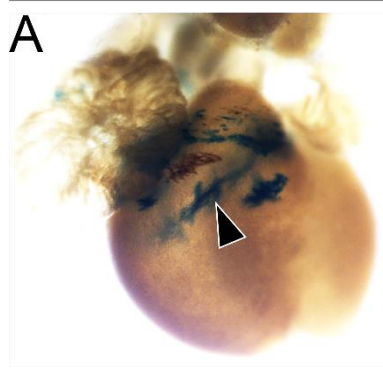


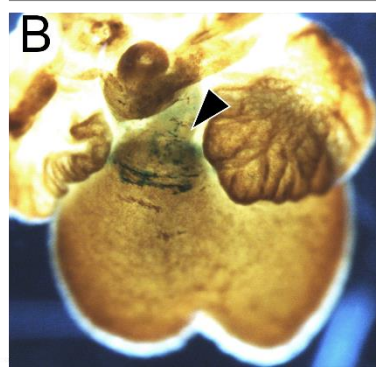
Figure S2. AMCs develop in the OFT of the heart from E10.5 onwards

(A-D) Frontal sections of the Outflow Tract area of WT hearts. The myocardium can be appreciated by immunofluorescence for troponin T (green) and mesothelial cells by immunofluorescence for Wt1 (red). (A,B) Arrowheads point at arterial mesothelial cells. All scale bars: 100µm. OFT: Outflow Tract (A,B). Ao: Aorta; PA: Pulmonary artery (C-D).

isl1-mER-Cre-mER; R26-**LacZ**; R26-**YFP** E14.5
ind: E8.5



ind: E9



Hoxb1-Cre; R26-**YFP** E14.5

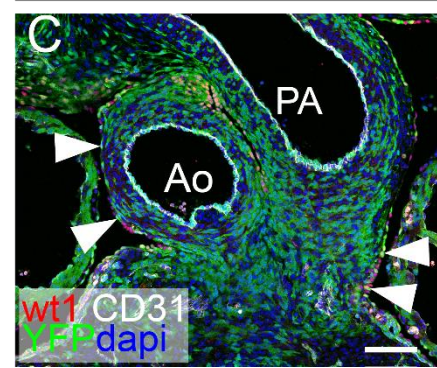


Figure S3. AMCs are derivatives of the posterior SHF

(A-B) Lineage tracing of early and late isl1+ progenitors. (A) Representative heart induced at E8.5 where most labelled cells are localised in the right ventricle (black arrowheads). (B) Representative heart induced at E9 where most labelled cells are localised in the great arteries and OFT area (black arrowheads). (C) Lineage tracing of Hoxb1+ progenitors with the YFP reporter (Green). We can appreciate the presence of YFP +Wt1 + AMCs in the Aorta as well as the pulmonary artery (white arrowheads). scale bar: 100µm. Ao: Aorta; PA: Pulmonary artery (C).

		Cell type																											
			reporter	Ms only	SM only	Fb only	EC only	CM only	valv only	SM/Fb	SM/Fb	SM/valv	EC/valv	EC/Fb	CM/Fb	CM/valv	Ms/Fb/SM	SM/CM/valv	SM/EC/Fb	Ms/Fb/valv	Ms/Fb/EC/SM	EC/SM/valv/CM	SM/Fb/valv/CM	EC/Fb/valv/CM	Ms/Fb/SM/valv	Ms/Fb/SM/CM/valv	Ms/Fb/EC/SM/valv	Ms/Fb/EC/SM/CM/valv	Ms/Fb/EC/SM/CM/valv
Ao	LacZ	0	2	0	4	1	2	1	3	3	0	0	0	0	0	2	0	0	0	2	0	0	0	0	0	0	1	1	1
	YFP	0	3	1	3	0	0	2	1	1	0	0	0	0	0	1	0	0	0	2	0	0	0	0	0	0	0	0	0
	both	0	0	0	0	0	0	1	0	0	0	1	0	1	0	1	0	0	0	0	0	0	0	0	0	0	1	0	0
PA	LacZ	0	4	2	1	5	0	0	1	1	1	1	1	1	1	1	1	1	0	0	1	0	0	1	6	0	0	0	
	YFP	0	1	2	2	0	1	0	1	0	0	0	0	0	0	0	0	0	1	0	0	0	1	0	0	0	0	0	
	both	0	0	0	0	0	0	0	0	0	0	0	0	0	1	0	0	0	0	0	0	1	0	0	0	0	0	0	

Ao Aorta

PA Pulmonary artery

Ms Mesothelial cells

SM Smooth muscle cells

Fb Fibroblasts

EC Endothelial cells

CM Cardiomyocytes

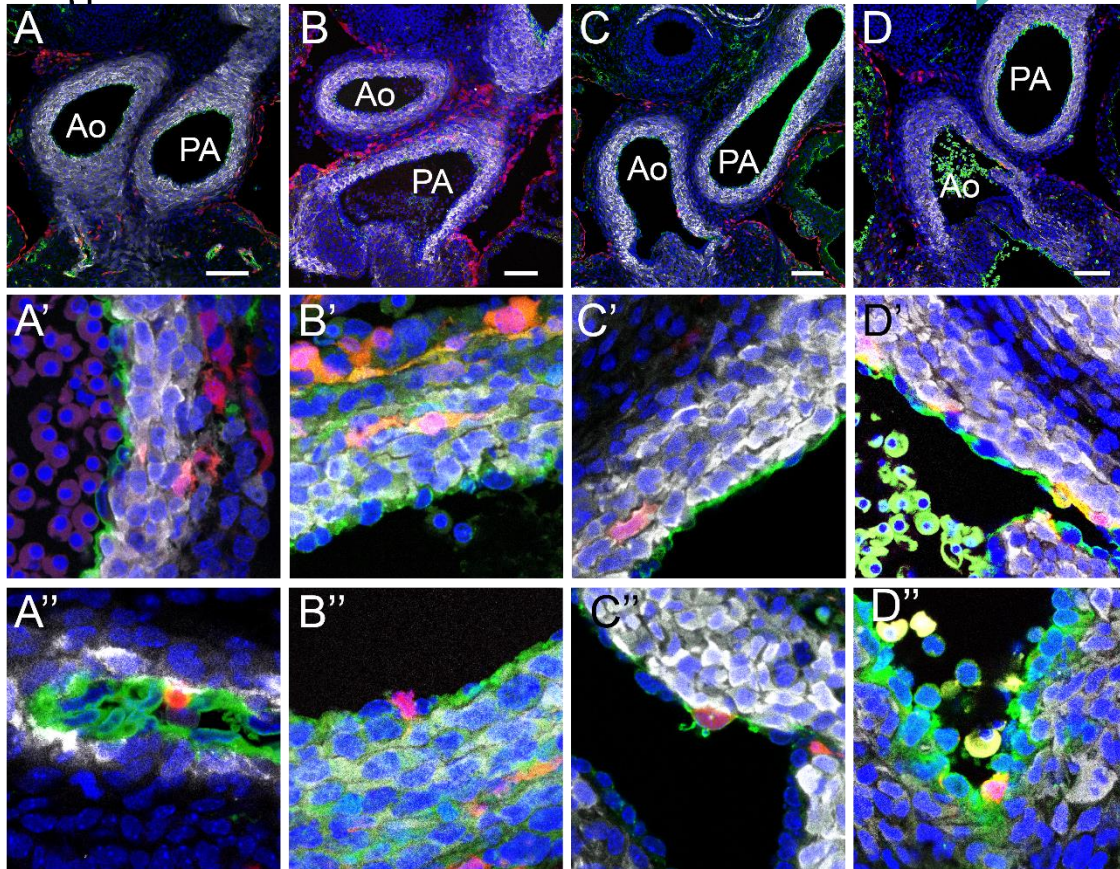
valv valvular mesenchymal cells

Figure S4. AMCs are clonally related to cells of the great arteries

The table represents the composition of cell clusters in the Aorta (Ao) and Pulmonary artery (PA). Each number represents the number of groups observed. The colours refer to the type of reporter expressed. This data together with show that arterial mesothelial cells are clonally related to cells of the great arteries.

Wt1-CreERT2; Rosa26-TdTomato E14.5

Tom CD31 SM22 α Dapi



Wt1-CreERT2 ER TropT Dapi

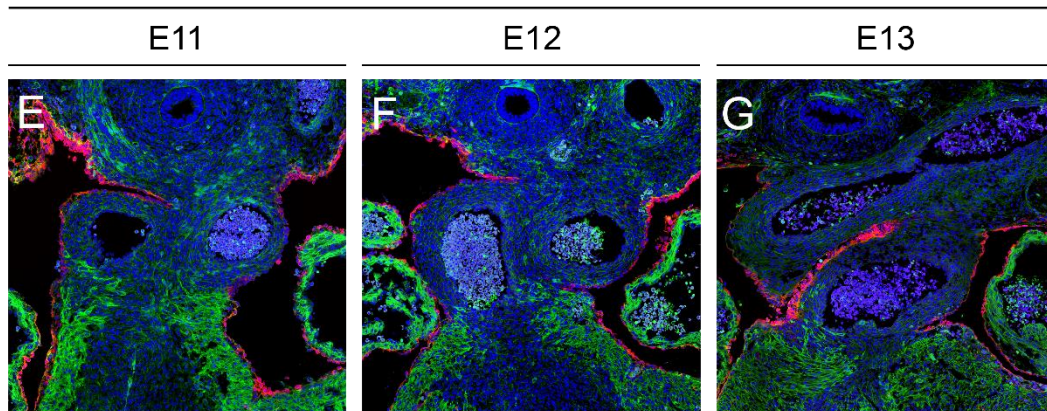
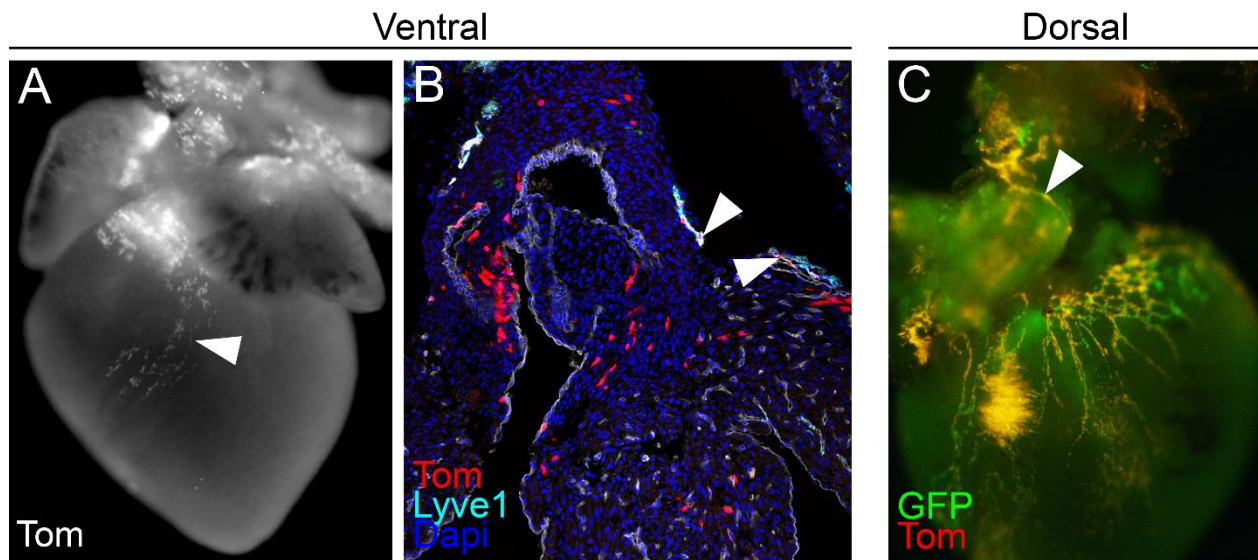


Figure S5. AMCs continuously give rise to SMCs and ECs of the great arteries

(A-D) Wt1-CreERT2 lineage tracing of embryos induced from E9.5 to E12.5 and harvested at E14.5. (A'-D') High magnifications of these hearts in which Tom+ smooth muscle cells (SM22 α +) can be appreciated. (A''-D'') High magnifications of these hearts in which Tom+ endothelial cells (CD31 +) can be appreciated. where most labelled cells are localised in the right ventricle (black arrowheads). (E-G) Localisation of the inducible Cre recombinase visualised by immunofluorescence of the ER protein (Red). ER is expressed in mesothelial cells but not in smooth muscle nor endothelial cells. Scale bars: 100 μ m. Ao: Aorta; PA: Pulmonary artery (A-D).



D

Stage	heart ID	Ventral			Dorsal	n groups with ventral LECs		
		LECs	pAMC	dAMC		ventral LECs	Dorsal LECs	ventral and dorsal
E15.5	AXK125.5	X	X	X		4/240	0/240	0/240
	AXK125.11	X	X	X				
	AXO274.2	X	X	X				
	AXK229.2	X						
E16.5	AXO464.1	X	X	X		4/71	3/71	2/71
	AXO464.6	X		X				
	AXK87.2	X		X				
	AXO460.3	X		X				
	AXO130.6	X	X		X			
	AXO130.4	X	X	X	X			
	AXK130.5				X X			
	AXO471.1				X			
P0	AXK40.6	X		X		1/130	1/130	0/130
	AXO14.2				X			

Figure S6. Analysis of lymphatic groups at various stages

(A-B) Specimens containing fluorescent lymphatic groups generated inducing RERT embryos at E8.5 and harvesting hearts at E16.5. (A) Tomato cells sparsely distributed in the ventral part of the heart (arrowheads). (B) Identification of Tom⁺ cells on sections. (C) Tom⁺ and GFP⁺ dorsal lymphatic clones. Recombined cells are forming a wide and highly organised network. Extra-cardiac GFP⁺ and Tom⁺ lymphatic cells can be observed (arrowheads). (D) Summary of lymphatic groups observed in their colour (Tomato: red or GFP: green crosses). The resulting count out of all hearts of each category is represented in the second half of the table. Overall ventral and dorsal lymphatic groups seem different and mostly arise independently. LECs : Lymphatic endothelial cells, pAMC: proximal Arterial mesothelial cell, dAMC: distal arterial mesothelial cell.

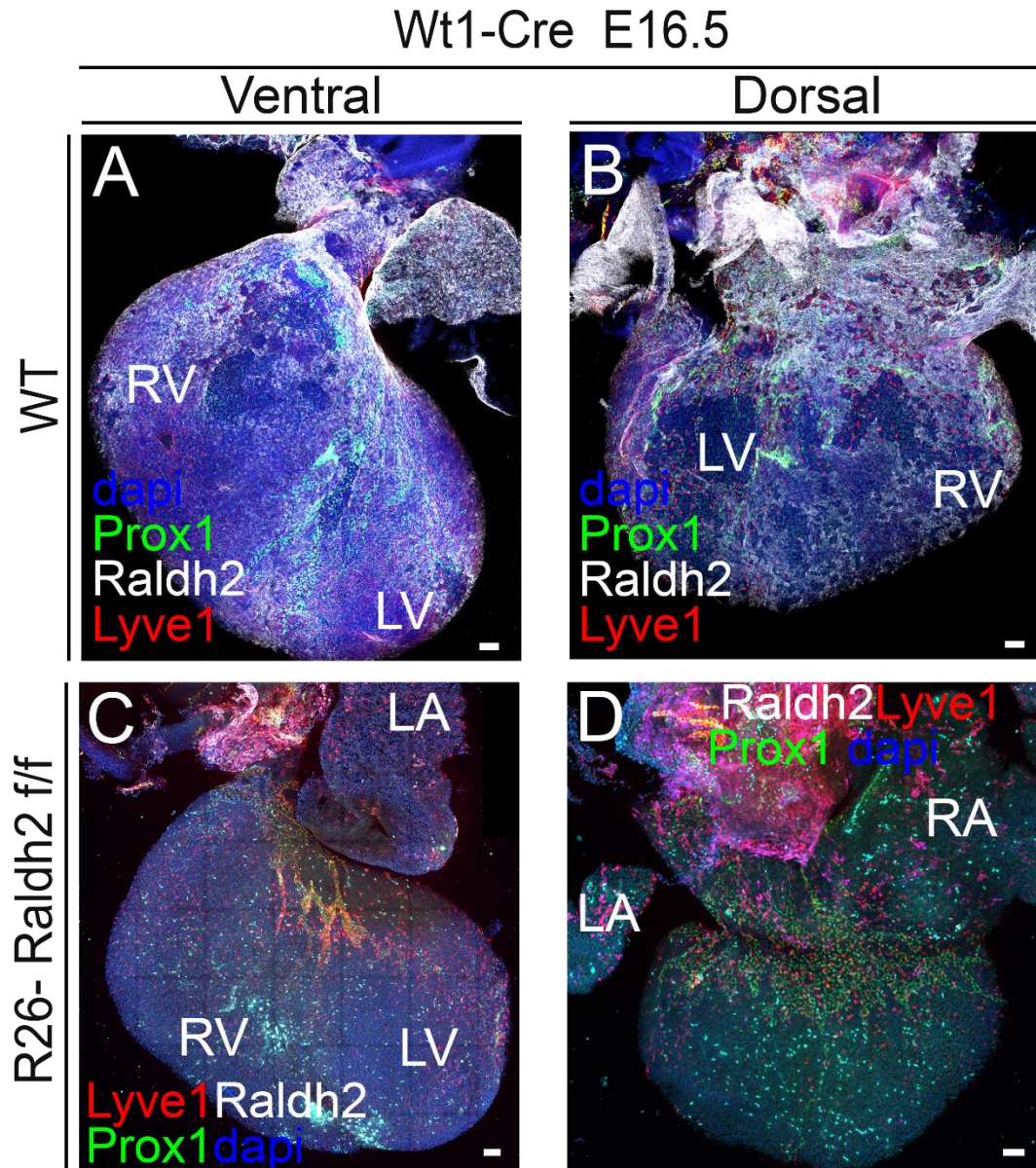


Figure S7. Raldh2 is successfully depleted in the mesothelium of Wt1-Cre; Raldh2 f/f embryos

(A-B) Z-projections of WT E16.5 hearts. (A-B) Ventral view showing normal vasculature (Prox 1 +; Lyve1 +) and normal Raldh2 expression in mesothelial cells. (C-D) Z-projections of Wt1; R26-Raldh2 f/f mutant embryos. They exhibit an abnormal lymphatic vasculature and the complete lack of RALDH2 protein in the epicardium and AMCs. All scale bars: 100 μ m. RV; Right ventricle; LA: Left atrium; RA: Right atrium; LV: Left ventricle.

Material and methods

1. Animal procedures

1.1 Mice strains

Animals were handled in accordance with CNIC Ethics Committee, Spanish laws and the EU Directive 2010/63/EU for the use of animals in research. All mouse experiments were approved by the CNIC and Universidad Autónoma de Madrid Committees for “Ética y Bienestar Animal” and the area of “Protección Animal” of the Community of Madrid with reference PROEX 220/15. For this study, Mice were maintained on mixed C57Bl/6 or CD1 background. The following mouse lines were used:

Cre inducible and constitutive mouse lines:

Polr2a-CreERT2 (RERT)	(Guerra et al., 2003)
Isl1-Cre	(Cai et al., 2003)
Isl1-mER-Cre-mER	(Laugwitz et al., 2005)
Mef2c-AHF-Cre	(Verzi et al., 2005)
Wt1CreERT2	(Zhou et al., 2008)
Wt1Cre	(Wessels et al., 2012)
Hoxb1IRES-Cre	(Arenkiel et al., 2003)
Vegfr3-CreERT2	(Martinez-Corral et al., 2016)

Enhancer trap and Knock outs:

Raldh2L-/-	(Vermot et al., 2003)
Tbx1tm1Pa mice	(Jerome and Papaioannou, 2001)

Enhancer trap and Reporter lines:

Mlc1v-nlacZ-24 (Fgf10-nlacZ enhancer trap)	(Kelly et al., 2001)
R26R-LacZ	(Soriano, 1999)
R26R-EYFP	(Srinivas et al., 2001)
R26R-tdTomato	(Madisen et al., 2010)
R26-mTmG	(Muzumdar et al., 2007)
R26-GFP	(Sousa et al., 2009)

Mice were genotyped by PCR as stated in the original reports.

1.2 Tamoxifen preparation and maternal administration

Tamoxifen for intraperitoneal injection:

For induction of the RERT line, 10mg of 4-Hydroxy Tamoxifen (Sigma) was dissolved in 1ml absolute Ethanol and 9ml corn oil (Sigma) for a final concentration of 1mg/ml. The stock solution was then sonicated for 40 minutes on ice to prevent overheating. The 4-OHT solution was aliquoted and stored at 4°C for up to 4 weeks, and re-sonicated before being administered to mice.

Tamoxifen for oral gavage:

For induction of all the other Cre lines 200mg of Tamoxifen (Sigma) was dissolved in 10ml of corn oil (Sigma) for a final concentration of 20mg/ml (to the exception of VEGFR3-Cre for which mg of Tamoxifen were diluted in sesame oil). The stock solution was then sonicated for 20 minutes on ice. The solution was aliquoted and stored at RT for up to 3 months. Tamoxifen was administered by oral gavage using a 1ml syringe (Beckton Dickinson) via a feeding needle (BD Microlance) in a range of 1 to 4 mg/female.

1.3 Maternal administration of Retinoic acid:

RA was administered to pregnant CD1 mice by oral gavage using a 1ml syringe and a feeding needle. 6.75 mg of crystalline all-trans RA (302-79-4 Sigma) was diluted in 0.8 ml of Ethanol (EtOH) in 9.2 ml sesame oil. The solution was sonicated, aliquoted and stored in the dark at 4°C. Samples were sonicated before being administered to pregnant females. Pregnant mice were administered at E13.5 and E14.5 days of gestation with a 6.75mg RA dose. Control were administered equivalent volumes of the vehicle (i.e., EtOH in sesame oil) at the corresponding times.

1.4 Embryo harvest

Embryos were staged defining the morning of the vaginal plug as embryonic day (E) 0.5. Females were sacrificed by CO₂ inhalation followed by cervical dislocation. Mice embryos were extracted at different developmental stages as follow. The abdominal cavity of sacrificed females was opened to expose the Uterus. The uterus was then placed in ice-cold PBS in a petri dish in order to open the muscle layer, decidual layer and amnion. Once extracted, embryos were decapitated and their thorax opened at the level of the sternum. If the heart needed to be isolated, it was pulled out with forceps. Unless stated differently, all tissues were dissected in ice-cold PBS and fixed in PFA (Merck) 2% in PBS overnight at 4°C.

1.5 Neonatal heart harvest

After their birth, P0 (postnatal 0) mice were decapitated. Their thorax was then cut at the level of the sternum similarly to embryos and their heart pulled out. Hearts were place in ice-cold PBS to remove the lungs and fixed in PFA 2% in PBS overnight at 4°C.

1.6 Clonal analysis

For retrospective clonal analysis, we used mouse embryos with the inducer Polr2a-CreERT2 (RERT) and the reporter R26R-lacZ; R26R-YFP knock-in alleles in heterozygosis. This genotype was generated upon breeding mice that have the inducer and reporter allele in double homozygosis with mice that have the other reporter allele in homozygosis. Random Cre-mediated recombination was obtained using 4-hydroxy-tamoxifen (4OHT) dissolved in corn oil. A single dose of 4OHT (0.1mg, 0.0675mg or 0.05mg) was injected intraperitoneally into pregnant females at E8.5 days of gestation. Recombination triggered either LacZ or YFP expression in single cells and their progeny. The hearts of embryos were dissected and analysed at E14.5, E15 and in neonates at P0. Upon recombination, cells go through cell division and differentiation giving rise to cell

clusters of labelled cells. Out of 737 embryos harvested at E14.5 only 454 showed labelled cells because of low 4OHT induction.

1.7 Mouse blood serum preparation

Mouse blood was collected on sacrificed adult WT mice and serum was prepared as described previously (Greenfield, 2017).

2. Tissue processing

2.1 *In situ* hybridisation on Paraffin sections

2.1.1 Paraffin embedding

Upon ON fixation in 4% PFA at 4°C, embryonic tissues were rinsed several times in PBS, and dehydrated through gradual concentrations of EtOH:H₂O (30%, 50%, 70%, 85%, 90%, 96%, 100%) at room temperature. Samples were washed twice in xylol and twice in paraffin wax at 65°C. Embryos were oriented and embedded in warm paraffin and left at 4°C on to solidify.

2.1.2 *In situ* hybridisation

In situ hybridisation was performed on 7 µm-thick paraffin sections according to previously described protocols (Jostarndt K. et al., 1994; Kanzler B. et al., 1998). After sectioning samples were rehydrated and digested with proteinase K (10 µg/ml) at 37°C for 10 minutes. Riboprobe hybridisation was performed at 65°C ON. Section were washed on the next day, incubated with anti-DIG antibody and developed with BM-purple (Roche, ref. 11442074001). Images were acquired with a Nikon Eclipse 90i microscope.

2.2 Immuno-histochemistry and immuno-fluorescence

2.2.1 Antibodies used for immuno-histochemistry and immuno-fluorescence

Here is an exhaustive list of all the antibodies used for immuno-staining.

Primary antibodies used:

target	Host species	Concentration used	reference
GFP	Rabbit	1:200	632460 Living Colors
GFP	chicken	1:100	ab13970 abcam
GFP	chicken	1:400	GFP-1010 Aves labs
c-TnT	Mouse	1:200	MS-295 Thermo Scientific
CD31	Rat	1:100	553370 BD Pharmingen™
Wt1	Rabbit	1:200	ab89901 abcam
Raldh2	Rabbit	1:200	ab96060 abcam
CD140 α	Rat	1:100	558774 BD Pharmingen
SMAcy3	Mouse	1:400	C6198 Sigma
SM22 α	Rabbit	1:200	ab14106 abcam
Prox1	Goat	1:300	AF2727 R&D systems
Lyve1	Rabbit	1:200	103-PA50S ReliaTech
Lyve1	Rat	1:100	103-M130 ReliaTech
ER	Rabbit	undiluted	ab27595 abcam
β -galactosidase	Rabbit	1:500	56031 Cappel
Periostin	Rabbit	1:200	NBP1-30042 novusbio
Podoplanin	Hamster	1:200	10R-P155a Fitzgerald
Calponin	Rabbit	1:200	Ab46794 abcam

Secondary antibodies used:

Species reactivity	Conjugate	Concentration used	reference
Rabbit	633	1:500	A21071 life technologies™
chicken	488	1:500	A11039 life technologies™
Mouse	633	1:500	A21052 life technologies™
Rabbit	488	1:500	A11034 life technologies™
Rabbit	568	1:500	A11036 life technologies™
Rabbit	594	1:500	A11012 life technologies™
Mouse	488	1:500	A11029 life technologies™
Mouse	594	1:500	A11005 life technologies™
Mouse	568	1:500	A11004 life technologies™

Mouse	488	1:500	A11029 life technologies TM
Mouse	HRP	1:200	P 0447 Dako
Rabbit	HRP	1:200	P 0448 Dako
Rabbit	Biotin		111-066-003 Jackson ImmunoResearch

2.2.2 Whole mount immuno-histochemistry for the detection of clones

To visualize LacZ+ clones in whole mount, β -galactosidase (β -gal) activity staining was performed as previously described (Torres, 1997). Embryos were post-fixed in 4% paraformaldehyde (PFA).

To visualise YFP+ clones, hearts went through a two-step process follow:

-Whole mount immuno-staining (common protocol for immuno-histochemistry and immuno-fluorescence)

Hearts were permeabilised using 0.5% Triton X-100 in PBS overnight (ON) at 4°C. Hearts went through a process of endogenous peroxidase quenching using 0.03% hydrogen peroxide (H₂O₂) in PBS at room temperature (RT). Hearts were then blocked in PBST (PBS triton 0.1%) with 10% goat serum for 3 hours at RT. The samples were incubated for 3 days with the primary antibody (anti green fluorescent protein, living colors) at 4°C. Samples were washed in PBST for 3 hours and incubated in a biotinylated secondary antibody (Jackson ImmunoResearch) for 2 days at 4°C. Samples were finally washed for an extra 3 hours at RT.

-3,3'-diaminobenzidine (DAB) histochemistry (for whole mount and sections)

YFP signal was amplified with the Vectastain ABC Peroxidase kit and detected using the DAB Vectastain Elite ABC Kit. All procedures were performed as advised by the manufacturer.

As a result, YFP + cells and LacZ + cells could be observed as brown and blue labels respectively. Hearts were then stored in 80% glycerol at 4 °C.

Kits used:

Kit	Reference
Dako liquid DAB + substrate	K3468 Dako
Vector DAB peroxidase substrate	SK-4100KI01, Vector Laboratories
Vector Red alkaline phosphatase kit	SK-5100, Vector Laboratories
Vector VIP peroxidase substrate	SK-4600, Vector Laboratories
Vectastain Elite ABC HRP Kit	PK-6100, Vector Laboratories
Vectastain ABC Alkaline phosphatase	AK-500, Vector Laboratories

[2.2.3 Tissue processing for cryo-sectioning](#)

After overnight fixation, tissues were washed several times in PBS and cryopreserved with a solution of 15% sucrose in PBS overnight at 4°C. To build gelatin blocks tissues were incubated in a solution of sucrose 15% and gelatin 7.5% (Sigma Aldrich) in PBS at 37°C for 4 hours. The samples were then embedded in the same solution at RT. Gelatin blocks were left to cool down at 4°C and snap-frozen in a solution of isopentane at -70°C for 1 minute. Blocks were then stored at -80°C until cryo-sectioning. 8 µm-thick cryo-sections were obtained using a Leica CM1950 Automated Cryostat. Sections were collected on Superfrost+ slides (Fisherbrand) and stored at -20°C on short term or -80°C for the long term.

[2.2.4 Immuno-histochemistry on gelatin sections](#)

If slides had been stored in the cold, they were left to sit at 4°C before being put at Room temperature. Immuno-staining was usually performed on freshly cut gelatin sections. Slides were incubated at 37°C in PBS for 15 minutes to remove the gelatin and washes several times with PBS.

Immuno-histochemistry on sections followed the same steps as whole mount immuno-staining to the only difference that times of incubation were shorter. Permeabilization was performed between 10 and 30 min depending on the targeted antigen. Peroxidase block as well as protein blocks were performed for 30min each. All procedures were spaced by 3 times washes in PBST. After a final wash with PBS, sections were mounted with aquatex (108562 Merck) or dako fluorescence mounting medium (S3023).

To identify clones by immuno-histochemistry on sections the following kits were used.

2.2.5 Immuno-fluorescence

Tissues were fixed overnight at 4 °C in 2% paraformaldehyde in phosphate-buffered saline (PBS). For immunofluorescence on sections, tissues were gelatin-embedded and cryo-sectioned (method described in further chapters). All the steps to perform immuno-fluorescence in whole mount or on sections were the same as in the immuno-staining section in the previous chapter. We will only list the differences:

- Peroxidase quenching was performed only in the case of using HRP-conjugated secondary antibodies followed by a peroxidase detection-based tyramide fluorescent amplification kit. Here is a list of the tyramide kits used:

Fluorophore	Concentration used	reference
TSA plus Cyanine 3	1:100	NEL744001KT, Perkin Elmer
TSA plus Cyanine 5	1:100	NEL745001KT, Perkin Elmer
TSA plus Cyanine 5.5	1:100	NEL766001KT, Perkin Elmer
TSA plus Fluorescein	1:100	NEL741001KT, Perkin Elmer

-The universal TNB blocking reagent (FP1012) Perkin Elmer was used instead of goat serum to block unspecific proteins.

-For biotin-streptavidin based amplification, streptavidin proteins conjugated with a fluorophore were used after incubation with a biotinylated secondary antibody. Here is a list of the streptavidin conjugates used:

Fluorophore	Concentration used	reference
Cy3	1:300	016-160-084, JackSon ImmunoResearch
647	1:300	S21374, ThermoFisher
633	1:300	S21375, ThermoFisher
405	1:300	S-32351, ThermoFisher

- Embryos were mounted in Vectashield mounting medium (Vector Laboratories,USA).

3. Epicardial and arterial mesothelial dissection

We will describe the common steps for the mesothelial dissection of samples used for RNAseq and embryonic heart culture together. The major differences between both experiments were the nature and the temperature of the solutions used. To preserve RNAs, all solutions were ice-cold PBS, were sterile and RNase free. For tissue culture we used a dissection medium at 37 °C (conditions described later). Samples were dissected under a Leica MZ12F stereoscope. The hearts were placed in the appropriate solution and frankly cut at the border between the great arteries and myocardium. Each piece was placed in distinct petri dishes. Samples for RNA extraction and for tissue cultures were handled differently. In the first case, petri dish plates with a bed of 2% agarose/PBS and thin metal thread were used to pin down the samples. In the latter case, only the forceps were used to delicately handle embryonic hearts. In both cases, fine forceps (Dumont #55 No11255-20) were used to delicately lift the mesothelium layer of the great arteries or the epicardium. The forceps were then used to maintain the embryonic tissues in place while carefully peeling the mesothelial/sub-mesothelial layers (form one sheet). The entire mesothelium of the ventricle, atrium and OFT was collected for RNA extraction and placed into different eppendorf tubes kept in dry ice. For culture, only a small piece of mesothelium was harvested at the time.

4. Ex vivo explants and culture

Hearts were dissected in 10% Calf Serum in DMEM/F12 1% Penicillin-Streptomycin kept in a water bath at 37 °C when not in use. E14.5 Wt1-Cre; R26-mTmG Fluorescent hearts and their WT littermates, observed with a Leica MZ12F stereoscope (fitted with a fluorescent lamp), were placed in different petri dishes. The medium was replaced every 5 min to prevent cooling of the embryonic tissue. One heart was dissected at the time under the stereoscope. Meanwhile, the rest of hearts were placed in Petri dishes with dissection medium on a histology flat table set at 37 °C. In WT hearts, a small piece of epicardium was peeled off from the ventricle under the PA (as described previously). A piece of Pulmonary mesothelium was then placed on the naked

myocardium of the recipient WT heart. As a control, a homotypic piece of epicardium from a fluorescent donor was placed on the naked myocardium of WT recipients instead.

Right after dissection, the E14.5 transplanted hearts were placed in a solution of 49.5% Krebs Henseleit Buffer (with DMEM/F12 instead of water) and 49.5% in Mouse serum (supplemented with N2 1:200 and B10 1:50)1% Penicillin-Streptomycin. Hearts were cultured in rolling-bottles in a 5%CO₂/ 95%O₂ gas environment for three days. Three hearts were cultured per bottle separating AMC-transplanted hearts from epicardium-transplanted hearts.

Hearts were finally washed in PBS and fixed in PFA 2% PBS ON at 4 °C.

5. Tissue imaging

5.1 Tissue clearing for 3D imaging

To detect superficial signal, tissues were dehydrated in gradual concentrations of glycerol (20%, 40%, 60% 80%).

For thick samples or deep signal, tissues were cleared with cubic 1 solution as described in the literature (Susaki et al., 2014).

5.2 Microscopy Imaging

Whole mount tissue and sections were imaged with the following microscopes:

- With a Leica SP5 multiline inverted confocal microscope for E16.5 and P0 fluorescent hearts in whole mount.
- With a Leica SP8 inverted confocal and white light laser for all embryonic fluorescent sections. The white laser allows for excitation of all possible wavelengths between 405 and 670nm.
- With a Leica TCS SP8 coupled to a DMI8 inverted confocal microscope Navigator module and white light laser. We used this microscope to couple to acquire several

embryonic hearts from a same experiment together (E15.5 RA induced animals, E16.5 Raldh2 KO embryos and E17.5 isl-Cre hearts)

- With Zeiss LSM 780 multifoton upright microscope. A MaiTai laser line at 1000 nm was used for two-channel two-photon imaging of Td-tomato and GFP fluorescence of E15.5 and E16.5 hearts in whole mount.

Maximum intensity Z-projections of whole hearts were acquired using both the tiling and z-stack functions.

6.RNA extraction and RNA sequencing:

Upon dissection epicardial and arterial mesothelial tissues were snap-frozen in Eppendorf tubes placed on dry ice. For a same mouse litter, the epicardium of either the Ventricle or atria and the arterial mesothelium were pooled together respectively. RNA was then purified from each population using the RNeasy Micro kit (Qiagen). Stranded RNA-seq libraries were sequenced on an Illumina HiSeq 2500 system. Sequencing reads were pre-processed by means of a pipeline that used FastQC, to assess read quality, and Cutadapt to trim sequencing reads, eliminating Illumina adaptor remains, and to discard reads that were shorter than 30 bp. The resulting reads were mapped against the mouse transcriptome (GRCm38, release 76; aug2014 archive) and quantified using RSEM v1.17. Data were then processed with a differential expression analysis pipeline that used Bioconductor package limma for normalization and differential expression testing, defining blocks of samples obtained from the same tissue source. Six biological replicates for each population were obtained and analysed by RNA-sequencing.

7.RNAseq analysis

The raw data analysis of RNA-seq data were generated by CNIC Bioinformatic unit. Contaminant were eliminated from reads using the Cutadapt software (Martin, 2011). The resulting reads were mapped and quantified on the transcriptome (Ensembl gene-build 70) using RSEM v1.2.3 (Li and Dewey, 2011). Only genes with at least 2 counts per million

in at least five samples were considered for statistical analysis. Data were then normalized and differential expression tested using the Bioconductor package EdgeR (Robinson et al., 2010). Genes were considered as differentially expressed genes with a Benjamini-Hochberg adjusted P-Value ≤ 0.05 . Analysis of the data was performed using Gene set enrichment analysis and Ingenuity pathways analysis software (Biobase International).

Discussion

The work presented in this thesis brought insights into the lymphangiogenic properties of SHF progenitors, the role of the arterial mesothelium and the developmental dynamics of cardiac lymphatic vessels.

Existence of a niche of LEC progenitors in the pulmonary artery

Our results suggest the existence of a vascular niche of mesodermal progenitors in the wall of the pulmonary artery. Interestingly, lymphatic endothelial cells form in close proximity to arterial mesothelial cells and epicardial cells. RNAseq and immunofluorescence data showed an abrupt downregulation of *Raldh2* expression in proximal AMCs compared to epicardial cells. In addition, clonal analysis data reveal that LECs adopt distinct behaviours depending on their position in the PA and ventricle. LECs found at the base of the pulmonary artery are located in the sub-mesothelial portion of the PA. However, the cells that have reached the ventricle are visible in the epicardial layer. Interestingly SHF-EpiCs are not of mesothelial nature since they are *Prox1*⁺/*Wt1*⁻. LECs are most likely specified in a low Retinoic acid environment in the proximal PA and subsequently migrate down the ventricle where they receive high retinoic acid cues from the epicardium, which stimulates lymphangiogenesis.. Consistently, *Raldh2* mutant embryos presented dilated cardiac lymphatic vessels and reduced branching. In contrast, animals injected with RA presented thinner vessels and a hyper-remodelled lymphatic vasculature. These data are consistent with previous reports showing the need of RA signalling for lymphatic maturation (Bowles et al., 2014; Burger et al., 2014; Marino et al., 2011). The stronger phenotypes observed in the ventral part of hearts treated with RA could be explained by a “short-circuiting” effect on the specification and expansion of SHF-derived lymphatic progenitors. We suspect that RA inhibits the specification of LEC SHF progenitors in the PA by disrupting the low *Raldh2* environment at the base of the PA. This would explain why the lymphatic tree of the ventral part of the heart exhibit smaller vessels. These data together with the existence of sparse ventral clones in the random

clonal analysis, suggests that the lymphatic vasculature which forms by angiogenesis from the CV in the ventral part of the heart serves as a scaffold for the later addition of SHF-derived LECs. Indeed, the ventral lymphatic vasculature of RA treated hearts seemed “naked”. It would be interesting to check whether RA directly affects the specification and development of LEC-SHF progenitors by exposing *isl1*-Cre embryos to an excess of RA .

RA also seems to promote the maturation of cardiac lymphatics since the lymphatic sac-like structures in the PA are not maintained in an immature state in untreated animals. This area normally exhibits Low *Raldh2* levels. The exposition to RA seems to cause hyper-remodelling and maturation of PA lymphatic sac-like cells suggesting that low RA levels are meant to maintain lymphatic cells in an immature state.

LEC progenitors may also be under the influence of crosstalk signals between SHF progenitors and cardiac neural crest cells (CNCCs). On one hand, SHF progenitors express the transcription factor *Tbx1* among others. *Tbx1* has been shown to be critical for lymphatic development by regulating the expression of *VEGFR3* (Chen et al., 2010). The observation of an aggravated phenotype in the ventral lymphatic vasculature of *Tbx1*-null embryos translates specific alterations in SHF-progenitors. Indeed, *Tbx1* is critical for the deployment of SHF progenitors in the OFT (Jerome and Papaioannou, 2001; Rana et al., 2014; Theveniau-Ruissy et al., 2008). On the other hand, CNCCs are a known source of molecular cues such as *Neuropilin*, *BMP*, *Wnt*, *ephrin*, *TGFβ/BMP* and *semaphorin* signalling. (Feiner et al., 2001; Hutson and Kirby, 2007; Kawasaki et al., 1999; Kuriyama and Mayor, 2008). Interestingly, some of these signals are also involved in the specification and maturation of lymphatic vessels such as *neuropilin*, *semaphorin* and *Ephrin* signalling (Bouvrée et al., 2012; Davy and Soriano, 2007; Jurisic et al., 2012; Ochsenein et al., 2014). No link has been established between the presence of neural crest cells and LECs in the OFT. In the laboratory we ruled out an eventual cell contribution of CNCCs to OFT lymphatic cells by fate mapping of *Wnt1*+ progenitors (Fig. 19). However, neural crest cells have been shown to be involved in lymphatic development (Burger et al., 2014). It is thus possible that signals from the neural crest are acting on the specification of a lymphangiogenic niche in the Pulmonary artery. The behaviour adopted by LECs in the PA and ventricle might be linked to CNCC maturation and migration.

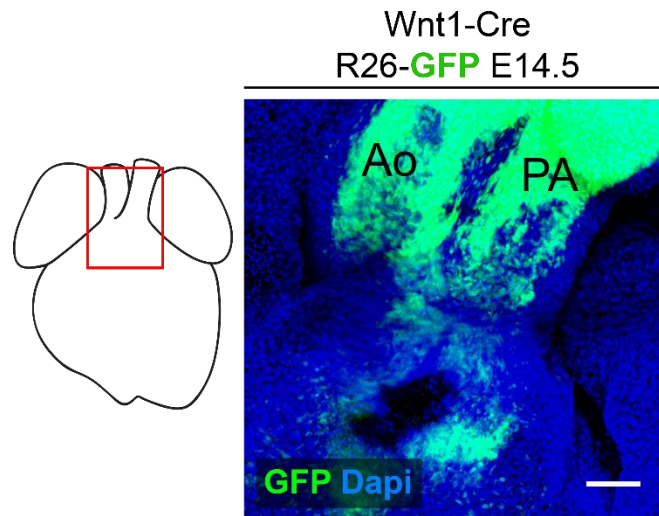


Figure 19. CNCCs progenitors do not form LECs in the OFT of the heart

Z projection of a Wnt1-Cre; R26-GFP heart at E14.5. The neural crest lineage is visible in green. We cannot observe LECs nor AMCs. Scale bar: 100 μ m

Lymphvasculogenesis might be regulated by AMC factors other than RA signalling. RNAseq data show that AMCs and sub-mesothelial cells express lymphatic genes such as *Foxc1* and *Foxc2*. Interestingly the arterial genes *Hey1* and *Hey2* were inhibited. These data suggest that AMCs might promote the specification of sub-mesothelial cells towards a lymphatic fate by the inhibition of arterial genes and the expression of lymphatic genes.

Data from the chick are consistent with the existence of lymphangiogenic signals in the great arteries. Indeed, Wilting and colleagues grafted the proepicardium of quail donors into chick embryos to see if LECs could derive from the proepicardium (Wilting et al., 2007). The graft constantly failed to produce LECs when transplanted orthotopically, indicating a non-proepicardial origin of the cardiac lymphatic vasculature. However, when the grafts were transplanted at the base of the heart, they integrated the chick lymphatic vessels, indicating an environment that promoted lymphatic specification in this area.

[A Role for AMCs in lymphangiogenesis?](#)

We showed that clones containing AMCs are of different nature depending on their proximity to the heart. Interestingly, about 20% of AMC clones are composed of both proximal and distal cells. Therefore, the addition of SHF-derived mesothelial cells to arteries is a continuum, without a strict lineage relationship along the arteries. The specification and contribution of AMCs to the great arteries is probably dependent on differential environmental cues along the great vessels. The fact that the cell behaviour of distal clones could be recapitulated with the *Wt1cre* line, but no LECs were found in the *Wt1* lineage suggests that LECs do not arise from AMCs unless a rare subset of AMCs not expressing *Wt1* would give rise to LECs, however we have not been able to detect clones establishing this relationship. In contrast, clones were found containing LECs both in the sub-epicardial end epicardial layer in the OFT myocardium. The temporal evolution of such clones suggests that LECs specified at the base of the aorta later colonize the myocardial area and eventually some of them emerge to the epicardial layer.

Early ventral lymphatic clones at E14.5 and E15 are composed of proximal arterial mesothelial cells. In contrast, later ventral lymphatic clones did not exhibit proximal AMCs. In some cases, we observed distal mesothelial cells instead. The fact that distal AMCs could be observed shows that such clones arose from SHF progenitors capable of giving rise to both distal and proximal clones. Proximal mesothelial cells are most likely incorporated into the pulmonary artery, reflecting a high turnover of the proximal sheet of arterial mesothelial cells. RNAseq data support such conclusions since the EMT actors *Twist1* and *Twist2*, are up-regulated in AMCs compared to epicardial cells. In addition, only in rare cases did the mesothelial cells of PA explants stayed on the epicardial surface. Instead *Wt1*⁺ cells consistently invaded the myocardium.

We have shown that *Wt1*⁺ AMCs are not integrated into the lymphatic vasculature. However, RNAseq and immunofluorescence data show that *Wt1* is downregulated in the arterial mesothelium. As a result, some AMCs might be expressing low or undetectable levels of *Wt1*. In that case, we cannot rule out that such cells may be incorporated into the cardiac lymphatic vasculature. Interestingly, lineage tracing with the *Wt1-Cre* transgene resulted in the labelling of a substantial number of cells associated to the lymphatic vessels (Fig. 20A). In addition, performing *Isl1-Mer-Cre-Mer* lineage tracing we found cells

lining against lyve1+/prox1+ cells (Fig. 20B). The study of lymphatic clones in whole mount also showed the presence of Prox1-/Lyve1- cells lying against LECs (Fig. 20C). These findings suggest that proximal AMC's are converted into LEC-associated cells. Collector and pre-collector lymphatic vessels in the body are coated by a layer of smooth muscle cells acquired during late post-natal life. In the region of the heart, lymphatic smooth muscle cells (LMCs) appear at first around LECs of the great arteries. It is only during adult life that cardiac LMCs can be appreciated (Juszyński et al., 2008). There is no evidence for the presence of LMCs in the embryonic heart (Flaht-Zabost et al., 2014). AMC's might thus mature into LMCs during late post-natal life. These cells may be similar to the pericytes found on capillary blood vessels.

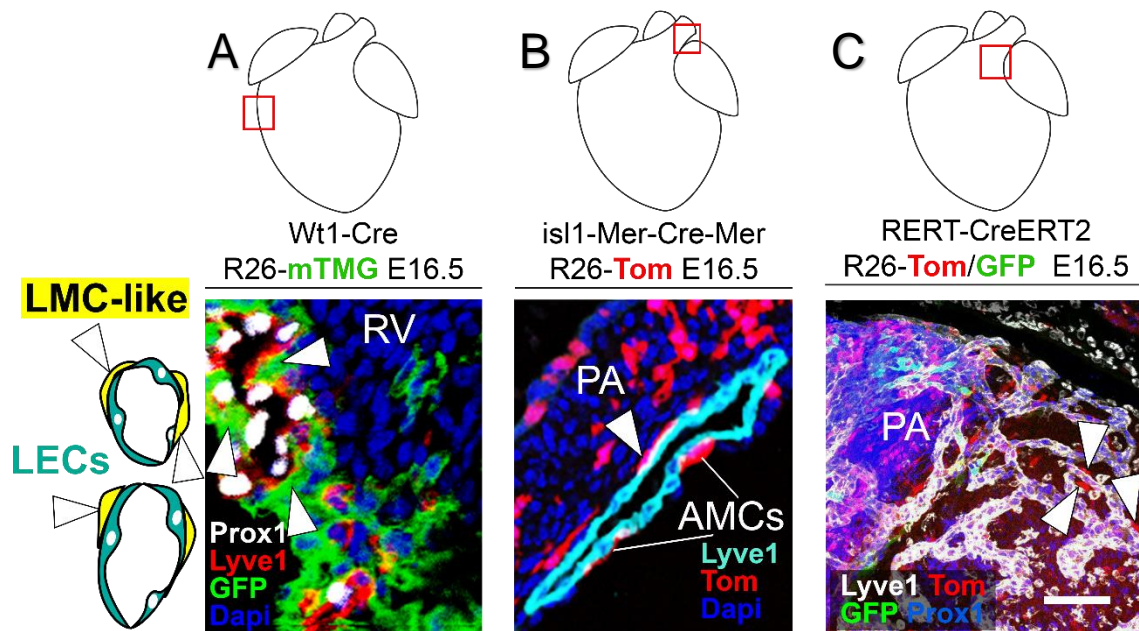


Figure 20. AMCs might be a source of LMC-like cells

(A) Heart section showing Wt1-Cre lineage in green (B) Heart section of an *ils1-Mer-Cre-Mer* heart induced at E9 (C) Z projection of a specimen from the clonal analysis with focus on the base of the Pulmonary artery (PA). We can see lymphatic vessels in all three panels. The arrowheads point at Lymphatic smooth muscle-like cells (LMC-like).

PA: Pulmonary artery; RV: Right ventricle; LECs: Lymphatic endothelial cell; AMCs: Arterial mesothelial cell

What about the Aorta?

The mesothelial proximal clones containing lymphatic endothelial cells are localised in the pulmonary artery. However, some proximal AMC clones could also be found in the Aorta. Therefore it is not clear if aortic proximal clones also possess lymphangiogenic properties. One way to address that issue would be to transplant the aortic sub-mesothelium/ mesothelium from fluorescent donors onto the ventricle of WT hearts and see if lymphatic vessels form. Prox1 and Lyve1 immunostaining in whole mount, show that lymphatic vessels generally form in the area corresponding to the territory of PA proximal lymphatic clones (Fig. 21A). However, in few individuals, the primary arterial lymphatic plexus appeared connected to the aorta (Fig. 21B). In addition, the unique ventral P0 clone we found, on the ventral part of the heart, displayed lymphatic cells on both the Ao and PA. We think that LEC progenitors specify in the PA, but some inter-individual variations may cause LECs to form at the base of the Aorta instead.

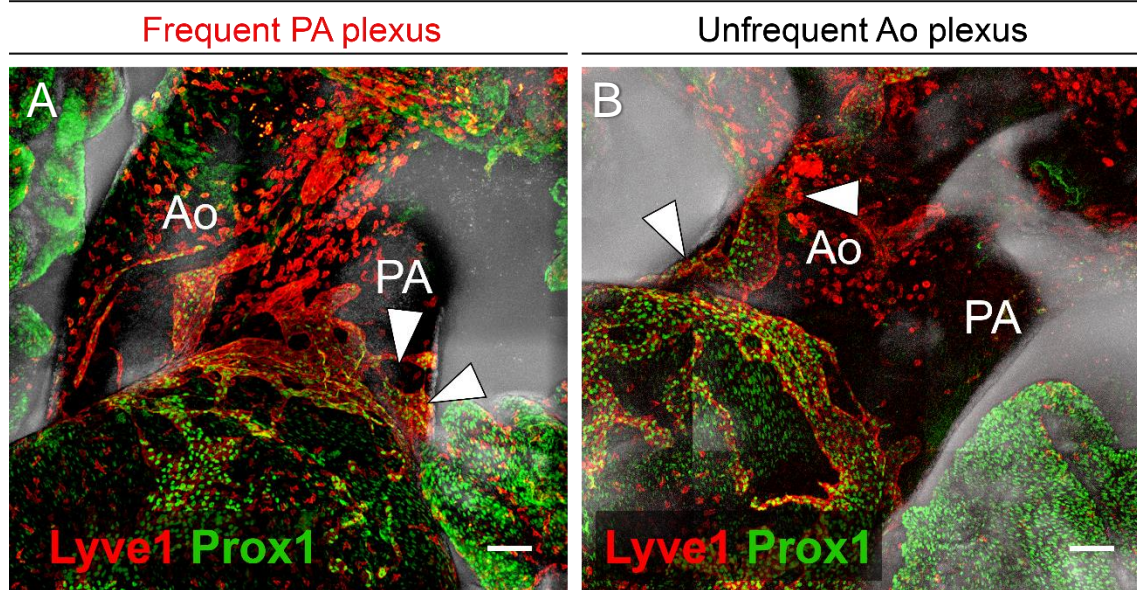


Figure 21. Morphology of the cardiac lymphatic vasculature at the level of the great vessels

(A,B) Z- projection of the frontal view of a hearts at E16.5 with focus on the great arteries. The cardiac lymphatics can be appreciated by the markers Lyve1 (red) and prox1 (green). (A) Most common situation. The primary lymphatic plexus usually forms on the Pulmonary artery (arrowheads). (B) in exceptional cases the primary lymphatic plexus forms on the Aorta (arrowheads). All scale bars: 100µm. Ao: Aorta; PA: Pulmonary artery;

The heterogeneous origins of the cardiac lymphatic vasculature

We will firstly discuss the results reported by the group of Paul Riley in 2015 because their work is the only study currently available on the origin of cardiac lymphatic vessels (Klotz et al., 2015).

Using the Tie2-Cre transgene, Linda Klotz and colleagues concluded that the cardinal vein is not the only source of cardiac lymphatic vessels. Despite exhaustive recombination of CV cells in Tie2-Cre embryos, the team reported incomplete recombination of the cardiac lymphatic vasculature. They confirmed these observations using the Tie2-Cre transgene to drive Prox1 deletion using a Prox1^{flox/flox} allele. Prox1 is a master regulator of lymphatic development indispensable for lymphatic formation (Johnson et al., 2008). Consequently, deleting prox1 from the Tie2 lineage is an effective

way to inhibit lymphangiogenesis in cardinal vein progenitors. As a result, the cardiac lymphatic vasculature of mutant embryos was hypoplastic. Therefore, the cardinal vein cannot be the sole source of lymphatic vessels or no lymphatic vessels would appear in the heart. It cannot be excluded that a portion of cardiac LECs may derive from incomplete gene deletion in a subset of CV cells. Another alternative is the existence of non-venous progenitors capable of forming LECs in the heart. Our discovery, placing the SHF as a key contributor of cardiac LECs, fits with these observations.

Linda Klotz and colleagues used a range of tissue-specific Cre lines to determine the origins of cardiac LECs. In particular, they used *Mesp1*-Cre and *Nkx2.5*-Cre to trace the fate of early and late mesodermal progenitors (Lints et al., 1993; Saga et al., 1999) respectively. However, no lymphatic vessels were found to belong to any of these lineages. At first glance, this results seem inconsistent with ours since the SHF is a mesodermal lineage (Kelly et al., 2001)(Saga et al., 2000)(Saga et al., 2000)(Saga et al., 2000). We have to keep in mind that the use of *Mesp1*-Cre or *Nkx2.5*-Cre with a fluorescent reporter result in strongly fluorescent hearts, because the entire myocardium is recombined. It is then difficult to observe the lymphatic vasculature by direct visualization at the stereoscope. In order to detect recombination in LECs Klotz and colleagues used confocal microscopy, however, to find SHF-derived cardiac lymphatics, a specific study of the ventral side of the heart is required.

In addition, ventral LEC progenitors in the SHF may not recombine efficiently, since the *Nkx2.5*Cre line does not completely recombine the SHF before its incorporation to the heart. Moreover, we think that ventral lymphatic cells arise from the latest SHF progenitors added to the arterial pole. Consistently, proximal AMC clones can be recapitulated using the line *Hoxb1*-Cre, which labels the posterior SHF arterial pole precursors. The fact that we were able to label lymphatics development in the ventral part of the heart using *Mef2c*-Cre, and *isl1*mER-Cre-mER at E9 suggests that lymphatic progenitors are located in the posterior region of the anterior SHF, understood as the SHF region that contributes to the arterial pole of the heart. This region would be the last added to the arterial pole and adjacent to the splanchnic mesoderm that contributes to the base of the great arteries. This hypothesis is consistent with the fact that proximal clones are composed of valvular

cells as well as cardiomyocytes of the base of the pulmonary artery but not to cardiomyocytes in the right ventricle or atria. De Bono and colleagues showed the existence of a transitory region at the interface between the AHF and pSHF that simultaneously expresses Mef2c-AHF-driven Cre, Tbx1 and Tbx5 (De Bono et al., 2018). Complementary fate mapping of Tbx5+ progenitors would provide insights into the exact location of LEC progenitors in the SHF.

The existence of alternative sources of cardiac lymphatic cells have been suggested by Klotz and co-workers. The group reported possible contribution of the Yolk Sac haemogenic endothelium to the cardiac lymphatic vasculature using *Pdgfr β -CreERT2* for lineage tracing (Klotz et al., 2015). However, Ulvmar and colleagues later showed that the *Pdgfrb*-Cre transgene is not appropriate to trace the fate of non-venous progenitors as it recombines part of the cardinal vein and jugular lymph sacs (Ulvmar et al., 2016). Several recent reports propose alternative origins of the lymphatic cells other than the cardinal vein, suggesting that the definitive lymphatic plexus forms both by lymphangiogenesis (sprouting off pre-existing vessels) from CV-derived vessels, and lymphvasculogenesis (de novo vessel formation) from different sources. Organs like the skin and the mesentery form their lymphatic vasculature from endothelial and non-endothelial progenitors (Martinez-corrall et al., 2015; Okuda et al., 2012; Pichol-thievend et al., 2018; Stanczuk et al., 2015; Wilting et al., 2006). In addition, there is growing evidence that LECs of different organs display different properties and genetic signatures (Petrova and Koh, 2018; Ulvmar and Mäkinen). These findings together with our findings reconcile the models of Sabin (Sabin, 1902) and Huntington and McClure (Huntington and McClure, 1910).

The lymphangiogenic properties of SHF progenitors introduce the concept of organ-specific lymphatic development

The discovery that SHF progenitors give rise to cardiac LECs, offers another perspective for the study of cardiogenesis and lymphangiogenesis.

On one hand It shows that the SHF is highly multipotent and is capable to provide the heart with nearly all cardiac cell types. We suspect the multipotent properties of SHF progenitors to rely on the expression of *isl1* transcription factor. Indeed, different reports suggest that *isl1*+ cells in different regions of the embryonic and adult heart are highly plastic (Bu et al., 2009; Laugwitz et al., 2005; Moretti et al., 2006; Qyang et al., 2007; Sun et al., 2007). It would be interesting to further challenge the contribution of SHF progenitors to other cardiac cell types. In addition, dissecting the molecular and cellular properties of SHF progenitors might offer new therapeutic strategies for the treatment of cardiomyopathies.

On the other hand, these discoveries imply that studying lymphangiogenesis should be done at the organ-level because LECs might derive from tissue-specific progenitors. Creating organ-specific LECs *in situ*, might be a way to create a capillary vasculature that fits perfectly the organ needs and environment. Indeed, LECs from different sources of progenitors may not be equivalent in terms of function (Petrova and Koh, 2018; Ulvmar and Mäkinen). In contrast, venous-lymphatic sprouting most likely creates collecting vessels meant to link the different organ plexuses to the thoracic duct. The reason why SHF-derived LECs exclusively form in the ventral part of the heart is not clear. It might be because the OFT region of the heart is a source of intense remodelling, it may be more “practical” to dispose of all OFT progenitors in a same location, however, specific disruption of this SHF-derive Lymphatic population would be required to determine whether and how they may play a specialized function in heart lymphatics.

Conclusions

- 1) Arterial mesothelial cells do not derive from the proepicardium but from the Second heart field.
- 2) The second heart field partially contributes to the smooth muscle and endothelial cells of the great vessels through contribution of arterial mesothelial cells.
- 3) In the pulmonary artery, proximal AMCs are clonally related to the lymphatic vasculature of the ventral part of the heart.
- 4) Proximal AMCs neither give rise to LECs nor to cardiomyocytes.
- 5) Most of the lymphatic cells of the dorsal part of the heart and part of the lymphatic cells of the ventral part of the heart are formed by angiogenesis of Cardinal vein progenitors.
- 6) The lymphatic vasculature of the ventral part of the heart depends on the late specification of SHF progenitors.
- 7) SHF progenitors are recruited in the mesothelial/sub-mesothelial region of the Pulmonary artery and colonize the ventricles by lymphangiogenesis.
- 8) The specification of LECs of the ventral part is conducted in a Raldh2 low environment.
- 9) RA signalling is involved in the subsequent remodelling of the lymphatic vasculature in the ventricles.

Bibliography

- Alberga, A., Boulay, J.L., Kempe, E., Dennefeld, C., and Haenlin, M. (1991). The snail gene required for mesoderm formation in *Drosophila* is expressed dynamically in derivatives of all three germ layers. *Development* 111.
- Arenkiel, B.R., Gaufo, G.O., and Capecchi, M.R. (2003). Hoxb1 neural crest preferentially form glia of the PNS. *Dev. Dyn.* 227, 379–386.
- Argüello, C., de la Cruz, M. V, and Gómez, C.S. (1975). Experimental study of the formation of the heart tube in the chick embryo. *J. Embryol. Exp. Morphol.* 33, 1–11.
- Arima, Y., Miyagawa-Tomita, S., Maeda, K., Asai, R., Seya, D., Minoux, M., Rijli, F.M., Nishiyama, K., Kim, K.-S., Uchijima, Y., et al. (2012). Preotic neural crest cells contribute to coronary artery smooth muscle involving endothelin signalling. *Nat. Commun.* 3, 1267.
- Banerjee, I., Fuseler, J.W., Price, R.L., Borg, T.K., and Baudino, T. a (2007). Determination of cell types and numbers during cardiac development in the neonatal and adult rat and mouse. *Am. J. Physiol. Heart Circ. Physiol.* 293, H1883–H1891.
- Van Den Berg, G., and Moorman, a. F.M. (2009). Concepts of Cardiac Development in Retrospect. *Pediatr. Cardiol.* 30, 580–587.
- Bergwerff, M., Verberne, M.E., DeRuiter, M.C., Poelmann, R.E., and Gittenberger-de-Groot, A.C. (1998). Neural Crest Cell Contribution to the Developing Circulatory System. *Circ. Res.* 82, 221–231.
- Bertrand, N., Roux, M., Ryckebüsch, L., Niederreither, K., Dollé, P., Moon, A., Capecchi, M., and Zaffran, S. (2011). Hox genes define distinct progenitor sub-domains within the second heart field. *Dev. Biol.* 353, 266–274.
- De Bono, C., Thellier, C., Bertrand, N., Sturny, R., Jullian, E., Cortes, C., Stefanovic, S., Zaffran, S., Théveniau-Ruissy, M., and Kelly, R.G. (2018). T-box genes and retinoic acid signaling regulate the segregation of arterial and venous pole progenitor cells in the murine second heart field. *Hum. Mol. Genet.* 27, 3747–3760.
- Bouvrée, K., Brunet, I., Del Toro, R., Gordon, E., Prahst, C., Cristofaro, B., Mathivet, T., Xu, Y., Soueid, J., Fortuna, V., et al. (2012). Semaphorin3A, Neuropilin-1, and PlexinA1 are required for lymphatic valve formation. *Circ. Res.* 111, 437–445.
- Bowles, J., Secker, G., Nguyen, C., Kazenwadel, J., Truong, V., Frampton, E., Curtis, C., Skoczylas, R., Davidson, T.-L., Miura, N., et al. (2014). Control of retinoid levels by CYP26B1 is important for lymphatic vascular development in the mouse embryo. *Dev. Biol.* 386, 25–33.
- Bruneau, B.G. (2008). The developmental genetics of congenital heart disease. *Nature* 451, 943–948.
- Bu, L., Jiang, X., Martin-Puig, S., Caron, L., Zhu, S., Shao, Y., Roberts, D.J., Huang, P.L., Domian, I.J., and Chien, K.R. (2009). Human ISL1 heart progenitors generate

diverse multipotent cardiovascular cell lineages. *Nature* 460, 113–117.

Burger, N.B., Stuurman, K.E., Kok, E., Konijn, T., Schooneman, D., Niederreither, K., Coles, M., Agace, W.W., Christoffels, V.M., Mebius, R.E., et al. (2014). Involvement of neurons and retinoic acid in lymphatic development: new insights in increased nuchal translucency. *Prenat. Diagn.* 34, 1312–1319.

Buttler, K., Kreysing, A., von Kaisenberg, C.S., Schweigerer, L., Gale, N., Papoutsis, M., and Wilting, J. (2006). Mesenchymal cells with leukocyte and lymphendothelial characteristics in murine embryos. *Dev. Dyn.* 235, 1554–1562.

Cai, C.L., Liang, X., Shi, Y., Chu, P.H., Pfaff, S.L., Chen, J., and Evans, S. (2003). Isl1 identifies a cardiac progenitor population that proliferates prior to differentiation and contributes a majority of cells to the heart. *Dev Cell* 5, 877–889.

Carver, E.A., Jiang, R., Lan, Y., Oram, K.F., and Gridley, T. (2001). The mouse snail gene encodes a key regulator of the epithelial-mesenchymal transition. *Mol. Cell. Biol.* 21, 8184–8188.

Chen, H.I., Poduri, A., Numi, H., Kivela, R., Saharinen, P., McKay, A.S., Raftrey, B., Churko, J., Tian, X., Zhou, B., et al. (2014). VEGF-C and aortic cardiomyocytes guide coronary artery stem development. *J. Clin. Invest.* 124, 4899–4914.

Chen, L., Mupo, A., Huynh, T., Cioffi, S., Woods, M., Jin, C., McKeehan, W., Thompson-Snipes, L., Baldini, A., and Illingworth, E. (2010). Tbx1 regulates Vegfr3 and is required for lymphatic vessel development. *J. Cell Biol.* 189, 417–424.

Chen, T.H.-P., Chang, T.-C., Kang, J.-O., Choudhary, B., Makita, T., Tran, C.M., Burch, J.B.E., Eid, H., and Sucov, H.M. (2002). Epicardial Induction of Fetal Cardiomyocyte Proliferation via a Retinoic Acid-Inducible Trophic Factor. *Dev. Biol.* 250, 198–207.

Christoffels, V.M., Mommersteeg, M.T.M., Trowe, M.-O., Prall, O.W.J., de Gier-de Vries, C., Soufan, A.T., Bussen, M., Schuster-Gossler, K., Harvey, R.P., Moorman, A.F.M., et al. (2006). Formation of the Venous Pole of the Heart From an *Nkx2-5* –Negative Precursor Population Requires *Tbx18*. *Circ. Res.* 98, 1555–1563.

Davy, A., and Soriano, P. (2007). Ephrin-B2 forward signaling regulates somite patterning and neural crest cell development. *Dev. Biol.* 304, 182–193.

Fahed, A.C., Gelb, B.D., Seidman, J.G., and Seidman, C.E. (2013). Genetics of Congenital Heart Disease. *Circ. Res.* 112, 707–720.

Feiner, L., Webber, A.L., Brown, C.B., Lu, M.M., Jia, L., Feinstein, P., Mombaerts, P., Epstein, J.A., and Raper, J.A. (2001). Targeted disruption of semaphorin 3C leads to persistent truncus arteriosus and aortic arch interruption. *Development* 128, 3061–3070.

Flaht-Zabost, A., Gula, G., Cizek, B., Czarnowska, E., Jankowska-Steifer, E., Madej, M., Niderla-Bielińska, J., Radomska-Leśniewska, D., and Ratajska, A. (2014). Cardiac mouse lymphatics: developmental and anatomical update. *Anat. Rec. (Hoboken)*. 297, 1115–1130.

Flaht, a, Jankowska-Steifer, E., Radomska, D.M., Madej, M., Gula, G., Kujawa, M., and Ratajska, a (2012). Cellular phenotypes and spatio-temporal patterns of lymphatic

vessel development in embryonic mouse hearts. *Dev. Dyn.* 241, 1473–1486.

François, M., Caprini, A., Hosking, B., Orsenigo, F., Wilhelm, D., Browne, C., Paavonen, K., Karnezis, T., Shayan, R., Downes, M., et al. (2008). Sox18 induces development of the lymphatic vasculature in mice. *Nature* 456, 643–647.

François, M., Short, K., Secker, G.A., Combes, A., Schwarz, Q., Davidson, T.-L., Smyth, I., Hong, Y.-K., Harvey, N.L., and Koopman, P. (2012). Segmental territories along the cardinal veins generate lymph sacs via a ballooning mechanism during embryonic lymphangiogenesis in mice. *Dev. Biol.* 364, 89–98.

Greenfield, E.A. (2017). Sampling and Preparation of Mouse and Rat Serum. *Cold Spring Harb. Protoc.* 2017, pdb.prot100271.

Guadix, J.A., Carmona, R., Muñoz-Chápuli, R., and Pérez-Pomares, J.M. (2006). In vivo and in vitro analysis of the vasculogenic potential of avian proepicardial and epicardial cells. *Dev. Dyn.* 235, 1014–1026.

Guadix, J.A., Ruiz-Villalba, A., Lettice, L., Velecela, V., Muñoz-Chápuli, R., Hastie, N.D., Pérez-Pomares, J.M., and Martínez-Estrada, O.M. (2011). Wt1 controls retinoic acid signalling in embryonic epicardium through transcriptional activation of Raldh2. *Development* 138, 1093–1097.

Guerra, C., Mijimolle, N., Dhawahir, A., Dubus, P., Barradas, M., Serrano, M., Campuzano, V., and Barbacid, M. (2003). Tumor induction by an endogenous K-ras oncogene is highly dependent on cellular context. *Cancer Cell* 4, 111–120.

Hägerling, R., Pollmann, C., Andreas, M., Schmidt, C., Nurmi, H., Adams, R.H., Alitalo, K., Andresen, V., Schulte-Merker, S., and Kiefer, F. (2013). A novel multistep mechanism for initial lymphangiogenesis in mouse embryos based on ultramicroscopy. *EMBO J.* 32, 629–644.

Harvey, N.L., and Oliver, G. (2004). Choose your fate: artery, vein or lymphatic vessel? *Curr. Opin. Genet. Dev.* 14, 499–505.

Hayashi, S., and McMahon, A.P. (2002). Efficient Recombination in Diverse Tissues by a Tamoxifen-Inducible Form of Cre: A Tool for Temporally Regulated Gene Activation/Inactivation in the Mouse. *Dev. Biol.* 244, 305–318.

Hong, Y.-K., Harvey, N., Noh, Y.-H., Schacht, V., Hirakawa, S., Detmar, M., and Oliver, G. (2002). Prox1 is a master control gene in the program specifying lymphatic endothelial cell fate. *Dev. Dyn.* 225, 351–357.

Huntington, G.S., and McClure, C.F.W. (1910). The anatomy and development of the jugular lymph sacs in the domestic cat (*Felis domestica*). *Am. J. Anat.* 10, 177–312.

Hutson, M.R., and Kirby, M.L. (2007). Model systems for the study of heart development and disease. Cardiac neural crest and conotruncal malformations. *Semin. Cell Dev. Biol.* 18, 101–110.

Ivins, S., Chappell, J., Vernay, B., Suntharalingham, J., Martineau, A., Mohun, T.J., and Scambler, P.J. (2015). The CXCL12/CXCR4 Axis Plays a Critical Role in Coronary Artery Development. *Dev. Cell* 33, 455–468.

- Jerome, L.A., and Papaioannou, V.E. (2001). DiGeorge syndrome phenotype in mice mutant for the T-box gene, *Tbx1*. *Nat. Genet.* 27, 286–291.
- Johnson, N.C., Dillard, M.E., Baluk, P., McDonald, D.M., Harvey, N.L., Frase, S.L., and Oliver, G. (2008). Lymphatic endothelial cell identity is reversible and its maintenance requires *Prox1* activity. *Genes Dev.* 22, 3282–3291.
- Jurismic, G., Maby-El Hajjami, H., Karaman, S., Ochsenbein, A.M., Alitalo, A., Siddiqui, S.S., Ochoa Pereira, C., Petrova, T. V, and Detmar, M. (2012). An unexpected role of semaphorin3a-neuropilin-1 signaling in lymphatic vessel maturation and valve formation. *Circ. Res.* 111, 426–436.
- Juszyński, M., Ciszek, B., Stachurska, E., Jabłońska, A., and Ratajska, A. (2008). Development of lymphatic vessels in mouse embryonic and early postnatal hearts. *Dev. Dyn.* 237, 2973–2986.
- Kaipainen, A., Korhonen, J., Mustonen, T., van Hinsbergh, V.W., Fang, G.H., Dumont, D., Breitman, M., and Alitalo, K. (1995). Expression of the *fms*-like tyrosine kinase 4 gene becomes restricted to lymphatic endothelium during development. *Proc. Natl. Acad. Sci. U. S. A.* 92, 3566–3570.
- Karkkainen, M.J., Haiko, P., Sainio, K., Partanen, J., Taipale, J., Petrova, T. V., Jeltsch, M., Jackson, D.G., Talikka, M., Rauvala, H., et al. (2004). Vascular endothelial growth factor C is required for sprouting of the first lymphatic vessels from embryonic veins. *Nat. Immunol.* 5, 74–80.
- Karunamuni, G., Yang, K., Doughman, Y.Q., Wikenheiser, J., Bader, D., Barnett, J., Austin, A., Parsons-Wingerter, P., and Watanabe, M. (2010). Expression of lymphatic markers during avian and mouse cardiogenesis. *Anat. Rec.* 293, 259–270.
- Katz, T.C., Singh, M.K., Degenhardt, K., Rivera-Feliciano, J., Johnson, R.L., Epstein, J. a., and Tabin, C.J. (2012). Distinct Compartments of the Proepicardial Organ Give Rise to Coronary Vascular Endothelial Cells. *Dev. Cell* 22, 639–650.
- Kawasaki, T., Kitsukawa, T., Bekku, Y., Matsuda, Y., Sanbo, M., Yagi, T., and Fujisawa, H. (1999). A requirement for neuropilin-1 in embryonic vessel formation. *Development* 126, 4895–4902.
- Kelly, R.G., Brown, N.A., and Buckingham, M.E. (2001). The arterial pole of the mouse heart forms from *Fgf10*-expressing cells in pharyngeal mesoderm. *Dev Cell* 1, 435–440.
- Keyte, A., and Hutson, M.R. (2012). The neural crest in cardiac congenital anomalies. *Differentiation* 84, 25–40.
- Kim, H., Nguyen, V.P., Petrova, T. V, Cruz, M., Alitalo, K., and Dumont, D.J. (2010). Embryonic vascular endothelial cells are malleable to reprogramming via *Prox1* to a lymphatic gene signature. *BMC Dev. Biol.* 10, 72.
- Kirby, M.L. (2007). *Cardiac development* (Oxford University press).
- Kirby, M.L., and Stewart, D.E. (1983). Neural crest origin of cardiac ganglion cells in the chick embryo: Identification and extirpation. *Dev. Biol.* 97, 433–443.
- Kirby, M.L., Gale, T.F., and Stewart, D.E. (1983). Neural crest cells contribute to normal

aorticopulmonary septation. *Science* 220, 1059–1061.

Klotz, L., Norman, S., Vieira, J.M., Masters, M., Rohling, M., Dubé, K.N., Bollini, S., Matsuzaki, F., Carr, C.A., and Riley, P.R. (2015). Cardiac lymphatics are heterogeneous in origin and respond to injury. *Nature* 522, 62–67.

Küchler, A.M., Gjini, E., Peterson-Maduro, J., Cancilla, B., Wolburg, H., and Schulte-Merker, S. (2006). Development of the zebrafish lymphatic system requires VEGFC signaling. *Curr. Biol.* 16, 1244–1248.

Kuriyama, S., and Mayor, R. (2008). Molecular analysis of neural crest migration. *Philos. Trans. R. Soc. B Biol. Sci.* 363, 1349–1362.

de la Cruz, M. V, Sánchez Gómez, C., Arteaga, M.M., and Argüello, C. (1977). Experimental study of the development of the truncus and the conus in the chick embryo. *J. Anat.* 123, 661–686.

Lai, L., Bohnsack, B.L., Niederreither, K., Hirschi, K.K., Ekblom, P., Kemler, R., and Doetschman, T. (2003). Retinoic acid regulates endothelial cell proliferation during vasculogenesis. *Development* 130, 6465–6474.

Laugwitz, K.-L., Moretti, A., Lam, J., Gruber, P., Chen, Y., Woodard, S., Lin, L.-Z., Cai, C.-L., Lu, M.M., Reth, M., et al. (2005). Postnatal isl1+ cardioblasts enter fully differentiated cardiomyocyte lineages. *Nature* 433, 647–653.

Lawson, K.A., Meneses, J.J., and Pedersen, R.A. (1991). Clonal analysis of epiblast fate during germ layer formation in the mouse embryo. *Development* 113, 891–911.

Lee, S., Kang, J., Yoo, J., Ganesan, S.K., Cook, S.C., Aguilar, B., Ramu, S., Lee, J., and Hong, Y.K. (2009). Prox1 physically and functionally interacts with COUP-TFII to specify lymphatic endothelial cell fate. *Blood* 113, 1856–1859.

Lescroart, F., Kelly, R.G., Le Garrec, J.F., Nicolas, J.F., Meilhac, S.M., and Buckingham, M. (2010). Clonal analysis reveals common lineage relationships between head muscles and second heart field derivatives in the mouse embryo. *Development* 137, 3269–3279.

Lescroart, F., Chabab, S., Lin, X., Rulands, S., Paulissen, C., Rodolosse, A., Auer, H., Achouri, Y., Dubois, C., Bondue, A., et al. (2014). Early lineage restriction in temporally distinct populations of Mesp1 progenitors during mammalian heart development. *Nat. Cell Biol.* 16.

Lin, S.-C., Dollé, P., Ryckebusch, L., Nosedá, M., Zaffran, S., Schneider, M.D., and Niederreither, K. (2010). Endogenous retinoic acid regulates cardiac progenitor differentiation. *Proc. Natl. Acad. Sci. U. S. A.* 107, 9234–9239.

Lints, T.J., Parsons, L.M., Hartley, L., Lyons, I., and Harvey, R.P. (1993). Nkx-2.5: a novel murine homeobox gene expressed in early heart progenitor cells and their myogenic descendants. *Development* 119, 969.

Ludwig, L.L., Schertel, E.R., Pratt, J.W., McClure, D.E., Ying, A.J., Heck, C.F., and Myerowitz, P.D. (1997). Impairment of left ventricular function by acute cardiac lymphatic obstruction. *Cardiovasc. Res.* 33, 164–171.

Madisen, L., Zwingman, T.A., Sunkin, S.M., Oh, S.W., Zariwala, H.A., Gu, H., Ng, L.L.,

Palmiter, R.D., Hawrylycz, M.J., Jones, A.R., et al. (2010). A robust and high-throughput Cre reporting and characterization system for the whole mouse brain. *Nat. Neurosci.* 13, 133–140.

Mäkinen, T., Jussila, L., Veikkola, T., Karpanen, T., Kettunen, M.I., Pulkkanen, K.J., Kauppinen, R., Jackson, D.G., Kubo, H., Nishikawa, S.-I., et al. (2001). Inhibition of lymphangiogenesis with resulting lymphedema in transgenic mice expressing soluble VEGF receptor-3. *Nat. Med.* 7, 199–205.

Männer, J. (1992). The development of pericardial villi in the chick embryo. *Anat. Embryol. (Berl.)* 186, 379–385.

Männer, J. (2013). Microsurgical Procedures for Studying the Developmental Significance of the Proepicardium and Epicardium in Avian Embryos: PE-Blocking, PE-Photoablation, and PE-Grafting. *J. Dev. Biol.* 1, 47–63.

Marino, D., Dabouras, V., Brändli, A.W., and Detmar, M. (2011). A role for all-trans-retinoic acid in the early steps of lymphatic vasculature development. *J. Vasc. Res.* 48, 236–251.

Martinez-corral, I., Ulvmar, M.H., Stanczuk, L., Tatin, F., Kizhatil, K., John, S.W.M., Alitalo, K., Ortega, S., and Makinen, T. (2015). Brief UltraRapid Communication Nonvenous Origin of Dermal Lymphatic Vasculature. 1649–1654.

Martinez-Corral, I., Stanczuk, L., Frye, M., Ulvmar, M.H., Diéguez-Hurtado, R., Olmeda, D., Makinen, T., and Ortega, S. (2016). Vegfr3-CreERT2mouse, a new genetic tool for targeting the lymphatic system. *Angiogenesis* 19, 433–445.

Martínez-Estrada, O.M., Lettice, L.A., Essafi, A., Guadix, J.A., Slight, J., Velecela, V., Hall, E., Reichmann, J., Devenney, P.S., Hohenstein, P., et al. (2010). Wt1 is required for cardiovascular progenitor cell formation through transcriptional control of Snail and E-cadherin. *Nat. Genet.*

Maruyama, K., Ii, M., Cursiefen, C., Jackson, D.G., Keino, H., Tomita, M., Van Rooijen, N., Takenaka, H., D'Amore, P.A., Stein-Streilein, J., et al. (2005). Inflammation-induced lymphangiogenesis in the cornea arises from CD11b-positive macrophages. *J. Clin. Invest.* 115, 2363–2372.

Merki, E., Zamora, M., Raya, A., Kawakami, Y., Wang, J., Zhang, X., Burch, J., Kubalak, S.W., Kaliman, P., Izpisua Belmonte, J.C., et al. (2005). Epicardial retinoid X receptor alpha is required for myocardial growth and coronary artery formation. *Proc. Natl. Acad. Sci. U. S. A.* 102, 18455–18460.

Mikawa, T., and Fischman, D.A. (1992). Retroviral analysis of cardiac morphogenesis: discontinuous formation of coronary vessels. *Proc. Natl. Acad. Sci. U. S. A.* 89, 9504–9508.

Mikawa, T., and Gourdie, R.G. (1996). Pericardial mesoderm generates a population of coronary smooth muscle cells migrating into the heart along with ingrowth of the epicardial organ. *Dev. Biol.* 174, 221–232.

Miquerol, L., Bellon, A., Moreno, N., Beyer, S., Meilhac, S.M., Buckingham, M., Franco, D., and Kelly, R.G. (2013). Resolving cell lineage contributions to the ventricular

conduction system with a Cx40-GFP allele: A dual contribution of the first and second heart fields. *Dev. Dyn.* 242, 665–677.

Moon, A. (2008). Chapter 4 Mouse Models of Congenital Cardiovascular Disease. *Curr. Top. Dev. Biol.* 84, 171–248.

Moorman, A., Webb, S., Brown, N.A., Lamers, W., and Anderson, R.H. (2003). Development of the heart: (1) formation of the cardiac chambers and arterial trunks. *Heart* 89, 806–814.

Moretti, A., Caron, L., Nakano, A., Lam, J.T., Bernshausen, A., Chen, Y., Qyang, Y., Bu, L., Sasaki, M., Martin-Puig, S., et al. (2006). Multipotent embryonic *isl1*⁺ progenitor cells lead to cardiac, smooth muscle, and endothelial cell diversification. *Cell* 127, 1151–1165.

Muzumdar, M.D., Tasic, B., Miyamichi, K., Li, L., and Luo, L. (2007). A global double-fluorescent Cre reporter mouse. *Genesis* 45, 593–605.

Navarro-Aragall, A.G., Plein, A., and Ruhrberg, C. (2018). Regulation and Function of Cardiac Neural Crest Cells ☆ (Elsevier Inc.).

Niederreither, K., Subbarayan, V., Dollé, P., and Chambon, P. (1999). Embryonic retinoic acid synthesis is essential for early mouse post-implantation development. *Nat. Genet.* 21, 444–448.

Nijmeijer, R.M., Leeuwis, J.W., DeLisio, A., Mummery, C.L., and Chuva de Sousa Lopes, S.M. (2009). Visceral endoderm induces specification of cardiomyocytes in mice. *Stem Cell Res.* 3, 170–178.

Ny, A., Koch, M., Schneider, M., Neven, E., Tong, R.T., Maity, S., Fischer, C., Plaisance, S., Lambrechts, D., Héligon, C., et al. (2005). A genetic *Xenopus laevis* tadpole model to study lymphangiogenesis. *Nat. Med.* 11, 998–1004.

Ochsenbein, A.M., Karaman, S., Jurisic, G., and Detmar, M. (2014). The Role of Neuropilin-1/Semaphorin 3A Signaling in Lymphatic Vessel Development and Maturation. (Springer, Vienna), pp. 143–152.

Okuda, K.S., Astin, J.W., Misa, J.P., Flores, M. V., Crosier, K.E., and Crosier, P.S. (2012). Lyve1 Expression Reveals Novel Lymphatic Vessels and New Mechanisms for Lymphatic Vessel Development in Zebrafish. *Development* 139, 2381–2391.

Papoutsi, M., Tomarev, S.I., Eichmann, A., Pröls, F., Christ, B., and Wilting, J. (2001). Endogenous origin of the lymphatics in the avian chorioallantoic membrane. *Dev. Dyn.* 222, 238–251.

Parker, S.E., Mai, C.T., Canfield, M.A., Rickard, R., Wang, Y., Meyer, R.E., Anderson, P., Mason, C.A., Collins, J.S., Kirby, R.S., et al. (2010). Updated national birth prevalence estimates for selected birth defects in the United States, 2004-2006. *Birth Defects Res. Part A Clin. Mol. Teratol.* 88, 1008–1016.

Pérez-Pomares, J.M., Phelps, A., Sedmerova, M., Carmona, R., González-Iriarte, M., Muñoz-Chápuli, R., and Wessels, A. (2002). Experimental Studies on the Spatiotemporal Expression of WT1 and RALDH2 in the Embryonic Avian Heart: A Model

for the Regulation of Myocardial and Valvuloseptal Development by Epicardially Derived Cells (EPDCs). *Dev. Biol.* 247, 307–326.

Pérez-Pomares, J.M., Phelps, A., Sedmerova, M., and Wessels, A. (2003). Epicardial-like cells on the distal arterial end of the cardiac outflow tract do not derive from the proepicardium but are derivatives of the cephalic pericardium. *Dev. Dyn.* 227, 56–68.

Petrova, T. V, and Koh, G.Y. (2018). Organ-specific lymphatic vasculature : From development to pathophysiology. 35–49.

Pichol-thievend, C., Betterman, K.L., Liu, X., Ma, W., Skoczylas, R., Lesieur, E., Bos, F.L., Schulte, D., Schulte-merker, S., Hogan, B.M., et al. (2018). A blood capillary plexus-derived population of progenitor cells contributes to genesis of the dermal lymphatic vasculature during embryonic development.

Pichol-Thievend, C., Betterman, K.L., Liu, X., Ma, W., Skoczylas, R., Lesieur, E., Bos, F.L., Schulte, D., Schulte-Merker, S., Hogan, B.M., et al. (2018). A blood capillary plexus-derived population of progenitor cells contributes to genesis of the dermal lymphatic vasculature during embryonic development. *Development* 145, dev160184.

Qyang, Y., Martin-Puig, S., Chiravuri, M., Chen, S., Xu, H., Bu, L., Jiang, X., Lin, L., Granger, A., Moretti, A., et al. (2007). The renewal and differentiation of Isl1+ cardiovascular progenitors are controlled by a Wnt/beta-catenin pathway. *Cell Stem Cell* 1, 165–179.

Rana, M.S., Théveniau-Ruissy, M., De Bono, C., Mesbah, K., Francou, A., Rammah, M., Domínguez, J.N., Roux, M., Laforest, B., Anderson, R.H., et al. (2014). Tbx1 coordinates addition of posterior second heart field progenitor cells to the arterial and venous poles of the heart. *Circ. Res.* 115, 790–799.

Sabin, F.R. (1902). On the origin of the lymphatic system from the veins and the development of the lymph hearts and thoracic duct in the pig. *Am. J. Anat.* 1, 367–389.

Saga, Y., Miyagawa-Tomita, S., Takagi, A., Kitajima, S., Miyazaki, J. i., and Inoue, T. (1999). MesP1 is expressed in the heart precursor cells and required for the formation of a single heart tube. *Development* 126.

Saga, Y., Kitajima, S., and Miyagawa-Tomita, S. (2000). Mesp1 expression is the earliest sign of cardiovascular development. *Trends Cardiovasc. Med.* 10, 345–352.

Schledzewski, K., Falkowski, M., Moldenhauer, G., Metharom, P., Kzhyshkowska, J., Ganss, R., Demory, A., Falkowska-Hansen, B., Kurzen, H., Ugurel, S., et al. (2006). Lymphatic endothelium-specific hyaluronan receptor LYVE-1 is expressed by stabilin-1+, F4/80+, CD11b+ macrophages in malignant tumours and wound healing tissue in vivo and in bone marrow cultures in vitro: implications for the assessment of lymphangiogenesis. *J. Pathol.* 209, 67–77.

Schneider, M., Othman-Hassan, K., Christ, B., and Wilting, J. (1999). Lymphangioblasts in the avian wing bud. *Dev. Dyn.* 216, 311–319.

Sebzda, E., Hibbard, C., Sweeney, S., Abtahian, F., Bezman, N., Clemens, G., Maltzman, J.S., Cheng, L., Liu, F., Turner, M., et al. (2006). Syk and Slp-76 Mutant Mice Reveal a Cell-Autonomous Hematopoietic Cell Contribution to Vascular Development.

Dev. Cell 11, 349–361.

Soriano, P. (1999). Generalized lacZ expression with the ROSA26 Cre reporter strain. Nat. Genet. 21, 70–71.

Sousa, V.H., Miyoshi, G., Hjerling-Leffler, J., Karayannis, T., and Fishell, G. (2009). Characterization of Nkx6-2-Derived Neocortical Interneuron Lineages. Cereb. Cortex 19, i1–i10.

Srinivas, S., Watanabe, T., Lin, C.S., William, C.M., Tanabe, Y., Jessell, T.M., and Costantini, F. (2001). Cre reporter strains produced by targeted insertion of EYFP and ECFP into the ROSA26 locus. BMC Dev. Biol. 1, 4.

Srinivasan, R.S., Dillard, M.E., Lagutin, O. V, Lin, F.-J., Tsai, S., Tsai, M.-J., Samokhvalov, I.M., and Oliver, G. (2007). Lineage tracing demonstrates the venous origin of the mammalian lymphatic vasculature. Genes Dev. 21, 2422–2432.

Stanczuk, L., Martinez-Corral, I., Ulvmar, M.H., Zhang, Y., Laviña, B., Fruttiger, M., Adams, R.H., Saur, D., Betsholtz, C., Ortega, S., et al. (2015). CKIT lineage hemogenic endothelium-derived cells contribute to mesenteric lymphatic vessels. Cell Rep. 10, 1708–1721.

Sun, Y., Liang, X., Najafi, N., Cass, M., Lin, L., Cai, C.L., Chen, J., and Evans, S.M. (2007). Islet 1 is expressed in distinct cardiovascular lineages, including pacemaker and coronary vascular cells. Dev. Biol. 304, 286–296.

Susaki, E.A., Tainaka, K., Perrin, D., Kishino, F., Tawara, T., Watanabe, T.M., Yokoyama, C., Onoe, H., Eguchi, M., Yamaguchi, S., et al. (2014). Whole-Brain Imaging with Single-Cell Resolution Using Chemical Cocktails and Computational Analysis. Cell 157, 726–739.

Taira, A., Uehara, K., Fukuda, S., Takenaka, K., and Koga, M. (1990). Active Drainage of Cardiac Lymph in Relation to Reduction in Size of Myocardial Infarction: - An Experimental Study. Angiology 41, 1029–1036.

Tam, P.P., and Behringer, R.R. (1997). Mouse gastrulation: the formation of a mammalian body plan. Mech. Dev. 68, 3–25.

Theveniau-Ruissy, M., Dandonneau, M., Mesbah, K., Ghez, O., Mattei, M.-G., Miquerol, L., and Kelly, R.G. (2008). The del22q11.2 Candidate Gene Tbx1 Controls Regional Outflow Tract Identity and Coronary Artery Patterning. Circ. Res. 103, 142–148.

Théveniau-Ruissy, M., Dandonneau, M., Mesbah, K., Ghez, O., Mattei, M.-G., Miquerol, L., and Kelly, R.G. (2008). The del22q11.2 candidate gene Tbx1 controls regional outflow tract identity and coronary artery patterning. Circ. Res. 103, 142–148.

Torres, M. (1997). 5 The Use of Embryonic Stem Cells for the Genetic Manipulation of the Mouse. Curr. Top. Dev. Biol. 36, 99–114.

Ulvmar, M.H., and Mäkinen, T. Heterogeneity in the lymphatic vascular system and its origin.

Ulvmar, M.H., Martinez-Corral, I., Stanczuk, L., and Mäkinen, T. (2016). Pdgfrb-Cre

targets lymphatic endothelial cells of both venous and non-venous origins. *Genesis* 54, 350–358.

Vermot, J., Niederreither, K., Garnier, J.-M., Chambon, P., and Dollé, P. (2003). Decreased embryonic retinoic acid synthesis results in a DiGeorge syndrome phenotype in newborn mice. *Proc. Natl. Acad. Sci. U. S. A.* 100, 1763–1768.

Verzi, M.P., McCulley, D.J., De Val, S., Dodou, E., and Black, B.L. (2005). The right ventricle, outflow tract, and ventricular septum comprise a restricted expression domain within the secondary/anterior heart field. *Dev. Biol.* 287, 134–145.

Villa del Campo, C., Lioux, G., Carmona, R., Sierra, R., Muñoz-Chápuli, R., Clavería, C., and Torres, M. (2016). Myc overexpression enhances epicardial contribution to the developing heart and promotes extensive expansion of the cardiomyocyte population. *Sci. Rep.* 6, 35366.

Virágh, S., and Challice, C.E. (1973). Origin and differentiation of cardiac muscle cells in the mouse. *J. Ultrastruct. Res.* 42, 1–24.

Wagner, M., and Siddiqui, M.A.Q. (2007). Signal transduction in early heart development (I): cardiogenic induction and heart tube formation. *Exp. Biol. Med. (Maywood)*. 232, 852–865.

Waldo, K., Miyagawa-Tomita, S., Kumiski, D., and Kirby, M.L. (1998). Cardiac neural crest cells provide new insight into septation of the cardiac outflow tract: aortic sac to ventricular septal closure. *Dev. Biol.* 196, 129–144.

Waldo, K., Zdanowicz, M., Burch, J., Kumiski, D.H., Stadt, H.A., Godt, R.E., Creazzo, T.L., and Kirby, M.L. (1999). A novel role for cardiac neural crest in heart development. *J. Clin. Invest.* 103, 1499–1507.

Waldo, K.L., Hutson, M.R., Ward, C.C., Zdanowicz, M., Stadt, H.A., Kumiski, D., Abu-Issa, R., and Kirby, M.L. (2005). Secondary heart field contributes myocardium and smooth muscle to the arterial pole of the developing heart. *Dev. Biol.* 281, 78–90.

Wang, S., Huang, W., Castillo, H.A., Kane, M.A., Xavier-Neto, J., Trainor, P.A., and Moise, A.R. (2018a). Alterations in retinoic acid signaling affect the development of the mouse coronary vasculature. *Dev. Dyn.* 247, 976–991.

Wang, S., Huang, W., Castillo, H.A., Kane, M.A., Xavier-Neto, J., Trainor, P.A., and Moise, A.R. (2018b). Alterations in retinoic acid signaling affect the development of the mouse coronary vasculature. *Dev. Dyn.* 247, 976–991.

Wang, X., Chen, D., Chen, K., Jubran, A., Ramirez, A., and Astrof, S. (2017). Endothelium in the pharyngeal arches 3, 4 and 6 is derived from the second heart field. *Dev. Biol.* 421, 108–117.

Wang, Y.-L., Wang, X.-H., Liu, Y.-L., Kong, X.-Q., and Wang, L.-X. (2009). Cardiac lymphatic obstruction impairs left ventricular function and increases plasma endothelin-1 and angiotensin II in rabbits. *Lymphology* 42, 182–187.

Wessels, A., van den Hoff, M.J.B., Adamo, R.F., Phelps, A.L., Lockhart, M.M., Sauls, K., Briggs, L.E., Norris, R. a., van Wijk, B., Perez-Pomares, J.M., et al. (2012). Epicardially

derived fibroblasts preferentially contribute to the parietal leaflets of the atrioventricular valves in the murine heart. *Dev. Biol.* 366, 111–124.

Wigle, J.T., and Oliver, G. (1999). Prox1 function is required for the development of the murine lymphatic system. *Cell* 98, 769–778.

Wigle, J.T., Harvey, N., Detmar, M., Lagutina, I., Grosveld, G., Gunn, M.D., Jackson, D.G., and Oliver, G. (2002). An essential role for Prox1 in the induction of the lymphatic endothelial cell phenotype. *EMBO J.* 21, 1505–1513.

Wilting, J., Papoutsis, M., Schneider, M., and Christ, B. (2000a). The lymphatic endothelium of the avian wing is of somitic origin. *Dev. Dyn.* 217, 271–278.

Wilting, J., Papoutsis, M., Schneider, M., and Christ, B. (2000b). The lymphatic endothelium of the avian wing is of somitic origin. *Dev. Dyn.* 217, 271–278.

Wilting, J., Aref, Y., Huang, R., Tomarev, S.I., Schweigerer, L., Christ, B., Valasek, P., and Papoutsis, M. (2006). Dual origin of avian lymphatics. *Dev. Biol.* 292, 165–173.

Wilting, J., Buttler, K., Schulte, I., Papoutsis, M., Schweigerer, L., and Männer, J. (2007). The proepicardium delivers hemangioblasts but not lymphangioblasts to the developing heart. *Dev. Biol.* 305, 451–459.

Yang, Y., García-Verdugo, J.M., Soriano-Navarro, M., Srinivasan, R.S., Scallan, J.P., Singh, M.K., Epstein, J.A., and Oliver, G. (2012). Lymphatic endothelial progenitors bud from the cardinal vein and intersomitic vessels in mammalian embryos. *Blood* 120, 2340–2348.

Yaniv, K., Isogai, S., Castranova, D., Dye, L., Hitomi, J., and Weinstein, B.M. (2006). Live imaging of lymphatic development in the zebrafish. *Nat. Med.* 12, 711–716.

Zhou, B., Ma, Q., Rajagopal, S., Wu, S.M., Domian, I., Rivera-Feliciano, J., Jiang, D., von Gise, A., Ikeda, S., Chien, K.R., et al. (2008). Epicardial progenitors contribute to the cardiomyocyte lineage in the developing heart. *Nature* 454, 109–113.

Zhou, Z., Wang, J., Guo, C., Chang, W., Zhuang, J., Zhu, P., and Li, X. (2017). Temporally Distinct Six2 -Positive Second Heart Field Progenitors Regulate Mammalian Heart Development and Disease Article Temporally Distinct Six2 -Positive Second Heart Field Progenitors Regulate Mammalian Heart Development and Disease. *CellReports* 18, 1019–1032.